

**APPLICATION OF ULTRAVIOLET LIGHT-EMITTING DIODES (UV-LEDs) FOR
WATER DISINFECTION BY MULTIPLE WAVELENGTHS AND PULSED
IRRADIATION**

by

Kai Song

M.Sc., Peking University, China, 2013

A THESIS SUBMITTED IN PARTIAL FULFILLMENT OF
THE REQUIREMENTS FOR THE DEGREE OF

DOCTOR OF PHILOSOPHY

in

THE FACULTY OF GRADUATE AND POSTDOCTORAL STUDIES
(Chemical and Biological Engineering)

THE UNIVERSITY OF BRITISH COLUMBIA

(Vancouver)

April 2018

© Kai Song, 2018

Abstract

Safe drinking water is essential to humans, thus natural raw water requires necessary treatment, especially removing pathogenic microorganisms for disinfection. In addition to conventional chemical disinfectant, ultraviolet (UV) radiation has been increasingly used for water disinfection. Recently a new UV source - UV light-emitting diodes (UV-LEDs) - has emerged with many special features, which is believed to be a promising alternative to conventional UV lamps for water disinfection. This research focused on two special features of UV-LEDs, multiple wavelengths and pulsed irradiation, to explore the effect and potential on water disinfection.

UV-LEDs in different UV wavelength ranges were combined in various manners to investigate the effect of multiple wavelengths on microorganisms inactivation in water. The results showed the effect of UV-LEDs multiple wavelengths depends on the wavelength combinations among UVA (315 – 400 nm), UVB (280 – 315 nm) and UVC (200 – 280 nm), the manner to apply different wavelengths (e.g. simultaneous, sequential), as well as different types of microorganisms (e.g. bacteria, virus). Combinations of UVC/UVB always achieved additive effect on microorganisms inactivation due to the same photochemical reactivation induced by UVC/UVB on DNA that follows the Second Law of Photochemistry. However, combining UVA with UVC/UVB simultaneously or applying UVA after UVC/UVB reduced the inactivation of bacterium *E. coli* due to DNA repair and photoreactivation effect of UVA. A special wavelength combination was developed by applying UVA as pretreatment followed by UVC inactivation, which achieved dramatic inactivation improvement and significant reactivation reduction on *E.*

coli. The effects and mechanisms of this special combination were thoroughly investigated and revealed in this research.

The effect of UV-LEDs pulsed irradiation was examined by applying pulsed irradiation with various pulsed patterns (frequency and duty rate) on different microorganisms in pure water and wastewater. Comparable inactivation were obtained by UV-LEDs continuous irradiation and various pulsed irradiation on all the four microorganisms examined, which clarified the role of pulsation on UV disinfection.

The findings in this research promote a better understanding on UV disinfection and are of considerable significance to take full advantage of UV-LEDs for water disinfection.

Lay Summary

Water disinfection is very important for humans to access safe drinking water. Ultraviolet (UV) radiation is an effective method for water disinfection. A newly emerging UV source - UV light-emitting diodes (UV-LEDs) – has many special features that may facilitate UV disinfection. This research closely looked at two special features of UV-LEDs, multiple wavelengths and pulsed irradiation, and aimed to investigate their effects on microorganisms inactivation and explore the potential for water disinfection. Through comprehensive investigation of various wavelength combinations in different UV ranges and pulsed irradiation with various pulse patterns for inactivation of different types of microorganisms in water, this research revealed the different effects of UV-LEDs multiple wavelengths and pulsed irradiation on water disinfection, and proposed the related mechanisms accordingly. The findings in this research will promote the practical applications of UV-LEDs for water disinfection by taking full advantage of their special features.

Preface

This research is conducted by me, Kai Song, under the supervision of Dr. Fariborz Taghipour and Dr. Madjid Mohseni at Department of Chemical and Biological Engineering in the University of British Columbia (UBC), Vancouver, Canada. I was in charge of literature review, research questions identification, research proposal development, experimental designs, and all the experimental work execution. During the whole process of research, Dr. Taghipour and Dr. Mohseni provided many insightful comments and suggestions to help improve this research.

Some parts of this research have been published in academic journals, while the others are in preparation for publication, which are listed as follows:

- A version of Chapter 1 and Chapter 2 has been published in Water Research:
Song, K., Mohseni, M. and Taghipour, F., 2016. Application of ultraviolet light-emitting diodes (UV-LEDs) for water disinfection: A review. *Water Research*. 94, 341–349.
- A version of Chapter 6 has been published in Chemical Engineering Journal:
Song, K., Taghipour, F. and Mohseni, M., 2018. Microorganisms inactivation by continuous and pulsed irradiation of ultraviolet light-emitting diodes (UV-LEDs). *Chemical Engineering Journal*. 343, 362-370.
- The manuscripts based on Chapter 4 and Chapter 5 are in preparation for publication.

For all of these publications and manuscripts, I conducted all the experimental work, data collection, data analysis and manuscripts writing. Dr. Taghipour and Dr. Mohseni helped improve experimental designs and data analysis, review and revise the manuscripts.

In addition to these publications, different parts of this research also have been presented in academic conferences:

- **Song, K.**, Taghipour, F., Mohseni, M. Application of ultraviolet light-emitting diodes (UV-LEDs) for water disinfection. RES'EAU-WaterNET AGM 2015, Kelowna, Canada, May 26-27, 2015.
- **Song, K.**, Mohseni, M., Taghipour, F. UV-LEDs microorganism inactivation by multiple wavelengths and pulse illumination. The 65th Canadian Chemical Engineering Conference, Calgary, Canada, October 4-7, 2015.
- **Song, K.**, Mohseni, M., Taghipour, F. Effect of wavelengths combinations by UV-LEDs on water disinfection. International Ultraviolet Association World Congress, Vancouver, Canada, Jan.31 - Feb.3, 2016.
- **Song, K.**, Taghipour, F., Mohseni, M. Ultraviolet light-emitting diodes (UV-LEDs): A new alternative for small systems water disinfection. RES'EAU-WaterNET AGM 2016, Whistler, Canada, Apr. 30 - May.1, 2016.
- **Song, K.**, Mohseni, M., Taghipour, F. Continuous and pulsed irradiation of ultraviolet light-emitting diodes (UV-LEDs) for water disinfection. RES'EAU-WaterNET AGM 2017, Victoria, Canada, May 26-27, 2017.
- **Song, K.**, Taghipour, F., Mohseni, M. Effect of pulsed irradiation by UV-LEDs on water disinfection. International Ultraviolet Association Americas Conference, Redondo Beach, United States, Feb.26-28, 2018

Table of Contents

Abstract.....	ii
Lay Summary	iv
Preface.....	v
Table of Contents	vii
List of Tables	xi
List of Figures.....	xii
List of Abbreviations	xviii
Acknowledgements	xix
Dedication	xx
Chapter 1: Introduction	1
1.1 Background	1
1.2 Thesis layout	5
Chapter 2: Literature review	6
2.1 UV mercury lamps for disinfection	6
2.2 Xenon lamps pulsed irradiation for disinfection.....	9
2.3 UV-LEDs for disinfection.....	11
2.4 Mechanisms of UV disinfection	15
2.5 Knowledge gaps.....	19
2.6 Research questions.....	20
2.7 Thesis objectives and scope	21
Chapter 3: Experimental methodology	24

3.1	Experimental apparatus.....	24
3.2	Selection of UV-LEDs.....	25
3.3	UV radiation measurement	26
3.4	Microorganism cultivation and enumeration	28
3.5	UV exposure and data analysis	29
Chapter 4: Microorganisms inactivation by UV-LEDs multiple wavelengths		31
4.1	Introduction.....	31
4.2	Experimental design.....	32
4.3	Results and discussion	34
4.3.1	Combinations of UVC- and UVB-LEDs on <i>E. coli</i> inactivation.....	34
4.3.2	Combinations of UVB- and UVA-LEDs on <i>E. coli</i> inactivation.....	37
4.3.3	Combinations of UVC- and UVA-LEDs on <i>E. coli</i> inactivation.....	39
4.3.4	Combinations of UVC- and UVA-LEDs on MS2 inactivation	44
4.4	Conclusions.....	47
Chapter 5: Microorganisms inactivation of UVA pretreatment followed by UVC disinfection.....		49
5.1	Introduction.....	49
5.2	Experimental design.....	50
5.2.1	Microorganisms inactivation	50
5.2.2	Reactivation examination.....	51
5.2.3	Mechanism investigation	53
5.3	Results and discussion	55
5.3.1	Effects of UVA pretreatment on <i>E. coli</i> inactivation.....	55

5.3.2	Effects of UVA pretreatment on MS2 inactivation	61
5.3.3	Effects of UVA pretreatment on <i>E. coli</i> reactivation.....	62
5.3.4	Roles of ROS on <i>E. coli</i> inactivation with UVA pretreatment	66
5.3.5	Roles of ROS on <i>E. coli</i> reactivation with UVA pretreatment	69
5.3.6	Determination of ROS during UVA pretreatment on <i>E. coli</i>	70
5.3.7	Proposed mechanisms for UVA pretreatment on microorganisms inactivation and reactivation.....	75
5.3.8	Energy and cost analysis for UVA pretreatment	77
5.4	Conclusions.....	82
Chapter 6: Microorganisms inactivation by UV-LEDs pulsed irradiation.....		84
6.1	Introduction.....	84
6.2	Experimental design.....	85
6.3	Results and discussion	87
6.3.1	Determination of UV fluence for pulsed irradiation.....	87
6.3.2	UV-LEDs pulsed irradiation on <i>E. coli</i> inactivation.....	90
6.3.3	UV-LEDs pulsed irradiation on coliform inactivation in wastewater	91
6.3.4	UV-LEDs pulsed irradiation on MS2 inactivation	94
6.3.5	Other features of UV-LEDs pulsed irradiation.....	95
6.3.6	Discussion.....	99
6.4	Conclusions.....	104
Chapter 7: Conclusions and recommendations		105
7.1	Overall conclusions.....	105
7.2	Contributions and significance of this research.....	107

7.3	Recommendations for future work	111
Bibliography		114
Appendices.....		132
Appendix A	Microorganisms cultivation and enumeration for UV disinfection	132
A.1	<i>E. coli</i> stock preparation	132
A.2	<i>E. coli</i> sample preparation and enumeration.....	132
A.3	MS2 phage stock preparation.....	134
A.4	MS2 phage sample preparation and enumeration.....	135
Appendix B	Supplementary data	137

List of Tables

Table 3.1 Specifications for UV-LEDs used in this research	26
Table 5.1 <i>E. coli</i> inactivation kinetics fitting results for 265 nm UVC with and without 365 nm UVA pretreatment. F represents UV fluence of 265 nm UVC in the unit of mJ/cm ² ..	60
Table 5.2 Energy efficiency and cost of UV-LEDs used in this research	78
Table 5.3 Energy consumption comparisons on 265 nm UVC-LED inactivation with and without 365 nm UVA-LED pretreatment. The third and fourth rows refer to 10 min, 30 min UVA pretreatment, respectively, in which the UV fluence data is derived from Table 5.1 for 6 log inactivation.	80
Table 5.4 Cost of UV-LEDs for 265 nm UVC inactivation with and without 365 nm UVA pretreatment.....	82
Table 6.1 UV fluence results from iodide-iodate (KI) and ferrioxalate (FeO _x) actinometry for 265 nm UV-LED continuous and pulsed irradiation at various frequencies (Hz) and duty rates (%). Calculated operation time is based on the definition of duty rate (Figure 6.1b), adjusted operation time is based on actual UV fluence measurement in order to ensure the equivalent UV fluence between continuous and pulsed irradiation.....	88
Table 6.2 Comparisons of total UV-LED "on" time between continuous and pulsed irradiation. Operation time for equivalent UV fluence is from Table 6.1. Total UV-LED "on" time during "on-off" cycles is based on the definition of duty rate in Figure 6.1(b).	96
Table 7.1 Summary of effects and mechanisms of applying UVA 365 nm on bacterium <i>E. coli</i> inactivation in different manners with different ranges of UV fluence.	109

List of Figures

Figure 1.1 The circuit (top) and band diagram (bottom) on how an LED works (reprinted from Wikipedia, Light-emitting diode with permission).....	3
Figure 2.1 Double-stranded DNA chain showing how the formation of pyrimidine dimers disrupts the structure of DNA chain (A = adenine, G = guanine, T = thymine, C = cytosine) (reprinted from Bolton and Cotton, 2008 with permission).....	7
Figure 2.2 Action spectra (relative response versus wavelength) for DNA, MS2, <i>Cryptosporidium</i> and <i>E. coli</i> (reprinted from Bolton and Cotton, 2008 with permission).....	7
Figure 2.3 Output spectra of low pressure and medium pressure lamps (not to scale) (reprinted from Kuo et al., 2003 with permission)	8
Figure 2.4 Illustration of energy output of continuous and pulsed UV for comparison (reprinted from Keener and Krishnamurthy, 2014 with permission)	10
Figure 3.1 Schematic diagram of experimental apparatus for UV-LEDs inactivation (not to scale)	24
Figure 4.1 Flow chart to illustrate UV-LEDs multiple wavelengths exposure. UV-LED #1 and UV-LED #2 represent each two different wavelengths among UVC (265 nm), UVB (285 nm), UVA (365 nm) for various dual-wavelength combinations.....	33
Figure 4.2 <i>E. coli</i> inactivation by 40 s 265 nm UVC-LED, 40 s 285 nm UVB-LED and simultaneous 40 s UVC/UVB-LEDs. Addition 265+285 nm represents the sum of log inactivation by 265 nm alone (i.e. the first column) and 285 nm alone (i.e. the second column). Error bars represent the standard deviation for triplicate runs.	34

Figure 4.3 <i>E. coli</i> concentration changes by sequential 265 nm UVC-LED and 285 nm UVB-LED exposure: (a) 40 s 265 nm followed by 40 s 285 nm, (b) 40 s 285 nm followed by 40 s 265 nm. For both sequential exposures, the overall concentration reduction was 4.6 log. Error bars represent the standard deviation for triplicate runs.	35
Figure 4.4 <i>E. coli</i> inactivation by 40 s 285 nm UVB-LED, 40 s 365 nm UVA-LED and simultaneous 40 s UVB/UVA-LEDs. Error bars represent the standard deviation for triplicate runs.....	38
Figure 4.5 <i>E. coli</i> concentration changes by sequential 285 nm UVB-LED and 365 nm UVA-LED exposure: (a) 40 s 365 nm followed by 40 s 285 nm, (b) 40 s 285 nm followed by 40 s 365 nm. Error bars represent the standard deviation for triplicate runs.	39
Figure 4.6 <i>E. coli</i> inactivation by 40 s 265 nm UVC-LED, 40 s 365 nm UVA-LED and simultaneous 40 s UVC/UVA-LEDs. Error bars represent the standard deviation for triplicate runs.....	40
Figure 4.7 <i>E. coli</i> concentration changes by sequential 265 nm UVC-LED and 365 nm UVA-LED exposure: (a) 40 s 365 nm followed by 40 s 265 nm, (b) 50 s 265 nm followed by 3 min 365 nm. Error bars represent the standard deviation for triplicate runs.	41
Figure 4.8 MS2 inactivation by 3 min 265 nm UVC-LED, 3 min 365 nm UVA-LED and simultaneous 3 min UVC/UVA-LEDs. Error bars represent the standard deviation for triplicate runs.....	45
Figure 4.9 MS2 concentration reduction by sequential 265 nm UVC-LED and 365 nm UVA-LED exposure: (a) 3 min 365 nm followed by 3 min 265 nm, (b) 3 min 265 nm followed by 3 min 365 nm. Error bars represent the standard deviation for triplicate runs.....	46

Figure 5.1 Flow chart to illustrate UVA pretreatment followed by UVC inactivation	51
Figure 5.2 <i>E. coli</i> inactivation by 365 nm UVA pretreatment with different times followed by 30 s 265 nm UVC irradiation. Error bars represent the standard deviation for triplicate runs.....	56
Figure 5.3 <i>E. coli</i> inactivation kinetics by 265 nm UVC with and without 365 nm UVA pretreatment. X-axis indicates UV fluence for 265 nm UVC. The UV fluence of 365 nm UVA pretreatment is 1.7 J/cm ² for 1 min, 17 J/cm ² for 10 min, 52 J/cm ² for 30 min. Error bars represent the standard deviation for triplicate runs.....	57
Figure 5.4 <i>E. coli</i> inactivation kinetics fitting for 265 nm UVC with and without 365 nm UVA pretreatment. X-axis indicates UV fluence for 265 nm UVC. The UV fluence of 365 nm UVA pretreatment is 1.7 J/cm ² for 1 min, 17 J/cm ² for 10 min, 52 J/cm ² for 30 min. Error bars represent the standard deviation for triplicate runs.....	60
Figure 5.5 MS2 inactivation by 365 nm UVA pretreatment with different times followed by 3 minutes 265 nm UVC irradiation. Error bars represent the standard deviation for triplicate runs.....	61
Figure 5.6 <i>E. coli</i> dark repair after 265 nm UVC inactivation and after 30 minutes 365 nm UVA pretreatment followed by 265 nm UVC inactivation for 3.3 log inactivation. Error bars represent the standard deviation for triplicate runs.	63
Figure 5.7 <i>E. coli</i> photoreactivation after 265 nm UVC inactivation and after 30 minutes 365 nm UVA pretreatment followed by 265 nm UVC inactivation for 3.3 log inactivation. Error bars represent the standard deviation for triplicate runs.....	64
Figure 5.8 <i>E. coli</i> inactivation kinetics by 265 nm UVC irradiation in the presence of different scavengers. Error bars represent the standard deviation for triplicate runs.	67

Figure 5.9 <i>E. coli</i> inactivation kinetics by 265 nm UVC irradiation after 365 nm UVA pretreatment in the presence of different scavengers. Error bars represent the standard deviation for triplicate runs.	67
Figure 5.10 <i>E. coli</i> photoreactivation after 30 min 365 nm UVA pretreatment followed by 265 nm UVC inactivation for 3.3 log inactivation in the absence and presence of mannitol. Error bars represent the standard deviation for triplicate runs.....	70
Figure 5.11 <i>E. coli</i> inactivation kinetics by 265 nm UVC irradiation after 30 min 365 nm UVA pretreatment in the presence of mannitol during different stages. Error bars represent the standard deviation for triplicate runs.....	71
Figure 5.12 Carbamazepine (CBZ) degradation kinetics under 365 nm UVA irradiation in the presence and absence of <i>E. coli</i> in water.	72
Figure 5.13 <i>E. coli</i> inactivation on agar plates by 265 nm UVC irradiation, by 365 nm UVA pretreatment followed by 265 nm UVC irradiation in the absence and presence of mannitol. Error bars represent the standard deviation for triplicate runs.....	73
Figure 6.1 Schematic diagram of pulsed UV-LED circuit and experimental apparatus (a); illustration of voltage waveform for pulsed UV-LED irradiation at 0.1 Hz frequency and 50% duty rate (b).....	86
Figure 6.2 Measured waveforms of UV-LED pulsed irradiation at 50% duty rate with 10 Hz (a), 100 Hz (b) and 1k Hz (c), as well as at 10% duty rate with 10 Hz (d)	89
Figure 6.3 <i>E. coli</i> inactivation by 265 nm UV-LED continuous and pulsed irradiation with various pulse patterns at equivalent UV dose 4.9 mJ/cm ² : (a) various frequencies at 50% duty rate; (b) various duty rates at 10 Hz frequency. Error bars represent the standard deviation for triplicate runs.	91

Figure 6.4 265 nm UV-LED continuous and pulsed irradiation with various pulse patterns at equivalent UV fluence 2.7 mJ/cm ² on inactivation of total coliform (a, b) and <i>E. coli</i> (c, d) in wastewater. Error bars represent the standard deviation for triplicate runs.	92
Figure 6.5 MS2 inactivation by 265 nm UV-LED continuous and pulsed irradiation with various frequencies at 50% duty rate with equivalent UV fluence 40 mJ/cm ² . Error bars represent the standard deviation for triplicate runs.	94
Figure 6.6 Temperature of UV-LED when operating in continuous and pulsed mode with various pulse patterns in the absence of heat sink: (a) various frequencies at 50% duty rate; (b) various duty rates at 10 Hz frequency.	98
Figure A.1 Growth curve of <i>E. coli</i> solution	133
Figure A.2 <i>E. coli</i> colonies on agar plates	134
Figure A.3 MS2 plaques on <i>E. coli</i> agar plates	136
Figure B.1 Dark control for <i>E. coli</i> concentration change after 50 s 265 nm UVC-LED exposure.	137
Figure B.2 The emission spectrum from fluorescent lamps for photoreactivation experiments	137
Figure B.3 Effect of different scavengers (0.5 mol/L mannitol, 1 mg/mL catalase, 1 mmol/L TEMPOL) on the viability of <i>E. coli</i> cells as control. Error bars represent the standard deviation for triplicate runs.	138
Figure B.4 The viability of <i>E. coli</i> cells under fluorescent lamps visible light and in dark as light and dark control for reactivation experiment. Error bars represent the standard deviation for triplicate runs.	138

Figure B.5 Effect of carbamazepine (CBZ, 400 ppb) on the viability of *E. coli* cells as control.

Error bars represent the standard deviation for triplicate runs..... 139

Figure B.6 Measured voltage waveform for UV-LED continuous irradiation..... 139

List of Abbreviations

AOPs	Advanced oxidation processes
CBZ	Carbamazepine
DNA	Deoxyribonucleic acid
<i>E. coli</i>	<i>Escherichia coli</i>
H ₂ O ₂	Hydrogen peroxide
LED	Light-emitting diodes
LP mercury lamps	Low pressure mercury lamps
MP mercury lamps	Medium pressure mercury lamps
MW	megawatt
nm	nanometer
•O ₂ ⁻	Superoxide radical
•OH	Hydroxyl radical
RNA	Ribonucleic acid
TEMPOL	4-hydroxy-2,2,6,6-tetramethylpiperidin-1-oxyl
UV	Ultraviolet
UVA	Ultraviolet A (in the wavelength range of 315 – 400 nm)
UVB	Ultraviolet B (in the wavelength range of 280 – 315 nm)
UVC	Ultraviolet C (in the wavelength range of 200 – 280 nm)

Acknowledgements

This research cannot be done without help from multiple resources. I would like to express my heartfelt appreciation to my two supervisors: Dr. Fariborz Taghipour and Dr. Madjid Mohseni. During the past four years, they kindly devoted numerous time and effort to teaching and guiding me on this project, so that I have been always encouraged, enlightened, and inspired by them. Even sometimes when I made mistakes, they still gave me the chance allowing me to correct and improve myself. What I learned from them in the past four years not only helped me accomplish this project, but also will continuously benefit me for the whole life.

I also would like to sincerely acknowledge my committee members Dr. Loretta Li and Dr. Heather Trajano. Their insightful comments and critical feedback considerably enriched this research. And also, their generous support and active participation on my committee meetings and exams played a significant role on helping me accomplish this PhD program.

I am truly grateful to all my colleagues in the two research groups of Dr. Taghipour and Dr. Mohseni. Whenever I need help in the lab or want to learn on unfamiliar topics, they are always willing to give me a hand and generously share their knowledge. Many thanks to my friends Nathaniel Lim and Min Feng from Michael Smith Laboratories for teaching me microbial assay techniques when I had a hard time initiating the microbial tests.

Special thanks to my family for understanding and supporting my pursuit of PhD study abroad. Their unconditional support always motivates me to work hard towards my goals in life.

Finally I would like to acknowledge the financial support from Natural Sciences and Engineering Research Council of Canada (NSERC) and Chinese Scholarship Council (CSC).

Dedication

To

My beloved fiancée

Dr. Qiulu (Mina) Chu

who constantly supported me

throughout the long challenging journey of my PhD study

emotionally, academically and financially.

Chapter 1: Introduction

1.1 Background

Drinking water safety is an important issue worldwide, especially in most developing countries and rural areas. Access to safe drinking water is essential to human survival and health. However, there are still millions of people around the world lacking access to safe drinking water and being threatened by waterborne diseases annually (Hatami, 2013, WHO, 2014). The development of efficient water treatment technologies, especially inactivation of pathogenic microorganisms in water, is of great significance for human health and well-being.

Ultraviolet (UV) radiation, an electromagnetic radiation with a wavelength from 100 nm to 400 nm, can effectively inactivate various microorganisms in water and has been increasingly applied for water disinfection (Hijnen et al., 2006). UV radiation has numerous advantages over conventional chemical disinfection methods (e.g. chlorination, ozonation). These include no chemical addition, no harmful disinfection by-products (DBPs) formation, and no introduction of disinfectant-resistance to bacteria (Mori et al., 2007). UV disinfection has been recommended as a substitute for chemical additives for surface water treatment (USEPA, 2006). There have been over 7000 municipal UV disinfection installations in the world for drinking water and wastewater treatment (Muller, 2011), and the small household UV disinfection systems are also available (Brownell et al., 2008). It is estimated that the global market for UV disinfection equipment has a potential to reach \$2.8 billion by 2020 (Allied Analytics LLP, 2014).

The main UV sources for current UV disinfection systems are low- or medium-pressure mercury lamps (Chevremont et al., 2013a). Although these lamps are widely used in water treatment systems, there are still many issues with them. Some of the major concerns are that the

UV lamps are fragile and contain toxic mercury, which is a hazardous substance to environment and requires proper disposal (Chevremont et al., 2013b, Close et al., 2006). Moreover, these lamps require significant amounts of energy to operate due to wall plug efficiency at around 15–35% and have a relatively short lifetime of about 10,000 hours (Autin et al., 2013, Chatterley and Linden, 2010).

In the past few years, with the rapid development and improvement of semiconductor industry, UV light-emitting diodes (UV-LEDs) have emerged as a new source to generate UV radiation (Muramoto et al., 2014). An LED is a semiconductor device that utilizes semiconductor materials to create a p-n junction. A p-n junction is an interface between two types of semiconductor materials, p-type and n-type. The "p" (positive) type contains an excess of holes, while the "n" (negative) type contains an excess of electrons (Wikipedia, p–n junction). With a suitable voltage applied to a p-n junction, the electrons and holes recombine at the junction to emit radiation and the wavelength of the radiation depends on the semiconductor materials (Figure 1.1). Commercial visible LEDs have been available for nearly 50 years and have diverse applications, especially in lighting industry, due to increasingly higher efficiency and lower cost (Ibrahim et al., 2014). Recently, the newly emerging UV-LEDs have followed a similar track and are expected to be economically viable in the coming years (Harris et al., 2013).

UV-LEDs at various wavelengths can be manufactured using different semiconductor materials. The most frequently used materials are III-nitride, including gallium nitride (GaN), aluminium gallium nitride (AlGaN) and aluminum nitride (AlN) (Khan et al., 2005). The wavelength of GaN-based UV-LEDs can be as short as 365 nm, which is in the UVA range (i.e. 315 – 400 nm) (Taniyasu et al., 2006b). The AlN UV-LEDs, on the other hand, are reported to emit UV radiation at 210 nm in the UVC range (i.e. 200 – 280 nm), which is the shortest

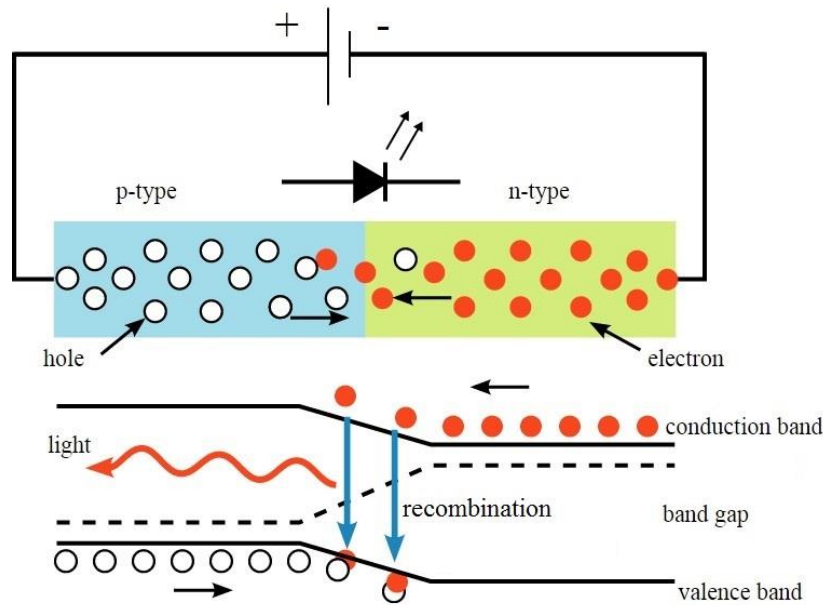


Figure 1.1 The circuit (top) and band diagram (bottom) on how an LED works (reprinted from Wikipedia, Light-emitting diode with permission)

wavelength among semiconductors (Taniyasu et al., 2006a). The wavelength from 210 to 365 nm (covering from UVC to UVA) is available from the emission of AlGa_N UV-LEDs, which are made of AlN and GaN with appropriate proportions (Taniyasu and Kasu, 2010). Since the wavelength is found to be an essential factor for water disinfection efficiency (Vilhunen et al., 2009), the ability of UV-LEDs to offer a great variety of wavelengths is well aligned with the needs of efficient disinfection, making it a potential option.

In addition to diversity in wavelengths, UV-LEDs possess several unique advantages compared to conventional UV mercury lamps, such as environmental friendliness (no mercury), compactness and robustness (more durable), faster start-up time (no warm-up time), potentially less energy consumption, longer lifetime, and ability to turn on and off with high frequency (Wurtele et al., 2011). It is predicted that by 2020, UV-LEDs at the wavelengths close to visible light (i.e. UVA) will operate at 75% wall plug efficiency with a lifetime longer than 100,000

hours, comparable with the operating parameters of current visible LEDs (Autin et al., 2013, Ibrahim et al., 2014). All these factors make UV-LEDs a promising alternative to conventional UV mercury lamps for water disinfection.

Currently there is limited research on how to apply the newly emerging UV-LEDs for water disinfection, especially how to take full advantage of their unique features that UV mercury lamps do not possess. One of such special features of UV-LEDs is wavelength diversity, which allows to select specific wavelengths for particular purposes and to generate various combinations for multiple wavelengths irradiation. Another special feature of UV-LEDs is the ability to turn on and off with high frequency, which enables the generation of pulsed irradiation with adjustable pulse patterns. Multiple wavelengths and pulsed irradiation may have different effects on microorganism inactivation compared to regular UV irradiation, and have a potential to improve inactivation based on the research on polychromatic UV radiation from medium-pressure mercury lamps and pulsed irradiation from xenon lamps (Elmnasser et al., 2007, Oguma et al., 2002). Given that UV-LEDs offer the broad adjustability and flexibility of the parameters for multiple wavelengths and pulsed irradiation, it is of great interest to explore the potential and capitalize these unique features for water disinfection. Therefore, the focus of this study is on these two special features of UV-LEDs for the exploration of the potential additional effects of multiple wavelengths and pulsed irradiation by UV-LEDs on inactivation of challenge microorganisms in water compared to that of regular UV irradiation. The novelty of this research lies in the first thorough investigation on the effect of multiple wavelengths and pulsed irradiation by UV-LEDs on water disinfection, which is neither viable for conventional UV lamps nor available yet in previous limited studies for UV-LEDs.

1.2 Thesis layout

This research was conducted through a series of well-designed experimental work to achieve the objectives of this project. The original experimental results, analysis and discussion, along with the related information gathered from the literature, are compiled in this dissertation, with a layout highlighted below:

Chapter 1 presents a general background of this study and a brief sketch of the dissertation layout.

Chapter 2 provides a comprehensive literature review on UV disinfection by various UV sources with the focus on UV-LEDs. Knowledge gaps are identified and research objectives are elaborated.

Chapter 3 describes the overall experimental methodology in detail including experimental apparatus, analytical techniques and data analysis methods.

Chapter 4 presents and discusses the effects of UV-LEDs multiple wavelengths on inactivation of representative microorganisms.

Chapter 5 elaborates the effects and mechanisms of UVA-LEDs pretreatment on UVC-LEDs disinfection of representative microorganisms.

Chapter 6 provides the investigation of UV-LEDs pulsed irradiation on inactivation of representative microorganisms.

Chapter 7 summarizes the overall conclusions, spells out the significance of this study, and provides recommendations for future work.

Chapter 2: Literature review

2.1 UV mercury lamps for disinfection

The effect of UV radiation largely depends on wavelength due to the different energy levels of photons. Thus, the electromagnetic spectrum of UV radiation can be subdivided into different ranges: UVA (315 – 400 nm), UVB (280 – 315 nm) and UVC (200 – 280 nm) (Bolton and Cotton, 2008). Although there is UVA radiation in natural sunlight, UVA is inefficient and impractical for disinfection due to its poor absorption by genetic materials in the cells of microorganisms such as DNA (Sinha and Hader, 2002). Therefore, in practice UV disinfection has to rely on the artificial UV sources emitting UVC and/or UVB radiation.

The most commonly used UV source for disinfection is mercury lamps (Bolton and Cotton, 2008). Low pressure (LP) mercury lamps emit nearly monochromatic UV radiation with the peak wavelength at 254 nm, which is close to DNA absorption peak at around 260 nm (Wurtele et al., 2011). The UV radiation from mercury lamps is strongly absorbed by DNA of microorganisms, producing direct DNA damage by the formation of pyrimidine dimers and making them unable to reproduce (Figure 2.1) (Bolton and Cotton, 2008).

Numerous research on water disinfection by low pressure mercury lamps has demonstrated that UV radiation at 254 nm is effective against most microorganisms including bacteria, bacterial spores, viruses, bacteriophages and protozoan cysts (Hijnen et al., 2006). However, it has been reported that the spectral sensitivity of microorganisms does not necessarily follow the DNA absorbance spectrum (Figure 2.2) and that the germicidal efficiency of UV radiation may vary from microorganism to microorganism (Chen et al., 2009, Mamane-Gravetz et al., 2005). Chen et al. (2009) investigated inactivation action spectrum of *B. subtilis* spores and found two

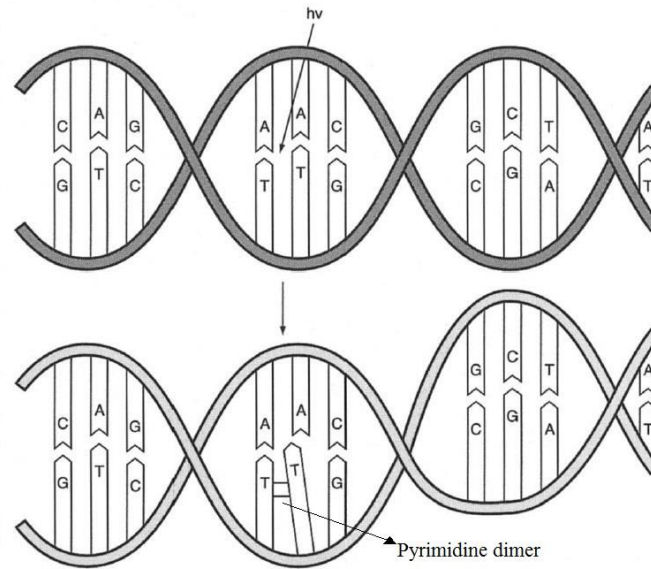


Figure 2.1 Double-stranded DNA chain showing how the formation of pyrimidine dimers disrupts the structure of DNA chain (A = adenine, G = guanine, T = thymine, C = cytosine) (reprinted from Bolton and Cotton, 2008 with permission)

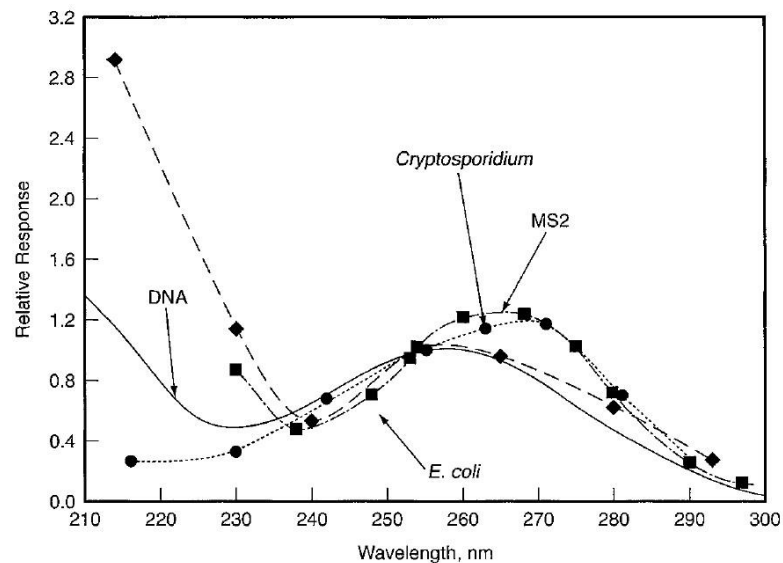


Figure 2.2 Action spectra (relative response versus wavelength) for DNA, MS2, *Cryptosporidium* and *E. coli* (reprinted from Bolton and Cotton, 2008 with permission)

peaks, one below 240 nm and another at around 270 nm. This study also showed inactivation rate constant at 254 nm is similar to that at 279 nm for *B. subtilis* spores inactivation and both of

them are lower than that at 270 nm, which means 254 nm is as effective as 279 nm but both of them are less effective than 270 nm. The studies on UV disinfection for *Cryptosporidium parvum* oocysts and bacteriophage T7 also indicated that 270 nm is more effective than 254 nm for these two microorganisms (Linden et al., 2001, Ronto et al., 1992). Although low pressure mercury lamps are effective for microorganism inactivation, these lamps are only able to produce UV radiation at 254 nm, which is not the most effective for some microorganisms. Unlike UV mercury lamps, UV-LEDs can be designed to emit various wavelengths and offer the possibility to select a particular wavelength targeting a specific pathogen of concern.

Unlike low pressure mercury lamps, medium pressure (MP) mercury lamps emit a polychromatic spectrum with various wavelengths from UVC to UVA and visible light (Figure 2.3) and have much higher output power than low pressure mercury lamps. An MP lamp can carry up to 30 kW while the typical output power of an LP lamp is around 40 W (Bolton and Cotton, 2008). In terms of germicidal UV intensity (typically for UVC range), MP lamps are

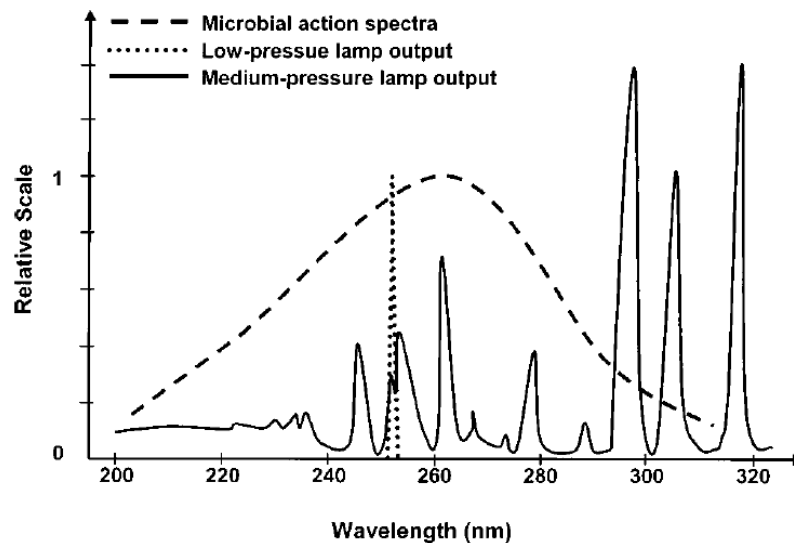


Figure 2.3 Output spectra of low pressure and medium pressure lamps (not to scale) (reprinted from Kuo et al., 2003 with permission)

approximately 15 to 20 times stronger than LP lamps. Therefore, they disinfect faster and have a greater penetration capability compared to LP lamps (USEPA, 1999). It is reported that MP mercury lamps have a higher inactivation effectiveness than LP lamps (Hijnen et al., 2006) and some microorganisms are more sensitive to shorter wavelengths below 240 nm emitted by MP lamps compared to 254 nm output of LP lamps (Figure 2.2). It is believed that the multiple wavelengths from MP lamps can damage not only DNA in the cell, but also other components, like membrane, protein in the microorganisms, which may account for the higher inactivation by MP lamps (Kalisvaart, 2004). Another benefit from MP mercury lamps is that polychromatic UV radiation could help reduce photoreactivation after UV disinfection. It has been demonstrated that some microorganisms like *E. coli* can repair themselves after exposure to LP mercury lamps, but cannot self-repair after exposure to MP mercury lamps (Oguma et al., 2002, Zimmer-Thomas et al., 2007, Zimmer and Slawson, 2002). Therefore, polychromatic UV radiation may play an important role for enhanced microorganism inactivation by MP mercury lamps. On the other hand, the broad polychromatic spectrum from MP mercury lamps is fixed and it cannot be selected and adjusted. So the energy for some wavelengths in the spectrum, which contribute little for inactivation, may be wasted.

2.2 Xenon lamps pulsed irradiation for disinfection

Another UV source to generate polychromatic radiation is xenon lamps. Xenon lamps can produce pulsed radiation instead of continuous radiation from mercury lamps. The pulsed radiation from xenon lamps has a broad spectrum ranging from UV (100 – 400 nm), visible light (400 – 700 nm), to infrared (700 – 1100 nm) (Oms-Oliu et al., 2010). Xenon lamps are mercury-free and non-toxic (Bohrerova et al., 2008). They do not require warm-up time and can emit pulsed radiation with high intensity. In a xenon lamp pulsed radiation generation system,

electrical energy is accumulated in a high power capacitor for a period of time (usually a fraction of a second) and then released to a xenon lamp within a very short time (nanoseconds to milliseconds) to generate pulsed radiation. Therefore, the power of high speed electronic pulses is magnified many times to generate short-duration and high peak energy pulses (Figure 2.4) (Elmnasser et al., 2007). The peak power of pulsed radiation from xenon lamps can be up to 35 MW. As a result, xenon lamps pulsed radiation has much higher emission power and penetration depth than mercury lamps, making it more effective and rapid for microorganism inactivation than continuous UV treatment (Oms-Oliu et al., 2010).

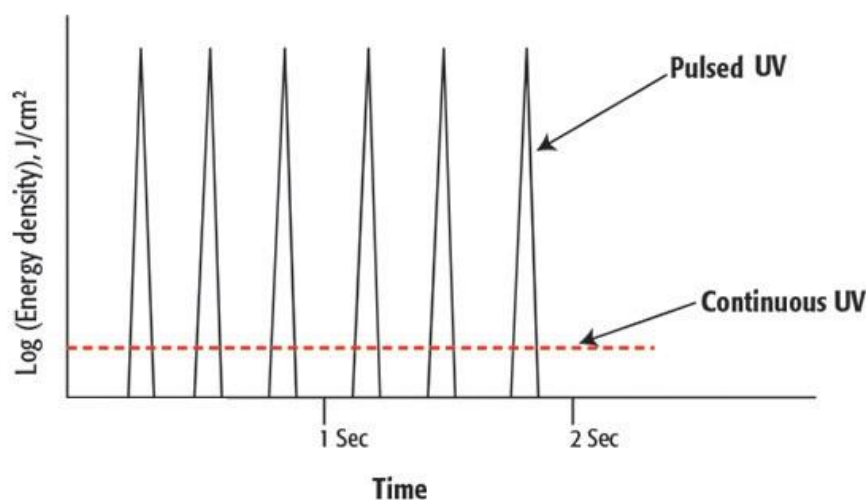


Figure 2.4 Illustration of energy output of continuous and pulsed UV for comparison (reprinted from Keener and Krishnamurthy, 2014 with permission)

The efficiency of xenon lamps pulsed irradiation has been well demonstrated on the inactivation of bacteria, spores and viruses for food decontamination and water disinfection (Bohrerova et al., 2008, Elmnasser et al., 2007, Oms-Oliu et al., 2010). It is reported to be 4 to 6 times faster than continuous UV irradiation for equivalent inactivation levels (Fine and Gervais, 2004). Moreover, with the same UV fluence (i.e. the amount of UV energy), it is approximately

2 times more effective for inactivation of bacterium *E. coli* and virus T4, T7 compared to mercury lamps continuous irradiation (Bohrerova et al., 2008).

2.3 UV-LEDs for disinfection

With the recent emergence of UV-LED as a new UV radiation source, there has been an increasing interest in UV-LEDs water treatment (Jo and Tayade, 2014, Song et al., 2016). However, the research on water disinfection by UV-LEDs is still limited compared to the extensive studies by conventional UV lamps. Due to the substantial differences between conventional mercury lamps and newly emerging UV-LEDs, the established methodologies on water disinfection by mercury lamps, such as experimental protocols, reactor designs, etc., are not expected to directly apply to UV-LEDs. Researchers applied various materials and experimental conditions for UV-LEDs water disinfection, which are thoroughly reviewed as following.

Due to the feature of wavelength diversity, UV-LEDs with different wavelengths in the range of UVA (315 – 400 nm), UVB (280 – 315 nm) and UVC (200 – 280 nm) have been applied for microorganism inactivation studies. Hamamoto et al. (2007) and Mori et al. (2007) applied UVA-LEDs at 365 nm for *E. coli* inactivation. The former research achieved 5.7 log inactivation at 315000 mJ/cm² UV fluence and the latter provided 3.9 log inactivation at 54000 mJ/cm² UV fluence. The UV fluence required by 365 nm UVA-LEDs are very high considering that typically the UV fluence required by 254 nm mercury lamps for 4 log *E. coli* inactivation is only around 8 mJ/cm² (Bolton and Cotton, 2008). With the help of TiO₂, Xiong and Hu (2013) established a photocatalytic disinfection system by UV-LEDs at 365 nm and the results still showed quite high UV fluence, 688 mJ/cm², for 3 log *E. coli* inactivation. These results

demonstrated that UVA-LED is not effective for microorganism inactivation, which is in agreement with the fact that UVA radiation is poorly absorbed by DNA of microorganisms.

Oguma et al. (2013) applied UVB-LEDs at 310 nm on *E. coli* inactivation and reported 0.6 log inactivation by a UV fluence of 56.9 mJ/cm², which is much lower than that required by 365 nm UVA-LEDs. Nonetheless, this is still far greater than the fluence required by 254 nm mercury lamps on *E. coli* inactivation. Therefore, UVB-LED is also not highly effective for microorganism inactivation.

Aoyagi et al. (2011) selected UVC-LEDs at 255 nm and 280 nm to study the inactivation effects on bacteriophages ϕ X174, Q β and MS2. The results indicated that UVC-LEDs at 255 nm is more effective than 280 nm for the inactivation of these bacteriophages and that the disinfection efficiency depends on the types of microorganisms and UV-LEDs wavelengths.

Another study on UVC-LEDs with 255 nm and 275 nm was reported from Bowker et al. (2011) for the inactivation of three microorganisms MS2, T7 and *E. coli*. The results showed that at a given UV fluence 275 nm UV-LEDs produced higher inactivation on T7 and *E. coli* than 255 nm UV-LEDs while they induced almost identical MS2 inactivation. These results do not seem to well follow the theory that wavelengths closer to DNA absorption peak at 260 nm are supposed to have higher inactivation effectiveness. This inconsistency indicated that spectral sensitivity of microorganisms may vary.

Since the wavelength of UV-LEDs can be customized, polychromatic radiation can be easily achieved by combination of UV-LEDs with selected wavelengths, which provides an opportunity to construct the potentially optimal spectrum for more effective inactivation of target microorganisms. Chevremont et al. (2012a) studied the inactivation effect of coupled UVA- and UVC-LEDs on mesophilic bacteria in wastewater. The UVA-LEDs alone at 365 nm and 405 nm

were less effective than UVC-LEDs alone at 254 nm and 280 nm. However, when combining UVA- and UVC-LEDs, the bacteria concentration sharply decreased after irradiation by 254/365 nm, 280/365 nm, 254/405 nm or 280/405 nm, indicating the combinations of UVA- and UVC-LEDs are more efficient than UVA-LEDs alone. Moreover, in terms of log inactivation, it was found that the combination of 280 nm and 365 nm provided higher log inactivation than the sum of each wavelength applied alone (i.e. $3.5 > 1.4 + 0.3 = 1.7$). The other three combinations showed similar phenomena: 254/365 nm ($2.4 > 0.8 + 0.3 = 1.1$), 254/405 nm ($2.2 > 0.8 + 0.3 = 1.1$) and 280/405 nm ($3.5 > 1.4 + 0.3 = 1.7$). This synergistic effect from the wavelength combinations was also reported by Nakahashi et al. (2014) which combined 254 nm mercury lamps and 365 nm UV-LEDs for *Vibrio parahaemolyticus* inactivation.

Contrary to the above, Oguma et al. (2013) combined 265 nm, 280 nm and 310 nm UV-LEDs for *E. coli* inactivation and did not observe the synergistic effect. The authors found combined wavelengths were less effective than each wavelength applied separately. They argued that the observed inefficient inactivation might have resulted from different indicator microorganisms and wavelength combinations as well as an inefficient thermal management of the UV-LEDs setup (Oguma et al., 2013). Despite these contrary findings, these studies suggest that combination of selected wavelengths might be a promising way to improve the disinfection efficiency of UV-LEDs, but more studies are needed as the experimental setup and conditions may have a determining factor.

The semiconductor structure of UV-LEDs enables them to respond electricity instantaneously. Thus pulsed radiation can be easily produced by connecting a pulse generator to UV-LEDs and applying pulse voltage to quickly turn on and off UV-LEDs. This special feature of UV-LEDs also allows to adjust the pulse parameters to obtain various pulse patterns, such as

different frequencies (how many on-off cycles in a second) and duty rates (the percentage of irradiation time in the total time of a cycle). Therefore, some studies applied the concept of pulsed irradiation from xenon lamps to UV-LEDs for disinfection. Wengraitis et al. (2013) applied pulsed UVC radiation by UV-LEDs at 272 nm for *E. coli* inactivation on the surface of agar plates and found *E. coli* sensitivity to 272 nm pulsed irradiation is up to 3.8 times higher than continuous irradiation. The pulse parameter for best inactivation was found to be 1 Hz frequency and 10% duty rate. Another study on UV-LEDs pulsed irradiation inactivation was reported by Li et al. (2010), which utilized 365 nm UVA-LEDs pulsed irradiation for inactivation of *Candida albicans* and *E. coli* biofilms. Their results showed the germicidal efficiency of 5-min exposure in pulse mode on *C. albicans* and *E. coli* biofilms was 6.34 and 2.53 times higher than that in continuous mode, respectively, indicating significantly greater germicidal ability by UV-LEDs pulsed irradiation than continuous irradiation. The highest inactivation for pulsed irradiation was found at 100 Hz frequency and 75% duty rate (Li et al., 2010). However, these two studies applied UV-LEDs pulsed irradiation to microorganisms on agar plates and biofilms instead of water disinfection. A recent study on water disinfection reported that 269 nm UV-LEDs pulsed irradiation at 9.1 Hz frequency and 9.1% duty rate was 1.8 times more efficient than continuous irradiation for inactivation of *Bacillus globigii* spores (Tran et al., 2014). In contrast, another study on water disinfection observed comparable performance between pulsed and continuous irradiation by 405 nm LEDs on *Staphylococcus aureus* inactivation for various pulse patterns (Gillespie et al., 2017). So far, there has been very limited research on UV-LEDs pulsed irradiation for water disinfection and the current few studies are inconclusive. Therefore, it is necessary to have a comprehensive study on the effect

of UV-LEDs pulsed irradiation on water disinfection and to explore the optimal parameters for potentially enhanced microorganism inactivation.

2.4 Mechanisms of UV disinfection

Many studies have investigated and discussed the mechanism of microorganisms inactivation by UV radiation, and various mechanisms have been proposed. It is well known that the basic mechanism is the impact of UV radiation on genetic materials such as DNA in cells, which depends on the wavelengths range of UV radiation such as UVC, UVB or UVA. UVC radiation has been proven to have a strong germicidal effect by acting directly on the DNA of microorganisms, leading to the formation of pyrimidine dimers and preventing them from reproducing without intermediate steps (Figure 2.1) (Chatterley and Linden, 2010, Chevremont et al., 2012a, Chevremont et al., 2012b, Hamamoto et al., 2007). Because DNA mainly absorbs UV radiation from 200 to 300 nm with an absorbance peak around 260 nm (Figure 2.2) (Wurtele et al., 2011), UVC radiation, especially those with the wavelengths around 260 nm, are the most efficient for microorganism inactivation. However, some of the direct damages to DNA are repairable by DNA-repair mechanisms, such as photoreactivation and dark repair (Oguma et al., 2001, Oguma et al., 2013, Sanz et al., 2007, Sinha and Hader, 2002). Since DNA repair is undesirable for microorganism inactivation, it is necessary to weaken or prevent the repair. DNA repair might be prevented by damaging the repair enzymes, which are proposed to be more vulnerable to high UV intensities (Sommer et al., 1998). Moreover, the absorption spectrum of proteins has a peak around 280 nm due to the different structures from DNA, which might help damage repair enzymes and prevent DNA repair (Kalisvaart, 2004).

Similar to UVC radiation, UVB can also induce direct DNA damage such as pyrimidine dimers, but in a less extent compared to those by UVC radiation due to the lower absorption by

DNA than UVC (Figure 2.2) (Gayan et al., 2014). Thus UVB is generally less effective than UVC for microorganisms inactivation. However, proteins typically have a relative absorption peak in UVB range at around 280 nm, which may have an impact on the inactivation of some microorganisms (Jagger, 1967). It is proposed that proteins damage by UVB radiation may enhance the inactivation of some viruses, such as adenovirus, which contain a high content of proteins (Beck et al., 2017, Oguma et al., 2016).

UVA radiation is poorly absorbed by DNA and is less efficient at inducing damage on DNA (Sinha and Hader, 2002). The absorption of UVA radiation and formation of pyrimidine dimers on DNA is about 10^5 times less efficient than that by UVC radiation (Cortat et al., 2013, Gayan et al., 2014). However, it still has the ability to inactivate microorganisms (Kalisvaart, 2004). The inactivation mechanism of UVA radiation has not been studied as widely as that of UVC radiation because the frequently used UV mercury lamps can only emit UVC radiation at 254 nm. The main mechanism of UVA inactivation involves an indirect effect by reactive intermediates and oxidative damage to DNA and other cellular components (Chatterley and Linden, 2010, Chevremont et al., 2012a, Chevremont et al., 2012b, Hamamoto et al., 2007, Hwang et al., 2013). The reactive intermediates are proposed to be reactive oxygen species (ROS), which are created by UVA radiation via photooxidation of oxygen (Cadet et al., 2015, Hoerter et al., 2005). Studies showed that addition of mannitol and catalase significantly protected microorganisms from UVA radiation by scavenging hydroxyl radicals ($\bullet\text{OH}$) and hydrogen peroxide (H_2O_2), respectively. Therefore, hydroxyl radicals and hydrogen peroxide are believed to be the major reactive oxygen species involved in UVA disinfection (Hamamoto et al., 2007, Li et al., 2010). These reactive intermediates induce oxidative damage to DNA, proteins, and cell membranes and cause growth delay (Eisenstark, 1987, Oppezzo and Pizarro,

2001, Pizarro, 1995, Pizarro and Orce, 1988, Ramabhadran and Jagger, 1976, Sinha and Hader, 2002). This process takes more time than the direct damage produced by UVC radiation (Chatterley and Linden, 2010). Although indirect damage by UVA radiation is less efficient than the direct damage by UVC radiation for microorganisms inactivation, the damage by UVA is believed to be irreparable, whereas the damage by UVC is reparable through DNA-repair mechanisms (Oguma et al., 2013, Xiong and Hu, 2013). UV damage by low-pressure mercury lamps, which emit UVC radiation at 254 nm, can be repaired relatively easily, but UV damage induced by medium-pressure mercury lamps, which produce UVC and UVA radiation together, is difficult to repair (Oguma et al., 2002, Zimmer and Slawson, 2002). Therefore, the prevention of microorganisms self-repair would be an advantage of UVA radiation for microorganisms inactivation. Furthermore, UVA radiation has higher penetrability and can penetrate further into the solution for a better disinfection of turbid water and wastewater (Chevremont et al., 2012a, Mori et al., 2007).

UVA radiation alone is not efficient for disinfection, but UVA radiation coupled with photocatalysts such as TiO_2 could efficiently produce reactive oxygen species for microorganism inactivation (Marugan et al., 2010). Because UVA sources such as UVA lamps and UVA-LEDs usually have higher output power than UVC lamps and UVC-LEDs, respectively, they are desirable for photocatalytic disinfection with photocatalysts. An interesting phenomenon called “residual disinfecting effect” was reported, in which further inactivation of *E. coli* was observed after a photocatalytic process using a combination of UVA radiation and TiO_2 (Xiong and Hu, 2013). The mechanism for residual disinfecting effect is proposed to be the cumulative damage of cellular components by reactive oxygen species or stable oxidants, such as H_2O_2 , which could

prevent the reproduction of damaged microorganisms (Pablos et al., 2013, Rincon and Pulgarin, 2004, 2007, Shang et al., 2009).

Many studies have been conducted on microorganism inactivation mechanisms using different wavelengths, such as UVC or UVA, with a focus on the effect on DNA damage. However, there is little information in the literature on DNA damage and inactivation mechanisms using a combination of different UV wavelengths (Nakahashi et al., 2014). Since a few studies have reported the synergistic effect of combining particular wavelengths (Chevremont et al., 2012a, Nakahashi et al., 2014), it is essential to identify the mechanisms. Chevremont et al. (2012a) argued that coupled wavelengths combined two UV properties: UVC induces direct damage on DNA, but such DNA damage can be repaired by enzyme photolyase, whereas the oxidative damage to bacterial membranes by UVA cannot be repaired. The research on an oxidative DNA product, 8-hydroxy-2'-deoxyguanosine (8-OHdG), which was induced by UVA alone, and a thymine dimer, cyclobutane pyrimidine dimers (CPDs), which was induced by UVC alone, suggested that the combination of UVA and UVC suppressed one or more recovery systems for DNA damage, such as CPDs, and oxidative stress from UVA may play a key role in this synergistic effect (Nakahashi et al., 2014). It is proposed that the coupled wavelengths of UVA and UVC may also reduce reactivation after exposure due to the combined effects of two types of UV wavelengths (Chevremont et al., 2012a).

The mechanisms of pulsed UV irradiation by xenon lamps with a high energy output and a broad spectrum have been widely studied for microorganisms inactivation and food decontamination. Yet, the mechanisms are still not well understood, and there is little research on pulsed irradiation by UV-LEDs. Pulsed UV radiation from xenon lamps has more instantaneous energy than continuous UV radiation from mercury lamps (Li et al., 2010), and additional

inactivation mechanisms have been proposed, including photochemical, photothermal, and photophysical effects (Elmnasser et al., 2007). Firstly, in addition to DNA damage by UV, it is believed that pulsed UV treatment can prevent DNA repair due to inactivation of the DNA-repair system and other enzymatic functions (Elmnasser et al., 2007). Secondly, the pulsed UV with more instantaneous energy may lead to localized overheating and membrane destruction (Krishnamurthy et al., 2007). Thirdly, the constant and repeated high intensity pulses might induce cell structure damage such as cell wall rupture, membrane damage, and cellular content leakage (Krishnamurthy et al., 2010). As a result of these additional effects, pulsed UV irradiation is reported to be 4 to 6 times faster than continuous UV irradiation for equivalent inactivation levels (Fine and Gervais, 2004). These proposed mechanisms are mainly based on studies of xenon lamps pulsed UV irradiation with a high energy output and a broad spectrum. Due to the different pulses generated by xenon lamps and UV-LEDs, the applicability of these mechanisms for UV-LEDs pulsed irradiation still needs further examination.

2.5 Knowledge gaps

Based on the literature review above, MP mercury lamps can provide polychromatic radiation for enhanced inactivation. However, within the very broad range of wavelengths in their fixed spectrum, it is difficult to identify and distinguish which wavelengths result in the additional effects and mechanisms. The newly emerging UV-LEDs provide great flexibility for wavelength combinations due to their unique feature of wavelength diversity. But how to construct the wavelength combinations for optimal inactivation remains unknown. There are very few studies so far on UV-LEDs wavelengths combinations, and their observations are not consistent with each other and thus not conclusive as reviewed above. Therefore, it is of great interest to conduct a comprehensive study on how to utilize the wavelength diversity of UV-

LEDs as a new opportunity and approach to tailor wavelength combinations for optimal inactivation, and to identify the additional mechanism of a particular combination.

The enhanced germicidal effect of xenon lamps pulsed irradiation has been well demonstrated by studies for food decontamination and water disinfection. However, pulses generated by xenon lamps are quite different from those of UV-LEDs in terms of spectrum, intensity, frequency, and duty rate. Thus, the direct applicability of the findings of xenon lamps pulsed irradiation to UV-LEDs pulsed irradiation is not expected. The very limited research on UV-LEDs pulsed irradiation presented inconsistent results and the effect of UV-LEDs pulsed irradiation on water disinfection is still inconclusive. Therefore, it is of considerable importance to perform a comprehensive study on UV-LEDs pulsed irradiation in order to examine the potentially enhanced germicidal effect, to investigate the optimal conditions, as well as to explore the additional mechanisms of inactivation.

In summary, the research on application of UV-LEDs for water disinfection is very limited currently, especially on the effects of multiple wavelengths and pulsed irradiation by UV-LEDs, which could potentially improve the inactivation of microorganisms. Considering that the special features of UV-LEDs as small-point UV sources with adjustable radiation patterns provide great flexibility for novel reactor designs and potential new applications, research efforts to fill the knowledge gaps as discussed above are of immense significance to take full advantage of these features such as wavelength diversity and pulsed irradiation for application of UV-LEDs.

2.6 Research questions

Based on the literature review and the knowledge gaps, the research questions can be stated as below:

(1) Since polychromatic UV radiation from MP mercury lamps can improve inactivation effectiveness and reduce reactivation potential compared to monochromatic LP mercury lamps, can multiple wavelengths from UV-LEDs have the similar effect? If yes, is there an optimal combination of selected wavelengths by UV-LEDs for most effective water disinfection?

(2) Since pulsed irradiation by xenon lamps can achieve more effective inactivation compared to continuous UV irradiation by mercury lamps, can pulsed irradiation by UV-LEDs have the same capability? If yes, is there an optimal pulse pattern by UV-LEDs for most effective inactivation?

(3) If multiple wavelengths and pulsed irradiation by UV-LED are found to have some additional effects as assumed in questions (1) and (2), are the mechanisms for these additional effects the same as MP mercury lamps and xenon lamps? If no, how to interpret?

2.7 Thesis objectives and scope

Based on the literature review, knowledge gaps and research questions, this project focuses on the application of two unique features of UV-LEDs, wavelength diversity and pulsed irradiation, for the inactivation of microorganisms in water. The main objective of this research is to investigate the effect of multiple wavelengths and pulsed irradiation by UV-LEDs on water disinfection, to understand the mechanism of the potentially enhanced inactivation and to explore the potential to capitalize them for improved inactivation by taking several UV-LEDs with different wavelengths and several typical microorganisms as representatives. The overall objective will be achieved through the following sub-objectives:

- Investigate the effect of multiple wavelengths by UV-LEDs with various combinations on the inactivation of representative microorganisms in water.

- Examine the effect of pulsed irradiation by UV-LEDs with various pulse patterns on the inactivation of representative microorganisms in water.
- Explore to understand the mechanism of the potentially additional inactivation effects from multiple wavelengths and pulsed irradiation by UV-LEDs provided the additional effects do exist and are discovered through the above two sub-objectives.

The scope of this work will be within the selected UV-LEDs wavelengths (265, 285, 365 nm) covering from UVC, UVB, to UVA, representative microorganisms (*E. coli*, MS2), typical wavelength combination manners (simultaneous, sequential), various pulse patterns (0.1, 1, 10, 100, 1k Hz frequency and 10%, 25%, 50%, 75%, 90% duty rate), which will be described in detail in the following chapter.

For the first sub-objective, the inactivation effect will be investigated under different conditions including various UV-LEDs wavelengths, different combinations and microorganism types. Then, results will be compared with the effect of single wavelength exposure and between different combination conditions and indicator microorganisms. Then, the effect of multiple wavelengths will be analyzed and identified based on these comparisons.

For the second sub-objective, various pulse patterns from UV-LEDs will be applied to examine the inactivation effect on the representative microorganisms. The continuous irradiation will be also applied as a reference in order to differentiate the role of pulsation. Then, the comparisons will be made between the effect of continuous and pulsed irradiation, and among different pulse patterns (frequency and duty rate) on inactivation of microorganisms for analyzing the effect of pulsed irradiation by UV-LEDs.

As to the third sub-objective, once additional or unusual effects on microorganisms inactivation are observed from UV-LEDs multiple wavelengths and pulsed irradiation through

the above two sub-objectives, further experiments will be performed accordingly to interpret those phenomena and to explore the mechanism of those additional effects. Then, the mechanism for those effects will be proposed and discussed based on the original experimental work in this study in conjunction with the established fundamental theories from literature.

Chapter 3: Experimental methodology

This chapter describes the overall experimental methodology, including experimental apparatus, materials, procedures, analytical techniques and data analysis methods, to fulfill the objectives of this research. Specific experimental designs and work for each sub-objective will be presented as part of corresponding chapters respectively (Chapters 4 to 6).

3.1 Experimental apparatus

In order to investigate the effect of multiple wavelengths by UV-LEDs on water disinfection, an experimental apparatus is designed and built, as shown in Figure 3.1. Two UV-LEDs with different wavelengths are located above a 9-cm diameter glass Petri dish with a 2-cm distance between water surface and UV-LEDs. The viewing angles of UV-LEDs are around $110^\circ \sim 130^\circ$ and the distance between the two UV-LEDs is 2 cm, so that the emitted UV radiation can cover the entire water surface. The two UV-LEDs are connected to two DC power supplies (Model: Aim TTI EX355R) separately so that they can be controlled independently to achieve

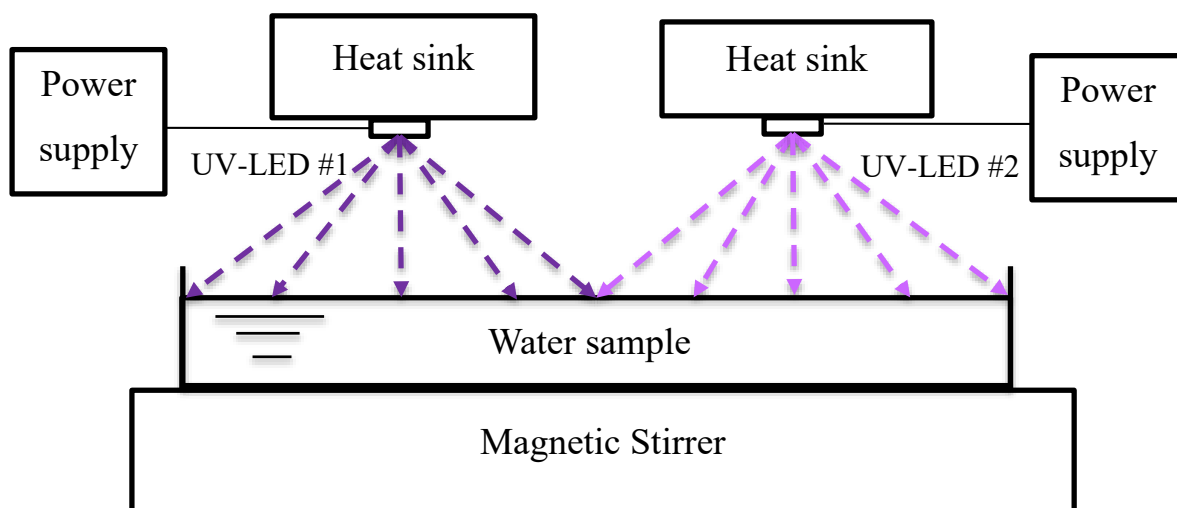


Figure 3.1 Schematic diagram of experimental apparatus for UV-LEDs inactivation (not to scale)

different combinations such as simultaneous or sequential exposure of two different wavelengths. Two aluminum-based heat sinks are used for heat dissipation of the UV-LEDs individually, as thermal management is critical to ensure the performance of UV-LEDs (Kheyrandish et al., 2017). During inactivation experiment, a 50-mL water sample containing microorganism cultures is placed in the glass Petri dish for UV exposure. A magnetic stirrer is used to homogenize the water sample during exposure for uniform irradiation. The whole apparatus is covered by a black box during experiment to avoid potential photoreactivation by ambient light.

3.2 Selection of UV-LEDs

Since this research focuses on the inactivation effectiveness of UV-LEDs with multiple wavelengths, the wavelengths in the experiments should cover a wide UV range such as UVA, UVB, and UVC. Based on the literature and commercial availability, several wavelengths of UV-LEDs are selected as follows:

- 1) 265 nm: representative for UVC, very close to DNA absorption peak, which is expected to be most effective for the inactivation of most microorganisms. It is the shortest wavelength for UV-LEDs commercially available in the market when this research was initiated.
- 2) 285 nm: represents UVB, the recently developed 285 nm UVB-LEDs have higher output power than UVC-LEDs.
- 3) 365 nm: represents UVA, mostly used in early studies on UV-LEDs water disinfection and photocatalysis. UVA-LEDs have been widely available in the market and have much higher output power and lower price compared to UVC-LEDs.

Based on these considerations, several UV-LEDs were selected for the experiments in this research. Their specifications are shown in Table 3.1. Various combinations were conducted

among these UV-LEDs such as UVC+UVA, UVC+UVB and UVB+UVA for the experiments. The single wavelength exposure by each UV-LED was also performed as control. During UV irradiation, the constant current was applied to each UV-LED at its maximum current for maximum output (Table 3.1).

Table 3.1 Specifications for UV-LEDs used in this research

UV Range	Wavelength (nm)	Voltage (V)	Current (mA)	Output Power (mW)	Viewing angle	Manufacturer
UVC	265	7.8	350	10	130 °	Nikkiso Co., Ltd, Japan
UVB	285	6.1	350	30	130 °	Nikkiso Co., Ltd, Japan
UVA	365	8.0	1000	2350	116 °	Seoul Viosys Co., Ltd, South Korea

3.3 UV radiation measurement

For a specific microorganism, inactivation effectiveness depends on the amount of UV radiation that is delivered to the microorganism in water sample (i.e. UV fluence), so it is essential to determine UV fluence during UV disinfection experiment. For conventional UV mercury lamps, a standard protocol using collimated beam apparatus has been well established during the past decades. The incident fluence rate at the surface of the water sample can be measured by a radiometer. Then the UV fluence delivered to microorganisms in water can be calculated as the product of fluence rate and exposure time with some necessary corrections (Bolton and Linden, 2003). However, due to substantial differences between conventional mercury lamps and newly emerging UV-LEDs, the collimated beam apparatus is not applicable for UV-LEDs to determine UV fluence (Song et al., 2016).

Another widely accepted method for UV fluence determination is chemical actinometry, which is based on known photochemical reactions induced by UV radiation (Kuhn et al., 2004). In the standard protocol on UV mercury lamps using collimated beam apparatus, chemical actinometry plays an important role on calibration of the radiometer detector and validation of the UV fluence measurement. In this research, based on the wavelengths of UV-LEDs, potassium iodide actinometry and ferrioxalate actinometry are used to determine the UV fluence delivered to the water surface over a period of irradiation. The protocol for potassium iodide and ferrioxalate actinometry has been well established, and the detailed procedure and quantum yield data at different wavelengths are followed from literature (Bolton et al., 2011, Goldstein and Rabani, 2008, Jagger, 1967, Rahn et al., 2006, Rahn et al., 2003). Then the UV fluence on the water surface is corrected by the water factor of actual water samples containing microorganisms to determine the UV fluence delivered to microorganisms suspension. The water factor is a factor for UV fluence correction which accounts for the decrease in UV intensity along the path that UV radiation passes through the water. The water factor is determined using the same method as that of UV lamps protocol since it is regardless of the types of UV sources (Bolton and Linden, 2003).

Note that to date, there is no standard protocol yet to accurately determine the absolute UV fluence delivered by UV-LEDs to a microorganism suspension (Song et al., 2016), so currently it is impractical to validate the UV fluence determination from chemical actinometry for UV-LEDs study. This issue has been recognized by researchers and industry leaders in the field of UV-LEDs, and recently the International Ultraviolet Association (IUVA) has announced an initiative to develop a standard protocol for UV-LEDs (IUVA, 2015). A recent study on UV-LEDs water disinfection adapted part of UV lamps protocol to correct the UV-LEDs fluence results from

chemical actinometry (Oguma et al., 2016), which demonstrates that chemical actinometry can be well used for current UV-LEDs studies with some corrections. However, whether the correction method in their study is well adaptable and widely acceptable still needs further careful investigation. And also, another two PhD projects in our group are currently ongoing with the target at solving this issue by experimental measurement and computer simulation, respectively. Therefore, in this research, all the conditions related to UV fluence determination, including experimental apparatus dimension, UV-LEDs specifications and water quality, are recorded and reported along with the results from chemical actinometry. All these data can ensure that the reported results are consistent and repeatable. Moreover, all the tests are conducted with the same apparatus and experimental conditions, with the only difference being that UV exposure is in single wavelength or multiple wavelengths, in continuous mode or pulsed mode. So that the same UV fluence results by actinometry can ensure the equivalent UV fluence delivered to microorganisms suspension, thus enable a solid comparison of inactivation effectiveness under different irradiation modes to identify the effects of multiple wavelengths and pulsed irradiation compared to single wavelength and continuous irradiation, respectively.

3.4 Microorganism cultivation and enumeration

Based on the literature, the most commonly used challenge microorganisms include *E. coli*, MS2, which are the representatives of bacteria and viruses, respectively, and are considered to be the main indicators of water quality and water disinfection effectiveness. *E. coli* is a typical bacterium usually as the fecal indicator in water. *E. coli* is susceptible to UV radiation and widely studied in water disinfection. MS2 is a typical bacteriophage which is more resistant to UV radiation compared to *E. coli*, thus typically used as a model microorganism for the assessment of Reduction Equivalent Fluence (REF) for validation testing of UV reactors in

North America (Mamane-Gravetz et al., 2005). Moreover, it is reported that some environmental bacteria may have different UV resistance compared to lab-grown pure strains. So it is necessary to test bacteria in wastewater such as total coliform. Therefore, in this research, pure *E. coli* and MS2 in lab buffered water, as well as total coliform and *E. coli* in wastewater were used as the challenge microorganisms to perform inactivation tests.

E. coli (ATCC 11229), MS2 (ATCC 15597-B1) and its host (*E. coli* ATCC 15597) were obtained from American Type Culture Collection (ATCC, Manassas, VA, USA) and cultivated by following the supplier's product data sheet. Agar plate method was used for microorganisms assay and colonies enumeration before and after UV exposure. The detailed procedures for microorganisms cultivation and enumeration in this project are adapted from literature (Adams, 1959, Bowker et al., 2011, USEPA, 2006) and illustrated in Appendix A.

Wastewater samples were obtained from the wastewater treatment pilot plant located at the University of British Columbia (UBC), Vancouver, Canada. The secondary effluent from activated sludge reactor was collected and filtered through 11 µm filter paper (Whatman, #1) to remove particles from wastewater. *E. coli* and total coliform in wastewater samples were assayed using Colilert Test Kit (IDEXX Laboratories, Inc., ME, USA) and the Most Probable Number (MPN) for each sample were determined by following Standard Methods for the Examination of Water and Wastewater (APHA et al., 2012).

3.5 UV exposure and data analysis

For each experimental condition of UV exposure, such as by single wavelength or multiple wavelengths, in continuous mode or pulsed mode, 50 mL microorganism suspension was placed in the glass Petri dish and exposed to UV radiation while stirring. Before and after UV exposure, the samples were taken to determine the concentration of microorganisms. The whole

experimental work including UV exposure and samples assays were conducted in a dark room with minimal red light in order to prevent the influence of potential photoreactivation from ambient light. The control was conducted in the same procedure without turning on the UV-LEDs. The test for each experimental condition was conducted independently three times with three measurement replicates for each sample.

In order to evaluate the inactivation effectiveness, the log inactivation of microorganisms is determined in this research. Concentration of microorganism in the water sample before UV irradiation is measured as the initial concentration, N_0 , while N_t is the concentration after exposure time t with UV irradiation. Then the ratio of N_0 to N_t is transformed to logarithmic form (USEPA, 2006):

$$\text{Log inactivation} = \text{Log}_{10} \frac{N_0}{N_t}$$

and then reported along with the corresponding UV fluence (mJ/cm^2), which indicates how many orders of magnitude of microorganism is inactivated under a certain UV fluence.

The log inactivation under different irradiation modes, such as by single wavelength or multiple wavelengths, in continuous mode or pulsed mode, are compared to determine the potential additional or unusual effects. The statistical analysis is conducted using a two-tailed paired t-test to determine the significance ($p < 0.05$).

Chapter 4: Microorganisms inactivation by UV-LEDs multiple wavelengths

4.1 Introduction

The microorganisms inactivation efficiency by UV radiation depends on wavelengths of UV due to the different energy levels of photons and their interaction with microorganisms cells, as reviewed in Chapter 2. The relative efficiency of UV radiation at different wavelengths in inactivating microorganisms (i.e. action spectrum) have been studied in the past decades and the action spectra for many microorganisms have been well established (Beck et al., 2014, Beck et al., 2015, Gates, 1930, Linden et al., 2001, Mamane-Gravetz et al., 2005). One of the special features of newly emerging UV-LEDs is wavelength diversity, which not only provides the chance to select a particular wavelength for most efficient inactivation of a specific microorganism, but also offers a unique opportunity to selectively combine multiple wavelengths for tailored polychromatic radiation.

Since the action spectra of microorganisms have been previously established for UV radiation at different wavelengths, they can be used as a guideline for UV-LEDs to select the optimal wavelength targeting the pathogen of interest. On the other hand, there is little research on how to combine different wavelengths and tailor the wavelength combinations for potentially improved inactivation or additional effect on microorganisms. Many studies on polychromatic UV from medium pressure mercury lamps have reported enhanced inactivation and reduced reactivation on some microorganisms, but the mechanism is still not well understood due to the fixed broad spectrum of these lamps. Therefore, in this chapter, the special feature of UV-LEDs is utilized to create various wavelength combinations and investigate the effect of multiple

wavelengths on microorganisms inactivation, as well as explore the potentially synergistic effect from wavelength combinations.

4.2 Experimental design

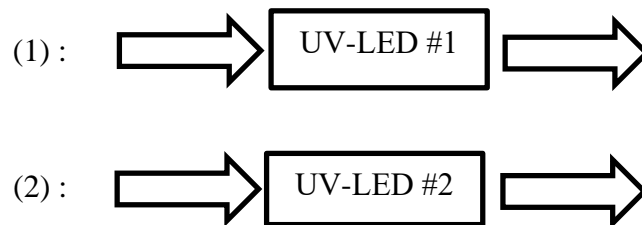
In order to investigate the effect of multiple wavelengths on microorganisms inactivation, various combinations were created by UV-LEDs including different wavelengths combinations and exposure modes. The selected UV-LEDs with different wavelengths (Table 3.1) were coupled, such as 265 + 285 nm, 265 + 365 nm and 285 + 365 nm (illustrated by UV-LED #1 + UV-LED #2 in Figure 4.1), to represent various combinations among UVA, UVB and UVC. Since UV radiation in different wavelength ranges may have different effects on microorganisms, the exposure sequence in wavelength combinations may also impact the inactivation effectiveness. Therefore, different exposure modes including simultaneous exposure and sequential exposure were performed as illustrated in Figure 4.1. For simultaneous exposure, two UV-LEDs with different wavelengths were turned on at the same time to irradiate the microorganism suspension. As to sequential exposure, one UV-LED was turned on firstly for a period of irradiation, and then turned off while the other UV-LED at a different wavelength was turned on for another period of irradiation. The results from various wavelength combinations were compared with single wavelength exposure by each UV-LED separately to analyze the impact of multiple wavelengths on inactivation effectiveness, and explore the potentially additional effect on microorganisms from multiple wavelengths compared to single wavelength exposure separately. Depending on different microorganisms, the UV exposure time for *E. coli* was 40 seconds while that for MS2 was 3 minutes.

Various wavelength combinations:

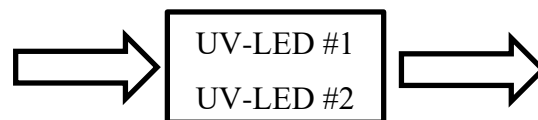
- 265 nm UVC + 285 nm UVB
- 285 nm UVB + 365 nm UVA
- 265 nm UVC + 365 nm UVA

For each wavelength combination above, the following exposure modes were performed (UV-LED #1 and UV-LED #2 represent the two different wavelengths in each combination above):

- Single wavelength exposure:



- Simultaneous exposure of two wavelengths:



- Sequential exposure of two wavelengths:

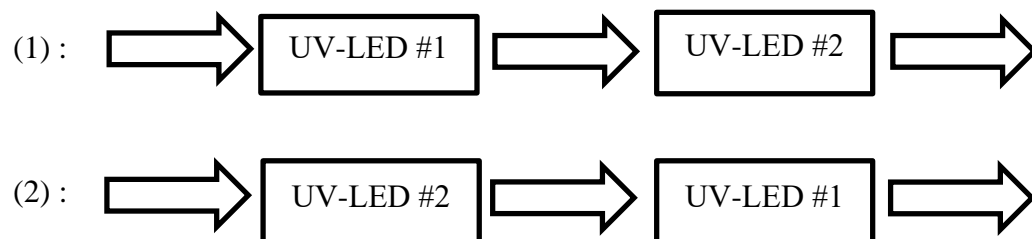


Figure 4.1 Flow chart to illustrate UV-LEDs multiple wavelengths exposure.

4.3 Results and discussion

4.3.1 Combinations of UVC- and UVB-LEDs on *E. coli* inactivation

265 nm and 285 nm UV-LEDs were combined to represent UVC and UVB radiation for the investigation of *E. coli* inactivation in water. The comparison of single wavelengths exposure and multiple wavelengths simultaneous exposure are shown in Figure 4.2. 40 seconds 265 nm UVC-LED exposure with the UV fluence of 4.2 mJ/cm² resulted in 1.8 log inactivation of *E. coli*, while 40 seconds 285 nm UVB-LED exposure with the UV fluence of 15.3 mJ/cm² achieved 2.8 log inactivation of *E. coli*. When combining together, 40 seconds simultaneous exposure of these two UV-LEDs resulted in 4.6 log inactivation, which is statistically comparable with the addition of log inactivation by each wavelength applied alone (i.e. 1.8 + 2.8 = 4.6).

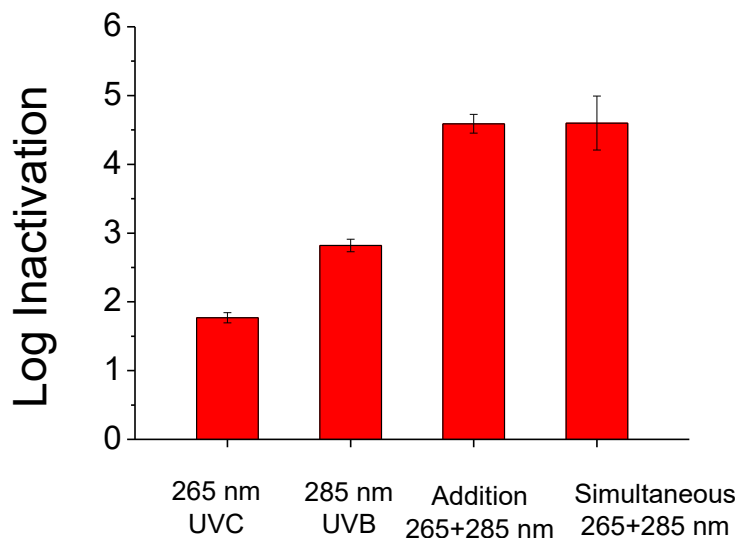


Figure 4.2 *E. coli* inactivation by 40 s 265 nm UVC-LED, 40 s 285 nm UVB-LED and simultaneous 40 s UVC/UVB-LEDs. Addition 265+285 nm represents the sum of log inactivation by 265 nm alone (i.e. the first column) and 285 nm alone (i.e. the second column). Error bars represent the standard deviation for triplicate runs.

The *E. coli* concentration changes under sequential exposure of these two wavelengths are shown in Figure 4.3. The first 40 seconds 265 nm UVC-LED exposure (4.2 mJ/cm^2) reduced *E. coli* concentration by 1.8 log, then the following 40 seconds 285 nm UVB-LED exposure (15.3 mJ/cm^2) further decreased *E. coli* concentration by 2.8 log, resulting in a total 4.6 log inactivation by the whole process of sequential exposure (Figure 4.3(a)). When reversing the sequence, as Figure 4.3(b) shows, *E. coli* concentration dropped by 2.8 log during 40 seconds 285 nm UVB-LED exposure, then continued to drop by another 1.8 log during the following 40 seconds 265 nm UVB-LED exposure, indicating a total 4.6 log inactivation by the whole process of sequential exposure. The statistical analysis showed no significant difference on the total log inactivation between the sequential exposure and the simultaneous exposure, as well as the addition of single wavelength exposure of 265 nm UVC-LED and 285 nm UVB-LED (i.e. 4.6 log inactivation in Figure 4.2 and 4.6 log concentration reduction in Figure 4.3).

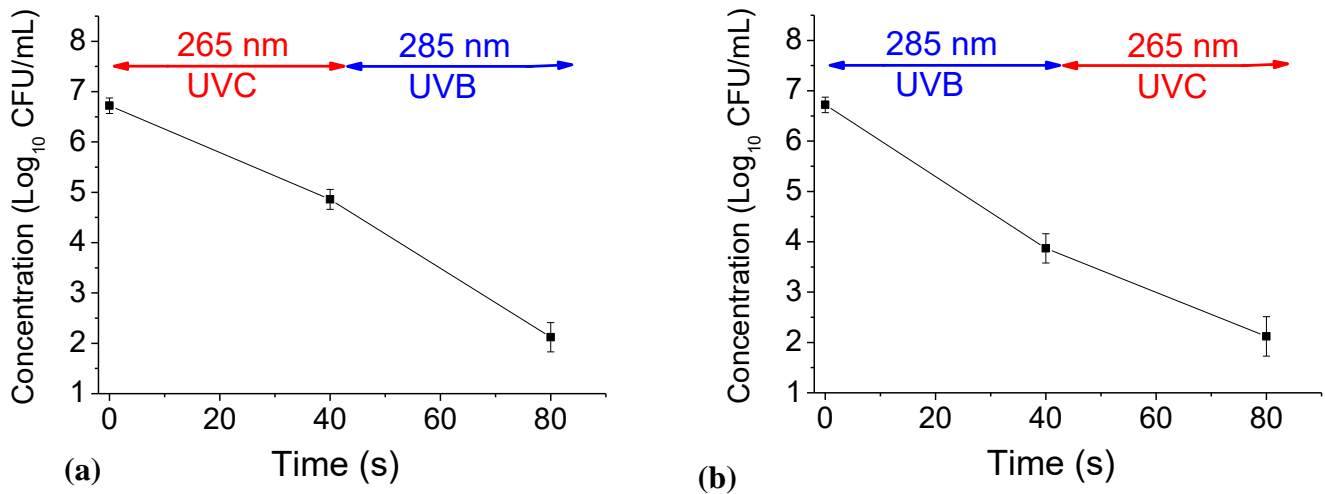


Figure 4.3 *E. coli* concentration changes by sequential 265 nm UVC-LED and 285 nm UVB-LED exposure:

(a) 40 s 265 nm followed by 40 s 285 nm, (b) 40 s 285 nm followed by 40 s 265 nm. For both sequential exposures, the overall concentration reduction was 4.6 log. Error bars represent the standard deviation for triplicate runs.

These results on simultaneous and sequential exposure for *E. coli* inactivation indicate that the combinations of 265 nm UVC-LED and 285 nm UVB-LED always achieve additive effect, i.e. when applying 265 nm UVC and 285 nm UVB radiation together, no matter simultaneously or sequentially, the total inactivation effectiveness is always comparable with the sum of each wavelength applied alone. This observation is in agreement with a recent study by Beck et al. (2017), which examined the inactivation effect of combination of 260 nm UVC-LED and 280 nm UVB-LED with varied fluence on four different types of microorganisms: bacterium *E. coli*, coliphage MS2, human adenovirus and *Bacillus pumilus* spores. Their observation indicated no synergy from any of the combinations by 260 nm and 280 nm in any fluence on any of these microorganisms in terms of inactivation effectiveness and DNA/RNA damage, in other words, only additive effect was observed on all of those combinations and microorganisms they examined. Moreover, another recent study by Li et al. (2017) combining 265 nm UVC-LED and 280 nm UVB-LED with different fluence ratios (50% : 50% and 25% : 75% for fluence ratio of 265 nm to 280 nm) for *E. coli* inactivation also observed only additive effect.

The basic fundamental mechanism for UVC and UVB radiation inactivation is disturbing the DNA in microorganism cells by the formation of pyrimidine dimers after the radiation is absorbed by DNA, as reviewed in Chapter 2. The different inactivation effectiveness of UVC and UVB is mostly due to the different UV absorption by DNA, thus resulting in different efficiency to induce pyrimidine dimers on DNA (Figure 2.2). Therefore, considering the same type of DNA damage induced by UVC and UVB radiation on microorganisms just with different efficiency, the above observation on UVC/UVB multiple wavelengths inactivation agrees with the Second Law of Photochemistry. This law states that for each photon of light absorbed by a chemical system, only one molecule is activated for a photochemical reaction (Bolton and

Cotton, 2008). In other words, each activated molecule by each photon is independent of each other, and the same amount of photons (e.g. UV fluence) always activate the same amount of molecules for a photochemical reaction (e.g. formation of pyrimidine on DNA for inactivation) with no additional amount of molecules being activated. Thus, the photochemical effect that UVC and UVB radiation with different wavelengths induce pyrimidine dimers on DNA for inactivation (Figure 2.1) should be independent of each other, and the overall photochemical effect should be the accumulation and sum of the effect from each wavelength separately. The observations on *E. coli* in this study and on four different types of microorganisms in the recent study by Beck et al. (2017) as well as another recent study by Li et al. (2017) all confirmed this expectation.

4.3.2 Combinations of UVB- and UVA-LEDs on *E. coli* inactivation

UVB and UVA radiation were combined using 285 nm UVB-LED and 365 nm UVA-LED for *E. coli* inactivation in water. As shown in Figure 4.4, 40 seconds 285 nm UVB-LED exposure (15.3 mJ/cm^2) resulted in 2.8 log inactivation, while 40 seconds 365 nm UVA-LED exposure (1.16 J/cm^2) led to 0.05 log inactivation. However, when combining together, 40 seconds simultaneous exposure of these two UV-LEDs achieved only 2.6 log inactivation, which is statistically lower than the 2.8 log inactivation by 40 seconds 285 nm exposure alone ($p < 0.05$), not to mention the addition of log inactivation by each wavelength applied alone. The simultaneous exposure of UVB- and UVA-LEDs obviously delivered higher total UV fluence than UVB-LED applied alone, thus it might be expected that the combination of these two UV-LEDs would provide higher log inactivation than UVB-LED applied alone. However, the experimental observation did not agree with this expectation. Then further investigation was performed in terms of sequential exposure to interpret this phenomenon.

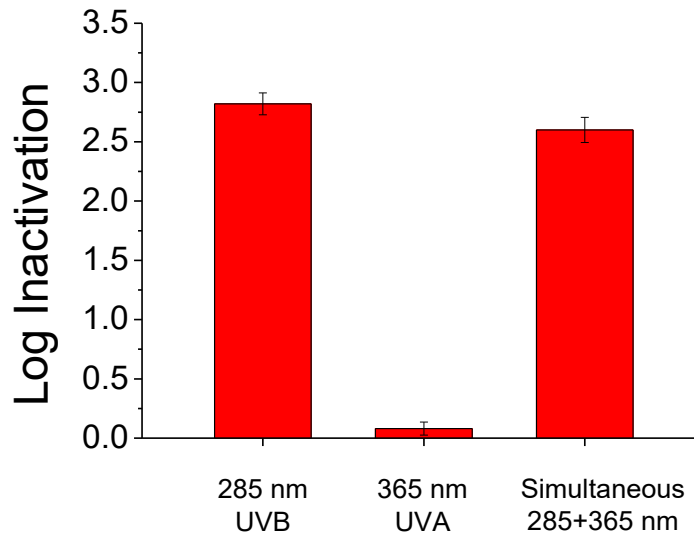


Figure 4.4 *E. coli* inactivation by 40 s 285 nm UVB-LED, 40 s 365 nm UVA-LED and simultaneous 40 s UVB/UVA-LEDs. Error bars represent the standard deviation for triplicate runs.

When UVB- and UVA-LEDs were applied sequentially, the *E. coli* concentration changes under different sequential exposure are shown in Figure 4.5. If applying 365 nm UVA-LED first, 40 seconds exposure reduced the *E. coli* concentration by 0.05 log, then the following 40 seconds 285 nm UVC-LED exposure resulted in a further concentration drop of 2.8 log, which is comparable with the additive inactivation of each UV-LEDs applied separately. However, if reversing the sequence to apply UVB-LED firstly followed by UVA-LED exposure, Figure 4.5(b) showed a very different effect. The *E. coli* concentration decreased by 2.8 log during the first 40 seconds 285 nm UVB irradiation, but then slightly increased by 0.2 log during the following 40 seconds 365 nm UVA irradiation, resulting in a total 2.6 log inactivation by the whole process of sequential 285 nm and 365 nm exposure. This effect seems consistent with the effect observed by simultaneous exposure of UVB- and UVA-LEDs, suggesting that combinations of UVB- and UVA-LEDs may reduce the inactivation effectiveness of *E. coli* compared to UVB-LED alone.

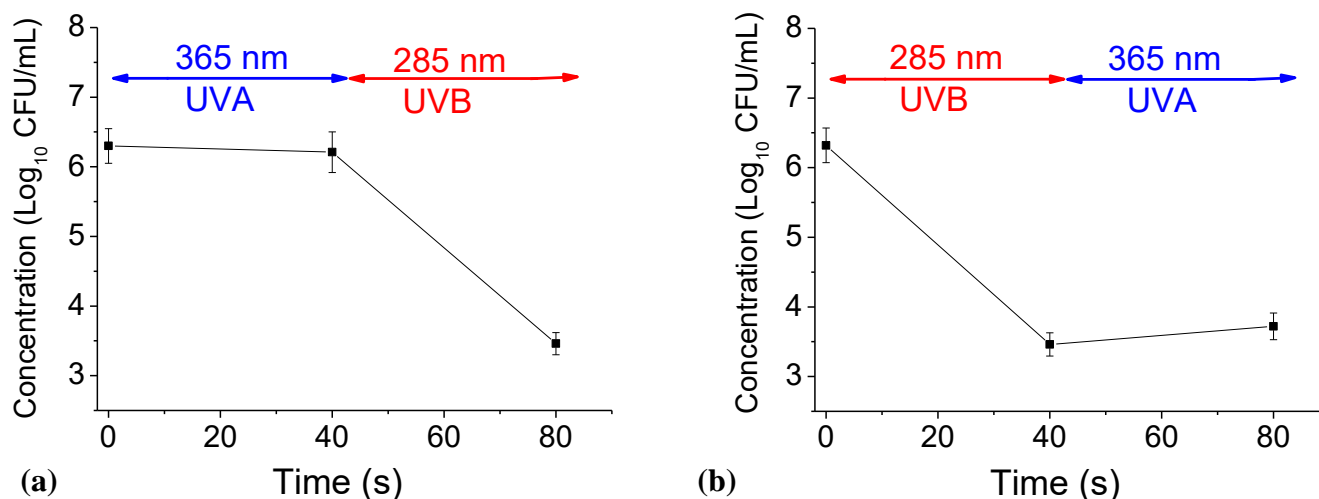


Figure 4.5 *E. coli* concentration changes by sequential 285 nm UVB-LED and 365 nm UVA-LED exposure:

(a) 40 s 365 nm followed by 40 s 285 nm, (b) 40 s 285 nm followed by 40 s 365 nm. Error bars represent the standard deviation for triplicate runs.

The results on sequential exposure of UVB- and UVA-LEDs not only distinguished the roles of UVB and UVA radiation but also revealed the importance of sequence on application of UV radiation in different wavelength ranges. When UVA is applied firstly before UVB, UVA can only slightly inactivate *E. coli* due to the low absorption of UVA radiation by DNA. However, if applying UVA after UVB, instead of inactivation, it was observed that UVA can increase the concentration of UVB-inactivated *E. coli*, clearly indicating that UVA radiation accounts for the decreased *E. coli* inactivation by combining UVB- and UVA-LED simultaneously or sequentially compared to applying UVB-LED alone. In order to further confirm this effect, UVC- and UVA-LEDs were also combined to further investigation.

4.3.3 Combinations of UVC- and UVA-LEDs on *E. coli* inactivation

Combination of UVC and UVA radiation were conducted using 265 nm UVC-LED and 365 nm UVA-LED as representatives for *E. coli* inactivation in water. As shown in Figure 4.6, 40 seconds 265 nm UVC-LED exposure (4.2 mJ/cm²) resulted in 1.8 log inactivation. However,

when applying it with 365 nm UVA-LED simultaneously for 40 seconds exposure, only 1.6 log inactivation was obtained, which is statistically less effective than 265 nm exposure alone ($p < 0.05$), let alone the sum of each wavelength applied separately. This observation indicates that although the simultaneous exposure of UVC- and UVA-LEDs delivered higher total UV fluence, it led to lower log inactivation than UVC-LED applied alone, which is similar as combinations of UVB- and UVA-LED for *E. coli* inactivation.

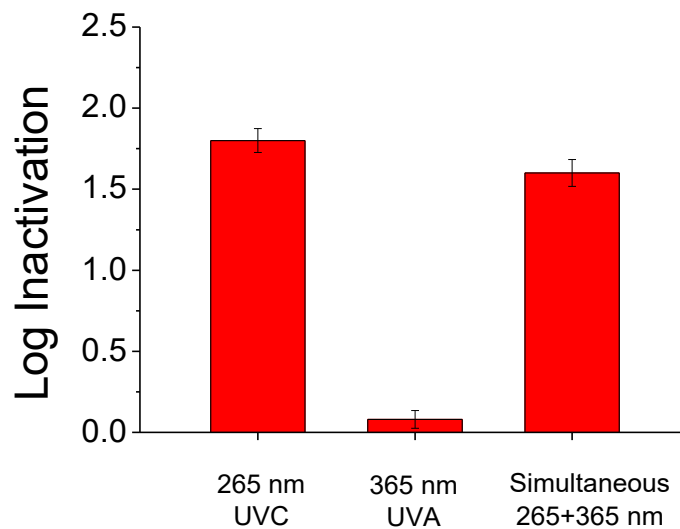


Figure 4.6 *E. coli* inactivation by 40 s 265 nm UVC-LED, 40 s 365 nm UVA-LED and simultaneous 40 s UVC/UVA-LEDs. Error bars represent the standard deviation for triplicate runs.

As for sequential exposure (Figure 4.7), when applying 365 nm UVA-LED first, 40 seconds exposure reduced the *E. coli* concentration by 0.05 log, then the following 40 seconds 265 nm UVC-LED exposure resulted in a further concentration drop of 1.8 log, which is comparable with the addition of inactivation effect by each UV-LED applied alone. However, if reversing the sequence of exposure, a different trend on *E. coli* concentration change was observed in Figure 4.7 (b). After initial 50 seconds 265 nm UVC-LED exposure, *E. coli* concentration dramatically dropped by 3.8 log. However, in the following 365 nm UVA-LED

exposure, instead of continuing inactivation, the *E. coli* concentration significantly increased by 1.1 log within 3 minutes (Note that the control experiment in Figure B.1 in Appendix B showed no concentration change when keeping *E. coli* in dark for 3 minutes after 50 seconds 265 nm UVC-LED inactivation). This observation is in agreement with the effect by simultaneous exposure of UVC- and UVA-LEDs, suggesting that applying UVA radiation for wavelengths combinations may reduce the inactivation effectiveness of *E. coli*. It is also noted that the *E. coli* concentration recovery by sequentially 50 seconds UVC followed by 3 minutes UVA (Figure 4.7(b)) is much stronger than that by 40 seconds UVB followed by 40 seconds UVA (Figure 4.5(b)), further implying the special effect of UVA radiation when coupled with UVC or UVB radiation.

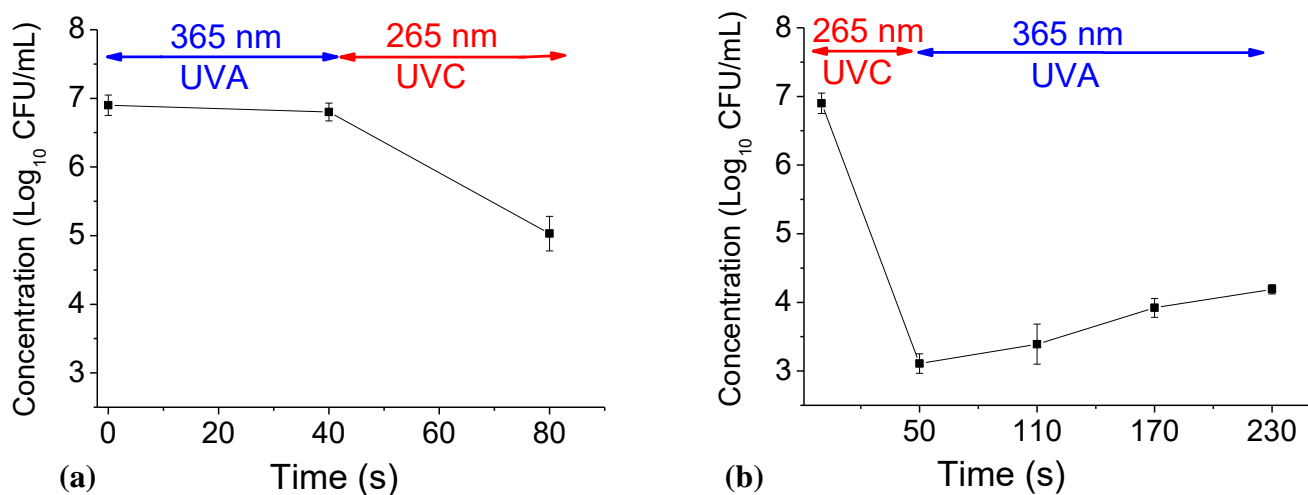


Figure 4.7 *E. coli* concentration changes by sequential 265 nm UVC-LED and 365 nm UVA-LED exposure:

(a) 40 s 365 nm followed by 40 s 265 nm, (b) 50 s 265 nm followed by 3 min 365 nm. Error bars represent the standard deviation for triplicate runs.

The results on sequential exposure of UVC- and UVA-LEDs clearly revealed the roles of UVC and UVA radiation, and demonstrated the significance of the manner to apply of UV radiation in different wavelength ranges. Moreover, the effects of wavelengths combinations by

UVC- and UVA-LEDs on *E. coli* inactivation are consistent with that by combined UVB- and UVA-LED, both indicating that UVA radiation can increase the concentration of UVC/UVB-inactivated *E. coli*, thus accounts for the reduced *E. coli* inactivation by combining UVC/UVB-LEDs with UVA-LED simultaneously or sequentially compared to applying UVC/UVB-LEDs alone.

This effect from UVA-involved wavelengths combinations is probably related to the different biological effects of UV radiation in different wavelength ranges. The effectiveness of UV disinfection depends not only on photochemical reactions (e.g. formation of pyrimidine dimers on DNA) but also on biological processes (e.g. self-repair of DNA, namely reactivation) (Harm, 1980). As reviewed in Chapter 2, UVC and UVB radiation are strongly absorbed by DNA, and mainly induce the photochemical reactions to form pyrimidine dimers on DNA to achieve inactivation. However, these photochemical reactions are mostly reversible, and the DNA damage induced by these photochemical reactions can be repaired by the biological processes in the cells, such as photoreactivation (Sinha and Hader, 2002). The enzyme photolyase in the cells can utilize the energy of light, preferably 300 – 500 nm (as called photoreactivating light), to repair DNA damage specifically against pyrimidine dimers (Gayan et al., 2014, Jagger, 1967, Thiagarajan et al., 2011). The functionalities of DNA damage repair for many organisms on the earth are developed over millions of years' evolution for the sake of survivability (Aravind et al., 1999, DiRuggiero and Robb, 2004). Many studies have demonstrated that *E. coli* has strong photoreactivation to repair UV-damaged DNA when exposure to fluorescent lamps visible light (300 – 500 nm) after UVC disinfection (Bohrerova and Linden, 2007, Oguma et al., 2001, Quek and Hu, 2008, Sommer et al., 2000, Zimmer and Slawson, 2002).

In this study, 365 nm UVA-LED was used to as a typical representative of UVA radiation. The UVA radiation with the wavelength from 315 nm to 400 nm is within the photoreactivating light range of 300 – 500 nm. Especially the enzyme photolyase in *E. coli* cells for DNA repair has the maximum absorption at around 370 nm to 420 nm (Payne and Sancar, 1990, Sancar, 2003). Thus, the energy from UVA radiation, such as 365 nm in this study, can also be utilized by the enzyme photolyase in *E. coli* to repair UVC/UVB-induced DNA damage. Moreover, photoreactivation is photoreactivating light fluence-dependent instead of time-dependent, and a study for standardized photoreactivation protocol compared different fluorescent lamps light for *E. coli* photoreactivation, which observed strong *E. coli* photoreactivation in the photoreactivating light fluence range of equivalent 0 – 1800 mJ/cm² at 368 nm regardless of the light sources and time (Bohrerova and Linden, 2007). The UV fluence of UVA-LED at 1200 mJ/cm² at 365 nm in this study is within this photoreactivating fluence range, thus can result in photoreactivation and reduce the inactivation effectiveness of *E. coli* when combining with UVB/UVC-LEDs together simultaneously or sequentially.

On one hand, UVA radiation is poorly absorbed by DNA and a large amount of UV fluence is required to achieve a decent inactivation by UVA (e.g. typically 10⁵ times more fluence required than that of UVC disinfection on *E. coli*) (Song et al., 2016). On the other hand, the energy of UVA radiation can be utilized by DNA repair enzyme to repair UVC/UVB-induced DNA damage for photoreactivation at a relatively low fluence (e.g. around 10² times more fluence compared to UVC inactivation of *E. coli*) (Bohrerova and Linden, 2007). Thus, there are two different effects of UVA radiation: inactivation effect at high fluence if directly applied on *E. coli* and photoreactivation effect at low fluence if applied on UV-damaged *E. coli*. As a result, when applying UVA radiation with UVC/UVB together, in the initial period with

relatively low UVA fluence, the photoreactivation effect is inevitably dominant among these two different UVA effects, resulting in decreased inactivation effectiveness. Moreover, the photoreactivation effect takes place only when UVC/UVB-damaged DNA is exposed to UVA radiation, but never happens on intact DNA since there is nothing to repair on undamaged DNA. Therefore, when UVA was applied before UVC/UVB, the *E. coli* inactivation was the same as each wavelength applied alone and no photoreactivation was observed (Figure 4.5(a), Figure 4.7(a)). But reduced *E. coli* inactivation was observed when applying simultaneous UVA with UVC/UVB or applying UVA after UVC/UVB due to the photoreactivation effect from UVA (Figure 4.4, Figure 4.5(b), Figure 4.6, and Figure 4.7(b)).

4.3.4 Combinations of UVC- and UVA-LEDs on MS2 inactivation

Based on the above results and discussion on UV-LEDs wavelength combinations for *E. coli* inactivation, there is only additive effect on *E. coli* by UVC- and UVB-LEDs combinations due to the same type DNA damage and the Second Law of Photochemistry. Since UVC and UVB radiation induce the same photochemical reactions on DNA or RNA of microorganisms, as reviewed in Chapter 2, the additive effect of UVC- and UVB-LEDs combinations can be extended to more microorganisms such as viruses based on the Second Law of Photochemistry. This has been proved by a recent study by Beck et al. (2017) which observed only additive effect by 260 nm UVC- and 280 nm UVB-LEDs combination on four different microorganisms including MS2. Unlike additive effect by UVC- and UVB-LEDs combinations, UVA-LEDs involved combinations with UVC- or UVB-LEDs induced a different effect for reduced *E. coli* inactivation due to the photoreactivation effect of UVA. Therefore, combinations of UVC- and UVA-LEDs were applied on coliphage MS2, as a representative of virus, to examine the potentially additional effect.

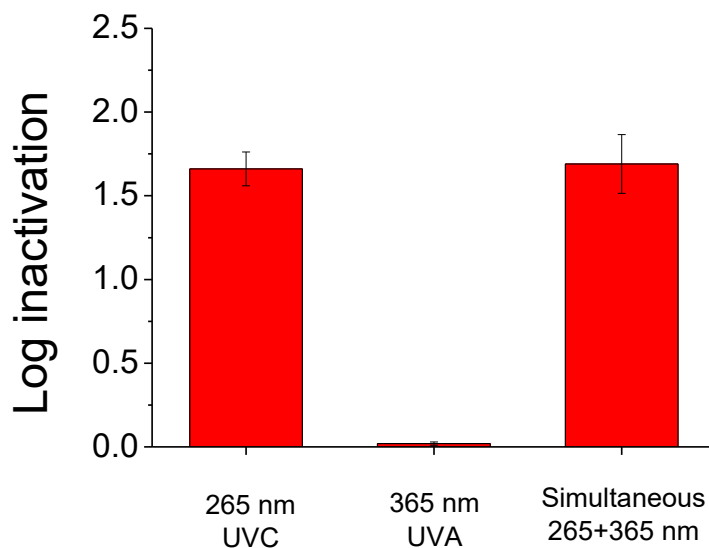


Figure 4.8 MS2 inactivation by 3 min 265 nm UVC-LED, 3 min 365 nm UVA-LED and simultaneous 3 min UVC/UVA-LEDs. Error bars represent the standard deviation for triplicate runs.

As shown in Figure 4.8, 3 minutes 265 nm UVC-LED exposure (20 mJ/cm^2) resulted in 1.6 log inactivation of MS2, while no appreciable inactivation was observed by 3 minutes 365 nm UVA-LED exposure (5400 mJ/cm^2). When applying these two UV-LEDs simultaneously for the same 3 minutes, 1.6 log inactivation of MS2 was obtained, which is comparable with the sum of each wavelengths applied alone. Unlike reduced *E. coli* inactivation by combining UVC- and UVA-LEDs simultaneously, there is no significant difference on MS2 inactivation between simultaneous 265 nm UVC-LED coupled with 365 nm UVA-LED and the sum of each UV-LED applied alone based on the statistical analysis.

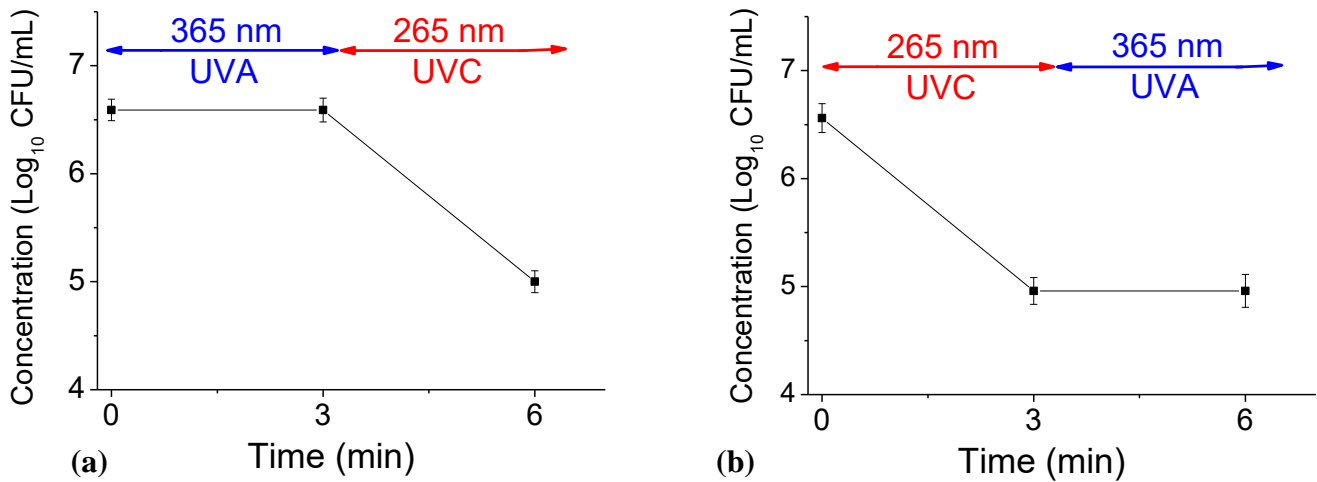


Figure 4.9 MS2 concentration reduction by sequential 265 nm UVC-LED and 365 nm UVA-LED exposure:

(a) 3 min 365 nm followed by 3 min 265 nm, (b) 3 min 265 nm followed by 3 min 365 nm. Error bars

represent the standard deviation for triplicate runs.

The MS2 concentration reduction under sequential exposure of these two wavelengths are shown in Figure 4.9. No matter applying UVA before UVC or UVC before UVA, 3 minutes 265 nm UVC-LED exposure always resulted in 1.6 log concentration reduction of MS2, while no detectable concentration change was observed by 3 minutes 365 nm UVA-LED exposure, which is the same as each wavelength applied alone. In other words, the sequential exposure of these two UV-LEDs always achieved the same log inactivation as the sum of each wavelength applied separately.

The results on combination of UVC- and UVA-LEDs for MS2 inactivation showed only additive effect regardless of simultaneous or sequential exposure, which is different from the reduced inactivation on *E. coli* by the same combination of UVC- and UVA-LEDs. This difference is probably due to the different species of microorganisms. Coliphage MS2 is a virus, which is significantly different from bacteria in terms of cell structure and functionality. Viruses usually consist of nucleic acid (DNA or RNA) surrounded by a protective coat of protein and do

not have the typical cellular structure as bacteria. Moreover, unlike bacteria, viruses are not able to reproduce by themselves due to the lack of metabolism functionality, so that they replicate only inside of the living cells of other organisms (Wikipedia, Virus). Due to the lack of key characteristics (such as cellular structure, metabolism), which are generally considered necessary to count as life, viruses have been considered as “organism at the edge of life” (Rybicki, 1990). Thus, previous studies on many viruses have demonstrated that no photoreactivation on viruses due to the lack of relative enzymes and cellular functionality (Bolton and Cotton, 2008, Harris et al., 1987, Hoyer, 1998). Therefore, due to the absence of biological processes such as photoreactivation in viruses, the impact of UV radiation, including UVC, UVB, UVA, on viruses, like MS2, is only photochemical effect on DNA or RNA following the Second Law of Photochemistry without additional effect.

4.4 Conclusions

UV-LEDs with the wavelengths at different UV ranges, including UVA, UVB, UVC, were combined for simultaneous and sequential exposure for inactivation of different types of microorganisms in water. Based on the comparisons of the inactivation effectiveness between wavelength combinations and single wavelength, the effect of multiple wavelengths on microorganisms inactivation were identified:

- (1) Combinations of UVC and UVB radiation always achieved additive inactivation on microorganisms, which can be explained by the same type of DNA damage induced by UVC/UVB and the Second Law of Photochemistry.
- (2) Combinations of UVA with UVC or UVB reduced the inactivation of bacterium *E. coli*, which can be interpreted by the biological processes on DNA repair in bacteria cells and the photoreactivation effect of UVA radiation.

- (3) Unlike *E. coli*, combinations of UVA with UVC have only additive effect on coliphage MS2 inactivation due to the absence of biological processes such as photoreactivation in viruses.

Chapter 5: Microorganisms inactivation of UVA pretreatment followed by UVC disinfection

5.1 Introduction

The microorganisms inactivation by UV radiation is mainly based on the UV-induced photochemical reactions on genetic materials (e.g. DNA) in the cells of microorganisms, mostly by UVC/UVB radiation as they are strongly absorbed by DNA. As for UVA radiation, due to its low absorption by DNA, it is inefficient to induce DNA damages for inactivation. However, there might be some biological effects other than the photochemical reactions on DNA by UVA radiation. As discussed in Chapter 4, one of the biological effects by UVA radiation on bacteria is that some enzymes in the cells may utilize the energy of UVA to repair the damaged DNA for photoreactivation. Considering that the metabolism in microorganisms cells involves many biological processes in addition to DNA repair, UVA radiation may impact some of these biological processes in cells. Thus there might be more biological effects by UVA radiation on microorganisms.

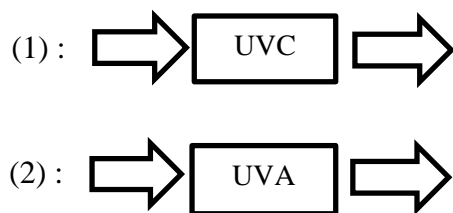
In this chapter, a new combination of UVA-LED and UVC-LED was developed for microorganisms inactivation to explore the potentially biological effects of UV radiation in different wavelengths. The effects of this combination on both inactivation and reactivation were examined. Then based on the observed effects, appropriate experiments were designed and performed accordingly to investigate the mechanism for the biological effects of this combination. Combining these experimental work together, the mechanism for microorganisms inactivation by this combination of UVA-LED and UVC-LED was discussed and proposed.

5.2 Experimental design

5.2.1 Microorganisms inactivation

Based on the results and discussion in Chapter 4, simultaneous exposure of UVA with UVC/UVB or applying UVA after UVC/UVB decreased the inactivation effectiveness of *E. coli* due to photoreactivation. So it is unfavorable to apply UVA with UVC/UVB simultaneously or after UVC/UVB for disinfection. Thus a feasible way to apply UVA radiation might be prior to UVC/UVB irradiation in order to avoid the UVC/UVB-damaged DNA exposing to UVA radiation for DNA repair. Therefore, a new combination of UVA and UVC was developed by applying UVA radiation prior to UVC irradiation with extended UVA exposure time as pretreatment before UVC disinfection. As shown in Figure 5.1, the single wavelength exposure by 265 nm UVC-LED or 365 nm UVA-LED was performed separately as a baseline for comparison. Then 365 nm UVA-LED pretreatment was conducted with different exposure times followed by 265 nm UVC-LED inactivation. The inactivation effectiveness by the process of UVA pretreatment followed by UVC was compared to those by single wavelength to explore the potentially additional effect.

Single wavelength exposure:



UVA pretreatment prior to UVC inactivation:

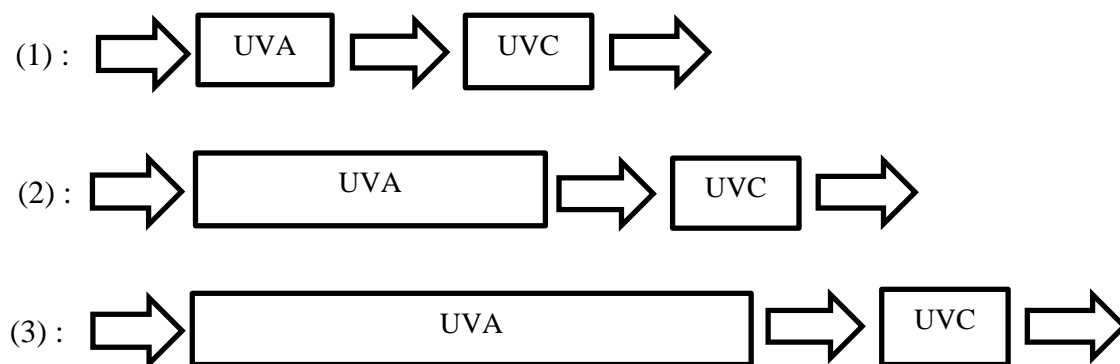


Figure 5.1 Flow chart to illustrate UVA pretreatment followed by UVC inactivation

5.2.2 Reactivation examination

As observed and discussed in Chapter 4, some microorganisms, specifically bacteria such as *E. coli*, may reactivate after UV disinfection under certain conditions like exposure to visible light or UVA. Thus reactivation may decrease the inactivation effectiveness and is unfavorable for UV disinfection. As a result, the potential reactivation post UV disinfection is usually taken into consideration in UV disinfection studies. Therefore, two main reactivation phenomena, photoreactivation (i.e. reactivation under visible light) and dark repair (i.e. reactivation in dark), were examined after UVC inactivation with or without UVA pretreatment.

After inactivation under various conditions, the irradiated water sample was transferred to two 9-cm diameter glass Petri dishes for photoreactivation and dark repair examination. For photoreactivation, the irradiated water sample was placed in a magnetic stirrer and exposed to two fluorescent lamps (Philips F15T8, 18W, cool white, 4100 K) while stirring for 4 hours. The emission spectrum from these fluorescent lamps was measured using an Ocean Optics USB2000+ spectrometer. The lamps emit visible light with the wavelengths of 300 – 700 nm (Figure B.2 in Appendix B for the emission spectrum). The water sample was placed 10 cm below the fluorescent lamps for exposure. The intensity of the lamps was measured using a Newport Optical 1917-R power meter with a 918D-ST-UV detector (measurement range: 200 – 1100 nm). The intensity was measured to be 4 mW/cm² at the surface of water sample. For dark repair, the irradiated water sample was placed in a magnetic stirrer in the dark while stirring for 4 hours. For both photoreactivation and dark repair test, samples were taken at 30-minute interval to determine microorganism concentration and the data was used to analyze the photoreactivation and dark repair effect for various UV-LEDs exposure conditions. The control was conducted in the same procedure using the unirradiated water samples.

In order to evaluate the reactivation effect, the following formula was used to calculate the percentage of reactivation (Quek and Hu, 2008):

$$repair \% = \frac{Log_{10}N_{rt} - Log_{10}N_t}{Log_{10}N_0 - Log_{10}N_t}$$

In which: N_0 -- Concentration of microorganism before UV disinfection (CFU/mL)

N_t -- Concentration of microorganism immediately after UV disinfection
(CFU/mL)

N_{rt} -- Concentration of microorganism after reactivation (CFU/mL)

The percentage of reactivation after different UV-LEDs inactivation conditions was compared to analyze their effects.

5.2.3 Mechanism investigation

As reviewed in Chapter 2, UVA inactivation may involve indirect effect by reactive intermediates such as reactive oxygen species (ROS). Thus appropriate experiments were designed and performed to investigate the role of ROS during the interaction of UV radiation and microorganisms in water.

The three main ROS include superoxide radical ($\bullet\text{O}_2^-$), hydroxyl radical ($\bullet\text{OH}$) and hydrogen peroxide (H_2O_2) (He and Hader, 2002, Hoerter et al., 2005). To investigate and clarify the role of each ROS, different scavengers were utilized to remove the corresponding ROS in the process of UV irradiation. These methods regarding scavengers are derived from previous studies and described as following with related references. 4-Hydroxy-TEMPO (TEMPOL) was used to remove $\bullet\text{O}_2^-$ radicals (Chen et al., 2011, Liang et al., 2016), mannitol was used to remove $\bullet\text{OH}$ radicals (Fridovich and Porter, 1981, Shen et al., 1997), catalase was used to remove H_2O_2 (Novo and Parola, 2008, Ruh et al., 2000). Note that during the process of UV irradiation on microorganisms in water, these ROS may present either in water or in the cells of microorganisms as intermediates, or a combination of both. Thus these scavengers were deliberately selected for this process because they can not only remove the corresponding ROS in water but also permeate the cells as intracellular scavengers of these ROS (Goldstein and Czapski, 1984, Lejeune et al., 2006, Reiter et al., 1995, Thamilselvan et al., 2000, Wilcox and Pearlman, 2008, Yamada et al., 2003). To perform the scavenger tests, TEMPOL, mannitol and catalase were purchased from Sigma-Aldrich Co. LLC. Before UV irradiation, each scavenger

was mixed with microorganism suspension for 1 mmol/L TEMPOL, 0.5 mol/L mannitol, 1 mg/mL catalase, separately. The microorganism suspension with each scavenger was stirred in dark for 30 minutes to ensure that the scavenger dissolved in the water and permeated the cells prior to UV exposure. Then inactivation and reactivation effects both in the presence and absence of these scavengers were examined and compared to identify the role of each ROS. The control experiment was conducted in the same procedure without exposure to UV radiation (Appendix B).

To detect the ROS in water, a probe compound carbamazepine (CBZ) was utilized to indirectly determine the concentration of $\bullet\text{OH}$ radicals. $\bullet\text{OH}$ radical is highly reactive and unstable, thus has to be indirectly measured. CBZ has a high reactivity with $\bullet\text{OH}$ radicals at a rate constant of $2.1 \times 10^9 \text{ M}^{-1} \text{ s}^{-1}$ (Vogna et al., 2004). Thus its degradation rate can be measured and then used to calculate the concentration of $\bullet\text{OH}$ radicals. Before UV irradiation, 400 ppb CBZ was mixed with microorganism suspension while stirring in dark for 30 minutes. During UV irradiation, the water samples were taken at the designated exposure times and filtered by 0.45 μm filters to remove the microorganism cells for the following high performance liquid chromatography (HPLC) analysis. The concentration of CBZ in each water sample was analyzed using HPLC (Dionex Ultimate 3000, Thermo Scientific), which equipped a UV detector at the detection wavelength of 211 nm and a 3.9 \times 150 mm Nova-Pak C-18 column with a 4- μm particle size. A sample of 100 μL was injected into the system. The mobile phase for HPLC analysis consisted of 30% acetonitrile and 70% acidified water with phosphoric acid (pH 2.4) at a flow rate of 1 mL/min and the operation temperature was 35 $^{\circ}\text{C}$. The CBZ standard for calibration were provided by Sigma-Aldrich (USA). The degradation kinetics of CBZ was

established to determine the $\bullet\text{OH}$ radical concentration. The concentration of $\bullet\text{OH}$ radicals in water in the absence of microorganisms was also determined as the control experiment.

In order to further identify the ROS in the cells of microorganisms, surface disinfection tests were designed and performed to exclude the water in the system during UV irradiation. The scavenger was mixed with microorganism suspension while stirring in dark for 30 minutes to ensure that the scavenger permeated the cells of microorganisms. Then 20 μL of microorganism suspension was spread on an agar plate. The agar plate was kept in dark for a while to allow it drying and to ensure the scavenger-permeated microorganism cells remained on the agar plate without water presenting. The agar plate with microorganisms was used to perform UV inactivation test in triplicate for each condition. The surface disinfection tests both in the presence and absence of scavenger were performed and compared to identify the role of ROS in the cells of microorganisms. Performing the experiments with and without water allowed separating the role of ROS in water and in microorganisms cells.

5.3 Results and discussion

5.3.1 Effects of UVA pretreatment on *E. coli* inactivation

E. coli suspension was exposed to different exposure times of 365 nm UVA-LED radiation as UVA treatment, followed by 265 nm UVC-LED irradiation for inactivation. As shown in Figure 5.2, 30 seconds 265 nm UVC exposure alone with the UV fluence of 3.7 mJ/cm^2 resulted in 1.3 log inactivation of *E. coli*. When applying 1 min 365 nm UVA pretreatment, the following 30 seconds 265 nm UVC exposure led to 1.3 log inactivation, which is equivalent as that without UVA pretreatment. However, when increasing 365 nm UVA pretreatment time to 10 minutes, the following 30 seconds 265 nm UVC exposure achieved 2.2 log inactivation in spite of only 0.08 log inactivation during UVA pretreatment (so called “pretreatment” due to the insignificant

inactivation during pretreatment), suggesting significantly synergistic effect (i.e. $2.2 > 1.3 + 0.08$). In terms of inactivation effectiveness, 69% inactivation improvement was achieved with the same 30 seconds 265 nm UVC irradiation (i.e. $(2.2 - 1.3) / 1.3 = 69\%$). When further extending 365 nm UVA pretreatment time to 30 minutes, the following 30 seconds 265 nm UVC exposure led to 3.3 log inactivation while 30 minutes of 365 nm UVA pretreatment only resulted in 0.2 log inactivation, further indicating significantly synergistic effect (i.e. $3.3 > 1.3 + 0.2$). The *E. coli* inactivation with UVA pretreatment under the same 30 seconds 265 nm UVC irradiation was remarkably improved by over 150% (i.e. $(3.3 - 1.3) / 1.3 = 154\%$). The results indicated that 365 nm UVA pretreatment can significantly improve the following 265 nm UVC inactivation and this inactivation improvement depends on the fluence of UVA pretreatment with a threshold to take effect. Unlike the decreased *E. coli* inactivation by applying UVA with UVC

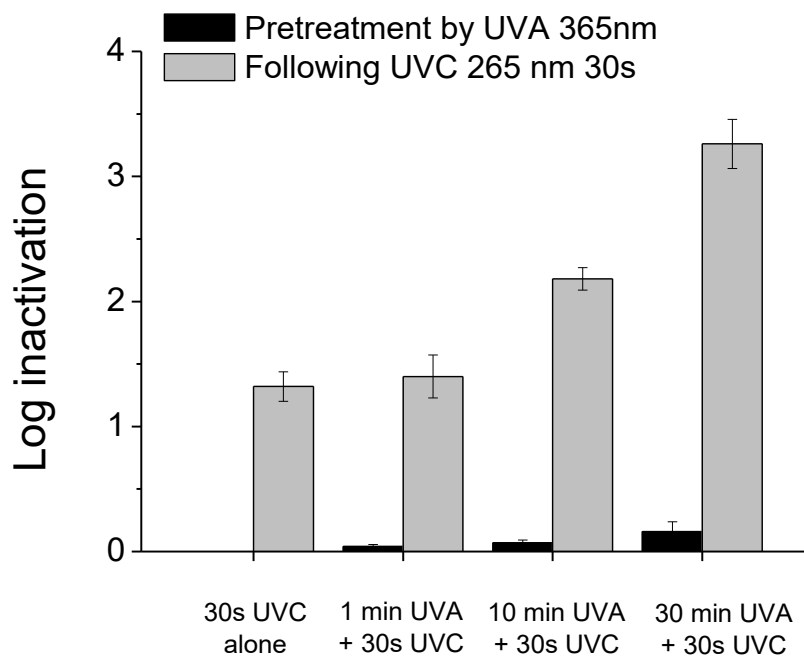


Figure 5.2 *E. coli* inactivation by 365 nm UVA pretreatment with different times followed by 30 s 265 nm UVC irradiation. Error bars represent the standard deviation for triplicate runs.

simultaneously or UVA after UVC in Chapter 4, this considerable synergistic effect by UVA pretreatment prior to UVC irradiation is highly favorable for UVC disinfection.

To further confirm this dramatic inactivation improvement by UVA pretreatment prior to UVC irradiation, the *E. coli* inactivation kinetics by 265 nm UVC irradiation was examined with different UVA pretreatment times. As shown in Figure 5.3, the *E. coli* inactivation kinetics by 265 nm UVC irradiation alone was comparable with that after 1 minute 365 nm UVA pretreatment. However, 10 minutes UVA pretreatment significantly improved the whole inactivation kinetics of 265 nm UVC irradiation, while 30 minutes UVA pretreatment even further enhanced the whole inactivation kinetics. Thus it further confirmed the significant synergistic effect and considerable inactivation improvement by UVA pretreatment. Since longer

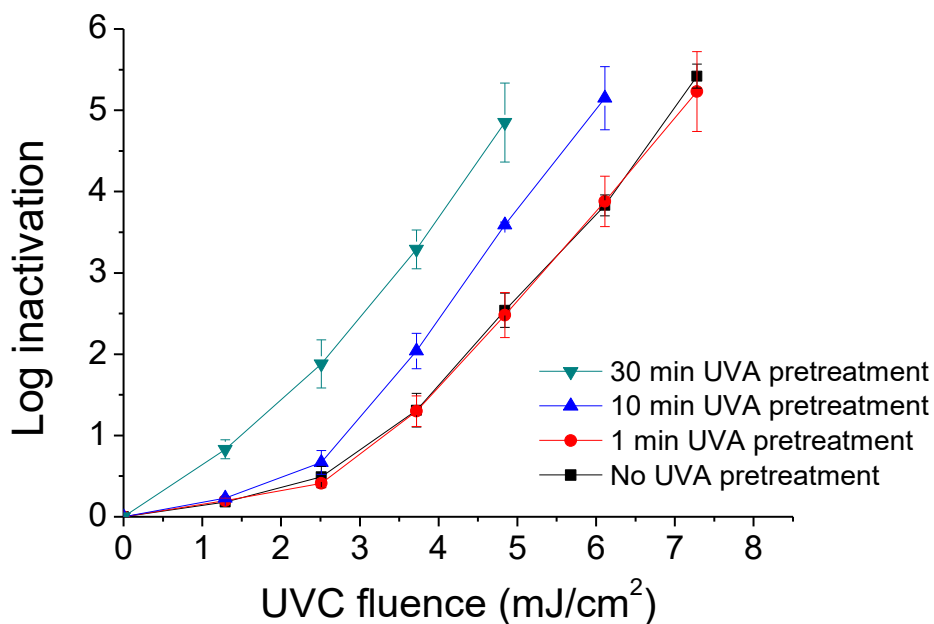


Figure 5.3 *E. coli* inactivation kinetics by 265 nm UVC with and without 365 nm UVA pretreatment. X-axis indicates UV fluence for 265 nm UVC. The UV fluence of 365 nm UVA pretreatment is 1.7 J/cm² for 1 min, 17 J/cm² for 10 min, 52 J/cm² for 30 min. Error bars represent the standard deviation for triplicate runs.

UVA pretreatment resulted in further improvement on UVC inactivation kinetics (Figure 5.3), it further suggested that UVA pretreatment accounted for the significant synergistic effect and the effect of UVA pretreatment on *E. coli* is fluence-dependent with a threshold to take effect.

Moreover, Figure 5.3 showed a shoulder effect in the *E. coli* inactivation kinetics by 265 nm UVC alone, in which little inactivation of *E. coli* was achieved at low UV fluence and the slope of kinetics curve was significantly lower than that at high UV fluence (Hijnen et al., 2006). This shoulder effect does not quite follow the Second Law of Photochemistry since the effect of photochemical reactions (e.g. formation of pyrimidine dimers on DNA under UVC radiation for inactivation) is supposed to be in direct proportion to the amount of photons (e.g. UV fluence). Thus the shoulder effect is believed to be closely related to the biological processes other than photochemical reactions in the cells and has been attributed to the self-repair ability such as photo repair and dark repair (Hoyer, 1998, Morton and Haynes, 1969). However, with 10 minutes UVA pretreatment, the shoulder effect in the following UVC inactivation kinetics was slightly reduced, while 30 minute UVA pretreatment almost completely eliminated the shoulder in the following UVC inactivation kinetics (Figure 5.3). The lack of shoulder in the UVC inactivation kinetics after 30 minutes UVA pretreatment suggested the suppression of biological processes such as self-repair during UVC irradiation, which probably resulted from elimination of self-repair ability by the UVA pretreatment. The bacteria cells can continuously repair the UV-induced DNA damage even during the process of UV irradiation, thus the cells with self-repair ability would be able to better resist the inactivation of UV irradiation (Quek and Hu, 2008). Therefore, the significant inactivation improvement in the whole kinetics (in addition to the shoulder at low UV fluence) of UVC inactivation followed by UVA pretreatment further

suggested that this effect may result from the elimination of self-repair ability. This hypothesis to interpret the effects of UVA pretreatment on *E. coli* inactivation will be further discussed later.

In order to quantify the improvement on the UVC inactivation kinetics of *E. coli* by UVA pretreatment, the linear relationship of log inactivation and UV fluence at high UV fluence excluding the shoulder at low fluence was fit using a shoulder model (Hijnen et al., 2006). As shown in Figure 5.4 and Table 5.1, the slope of the inactivation kinetics was always the same regardless of the absence or presence of various UVA pretreatment times. The slope of inactivation kinetics, formerly known as inactivation rate constant, indicates the UV sensitivity of a microorganism to UV in a specific wavelength. It can be concluded that UVA pretreatment did not change the UV sensitivity of *E. coli* to 265 nm UVC. However, the intercept of the inactivation kinetics varied with different 365 nm UVA pretreatment times. Although no significant change on the intercept of the inactivation kinetics (i.e. 2.98 vs. 2.84) was observed when applying 1 minute UVA pretreatment before UVC inactivation, 10 minute UVA pretreatment remarkably changed the intercept from 2.98 to 2.54. In other words, the whole inactivation kinetics was increased by 0.44 log inactivation under the same 265 nm UVC fluence. Furthermore, 30 minute UVA pretreatment changed the intercept from 2.98 to 0.79, indicating the inactivation was dramatically improved by 2.2 log. These results suggested that the UVC inactivation improvement after UVA pretreatment is due to the elimination of the shoulder in the inactivation kinetics instead of altering the inactivation rate constant. Moreover, these results quantitatively demonstrated the effect of UVA pretreatment on *E. coli* inactivation is UVA fluence-dependent with a threshold to take effect, and the threshold for 365 nm UVA pretreatment to take effect on *E. coli* is between 1.7 J/cm² (i.e. UV fluence of 1 min 365 nm that

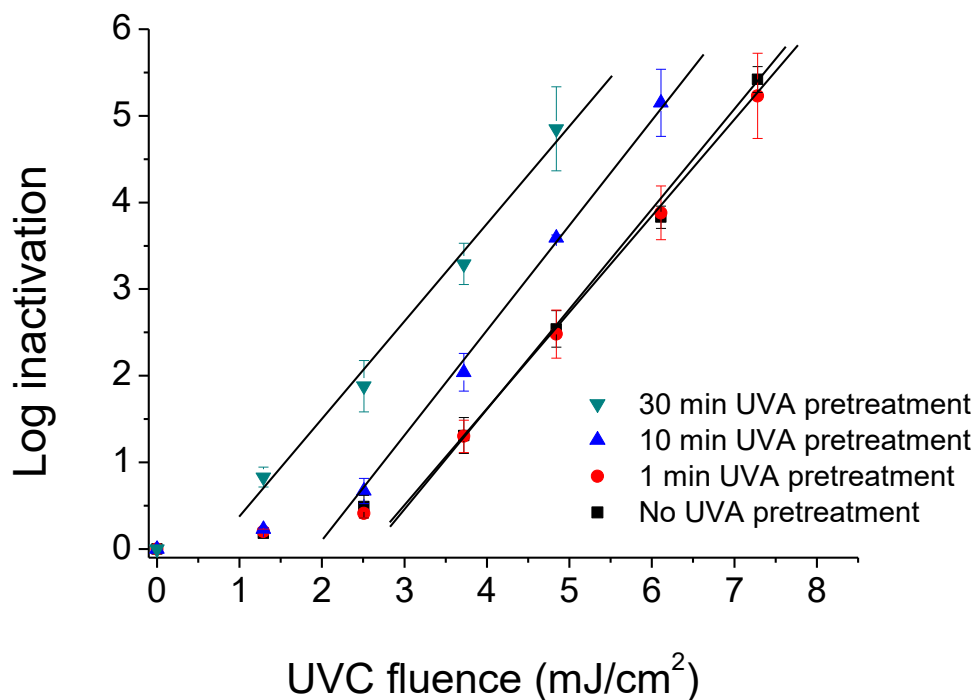


Figure 5.4 *E. coli* inactivation kinetics fitting for 265 nm UVC with and without 365 nm UVA pretreatment. X-axis indicates UV fluence for 265 nm UVC. The UV fluence of 365 nm UVA pretreatment is 1.7 J/cm² for 1 min, 17 J/cm² for 10 min, 52 J/cm² for 30 min. Error bars represent the standard deviation for triplicate runs.

Table 5.1 *E. coli* inactivation kinetics fitting results for 265 nm UVC with and without 365 nm UVA pretreatment. F represents UV fluence of 265 nm UVC in the unit of mJ/cm².

	Kinetics fitting	R ²
UVC without UVA pretreatment	Log inactivation = 1.14 F – 2.98	0.994
UVC after 1 minutes UVA (1.7 J/cm ²) pretreatment	Log inactivation = 1.11 F – 2.84	0.999
UVC after 10 minutes UVA (17 J/cm ²) pretreatment	Log inactivation = 1.26 F – 2.54	0.998
UVC after 30 minutes UVA (52 J/cm ²) pretreatment	Log inactivation = 1.13 F – 0.79	0.984

did not change UVC inactivation) and 17 J/cm² (i.e. UV fluence of 10 min 365 nm that significantly improved UVC inactivation).

5.3.2 Effects of UVA pretreatment on MS2 inactivation

The effect of UVA pretreatment on coliphage MS2 inactivation was examined through long time 365 nm UVA-LED exposure followed by 265 UVC-LED inactivation. As shown in Figure 5.5, 3 minutes of 265nm UVC alone with the UV fluence of 20 mJ/cm² resulted in 1.6 log inactivation of MS2 in water. When applying 365 nm UVA pretreatment, the following 3 minutes 265 nm UVC exposure always achieved 1.6 log inactivation after various different UVA pretreatment times up to 90 minutes, which is comparable to that without UVA pretreatment.

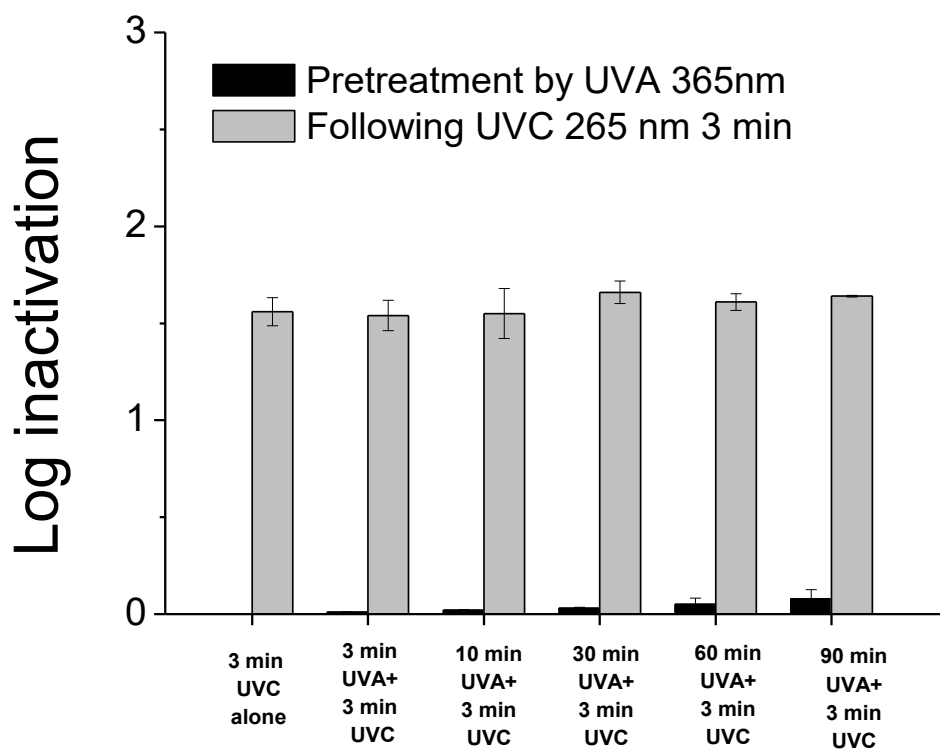


Figure 5.5 MS2 inactivation by 365 nm UVA pretreatment with different times followed by 3 minutes 265 nm UVC irradiation. Error bars represent the standard deviation for triplicate runs.

Unlike *E. coli* that exhibited the significant synergistic effect and considerable inactivation improvement by UVA pretreatment, no additional effect was observed for MS2 inactivation by UVA pretreatment, even at long periods of irradiation. This observation is similar to that of the effects of UV-LEDs multiple wavelengths described in Chapter 4, both indicating additional effects on *E. coli* inactivation but not on MS2 inactivation. Thus the absence of additional effect on MS2 inactivation by UVA pretreatment can be attributed to the same reason as that by UV-LEDs multiple wavelengths: the difference in the types of microorganisms. As discussed in Chapter 4, viruses, such as MS2, have minimal cellular functionality and biological processes, like repair enzymes. Thus the interaction of UV radiation with viruses depends only on the photochemical reactions on DNA or RNA following the Second Law of Photochemistry without additional effect.

5.3.3 Effects of UVA pretreatment on *E. coli* reactivation

Based on the results and discussion on the effects of UVA pretreatment on *E. coli* inactivation in Section 5.3.1, the significant synergistic effect and considerable inactivation improvement by UVA pretreatment on *E. coli* inactivation may be related to the suppression of self-repair ability of *E. coli*, such as photo repair and dark repair. Thus, to further investigate this hypothesis, the effects of UVA pretreatment on *E. coli* reactivation including photoreactivation and dark repair were examined.

Blank control experiments for photoreactivation and dark repair was conducted by stirring unirradiated *E. coli* samples under visible light or in dark. No change of *E. coli* concentration was observed during 4 hours in these control experiments (Figure B.4 in Appendix B). The dark repair of *E. coli* after 265 nm UVC inactivation and after 30 minutes 365 nm UVA pretreatment followed by 265 nm UVC inactivation for 3.3 log inactivation is shown in Figure 5.6. Both the

repair extent and trend were comparable for *E. coli* dark repair after UVC inactivation with or without UVA pretreatment. For both cases, the dark repair was up to 12% in the first hour and then no more recovery afterwards, indicating that after 3.3 log inactivation, only up to 0.4 log was recovered in the dark. Thus UVA pretreatment did not affect the dark repair of *E. coli* after UVC inactivation.

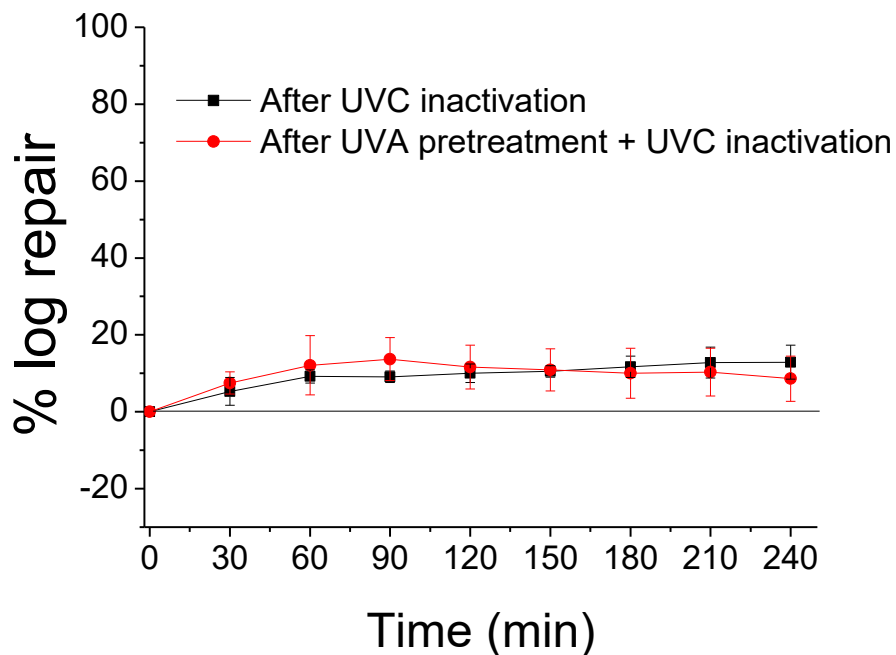


Figure 5.6 *E. coli* dark repair after 265 nm UVC inactivation and after 30 minutes 365 nm UVA pretreatment followed by 265 nm UVC inactivation for 3.3 log inactivation. Error bars represent the standard deviation for triplicate runs.

Figure 5.7 shows the photoreactivation of *E. coli* after 265 nm UVC inactivation and after 30 minutes 365 nm UVA pretreatment followed by 265 nm UVC inactivation for 3.3 log inactivation. After UVC inactivation, *E. coli* recovered up to 60% during 4 hours photoreactivation, indicating that after 3.3 log inactivation, 2 log was recovered during 4 hours exposure to visible light. This observation is in agreement with those in previous studies which

observed up to 80% recovery by photoreactivation after 254 nm UV mercury lamps inactivation of *E. coli* (Oguma et al., 2002, Quek and Hu, 2008), both demonstrating significant recovery through photoreactivation after UVC inactivation. However, after 365 nm UVA pretreatment followed by 265 nm UVC inactivation, the photoreactivation of *E. coli* was only up to 15% during 4 hours exposure to visible light (Figure 5.7), which means only up to 0.5 log was recovered after 3.3 log inactivation. This is dramatically lower than the photoreactivation after UVC inactivation without UVA pretreatment, suggesting the loss of photo repair ability of *E. coli* after the process of UVA pretreatment followed UVC inactivation. Unlike the strong photoreactivation after UVC-only inactivation, the significantly reduced photoreactivation after UVA pretreatment followed by UVC inactivation is another feature highly favorable for UVC

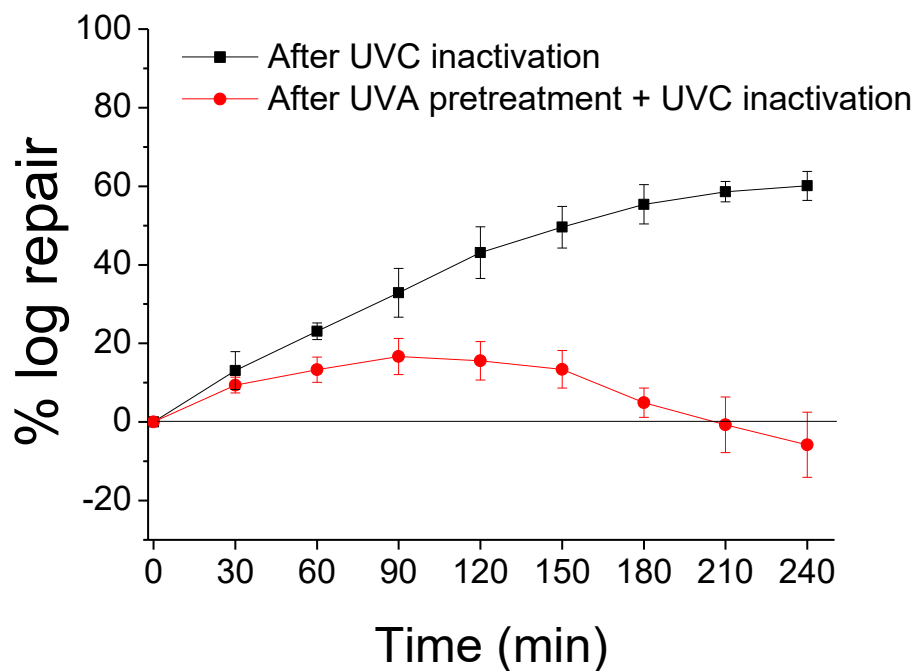


Figure 5.7 *E. coli* photoreactivation after 265 nm UVC inactivation and after 30 minutes 365 nm UVA pretreatment followed by 265 nm UVC inactivation for 3.3 log inactivation. Error bars represent the standard deviation for triplicate runs.

disinfection.

Moreover, with 365 nm UVA pretreatment prior to 265 nm UVC inactivation, the photoreactivation of *E. coli* was up to 15% during the first 2.5 hours exposure to visible light (Figure 5.7), in which the photoreactivation extent and trend is similar as that of dark repair (Figure 5.6). The dark repair process does not require the presence of visible light, thus can take place both in dark and under visible light (Nair, 2010, USEPA, 2006). Therefore, it implies that during the first 2.5 hours exposure to fluorescent lamps visible light the reactivation of 15% (Figure 5.7) may mostly account for dark repair of 12% (Figure 5.6). The insignificant difference (less than 3%, within the measurement error) suggests the complete loss of photo repair ability of *E. coli* after 30 minutes UVA pretreatment. Furthermore, after 2.5 hours exposure to visible light, the *E. coli* concentration started decreasing to even lower than the initial concentration after UVC inactivation (i.e. the two data points with negative percentage in Figure 5.7), suggesting further inactivation under the fluorescent lamps visible light. Considering that there are two small peaks in UVA range in the emission spectrum of the fluorescent lamps visible light (Figure B.2 in Appendix B), the drop of *E. coli* concentration further suggested that the *E. coli* cannot even resist the slight UVA emission in visible light due to the severe damage of self-repair systems after the process of UVA pretreatment followed by UVC inactivation.

As such, the effects of UVA pretreatment on *E. coli* reactivation not only revealed another important advantage from the process of UVA pretreatment followed by UVC inactivation, but also demonstrated the hypothesis that the significant synergistic effect and considerable inactivation improvement by UVA pretreatment on *E. coli* inactivation is related to the suppression of self-repair ability of *E. coli*, such as photo repair.

5.3.4 Roles of ROS on *E. coli* inactivation with UVA pretreatment

Two important beneficial effects were revealed in the process of UVA pretreatment followed by UVC inactivation on *E. coli*: considerable inactivation improvement and significant reactivation suppression. To the best of the author's knowledge, this is the first report of this process and its beneficial effects. Thus there is little information from literature for the mechanism of this process. Therefore, appropriate experiments were designed and performed to explore the mechanism for the effects of this process. The roles of reactive oxygen species (ROS) were examined during the process of UVA pretreatment followed by UVC inactivation.

Different scavengers were added to *E. coli* suspension to remove corresponding ROS under UV irradiation. The control experiments were also performed by only adding scavengers to *E. coli* suspension without UV irradiation. No change of *E. coli* concentration was observed during these control experiments (Figure B.3 in Appendix B), indicating that none of these scavengers has harmful effect to *E. coli* cells within the duration of the tests with UV irradiation. The *E. coli* inactivation kinetics by 265 nm UVC irradiation with different scavengers is shown in Figure 5.8. No significant difference was observed for the UVC inactivation kinetics in the absence and presence of each scavenger, indicating that none of the ROS, such as superoxide radical ($\bullet\text{O}_2^-$), hydroxyl radical ($\bullet\text{OH}$) or hydrogen peroxide (H_2O_2), was involved in UVC inactivation of *E. coli*. This observation is consistent with basic fundamental mechanism of UVC inactivation that DNA directly absorbs UVC radiation for the formation of pyrimidine dimers through the photochemical reactions without intermediate steps (as reviewed in Chapter 2).

Figure 5.9 shows the *E. coli* inactivation kinetics by 265 nm UVC irradiation after 365 nm UVA pretreatment with different scavengers. When TEMPOL (the scavenger of $\bullet\text{O}_2^-$) was added into the inactivation system, the *E. coli* inactivation kinetics was comparable with that

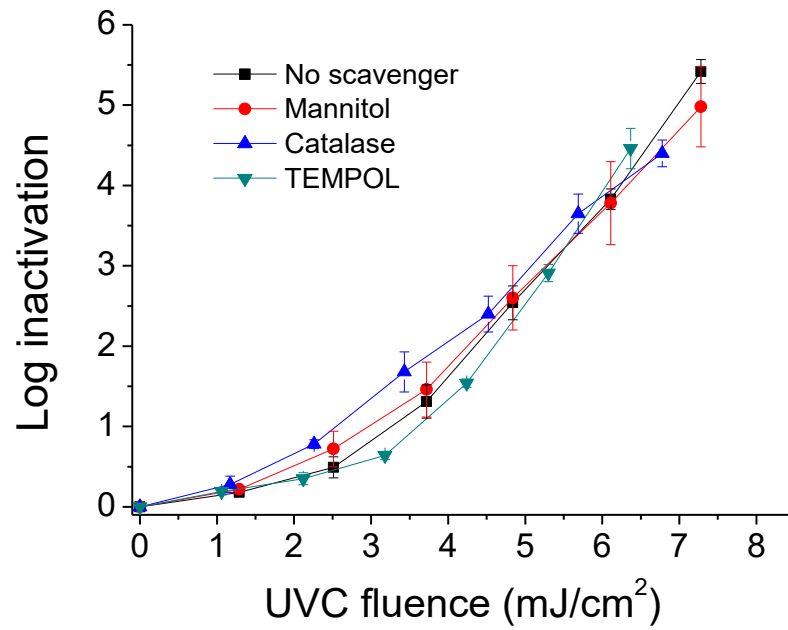


Figure 5.8 *E. coli* inactivation kinetics by 265 nm UVC irradiation in the presence of different scavengers.

Error bars represent the standard deviation for triplicate runs.

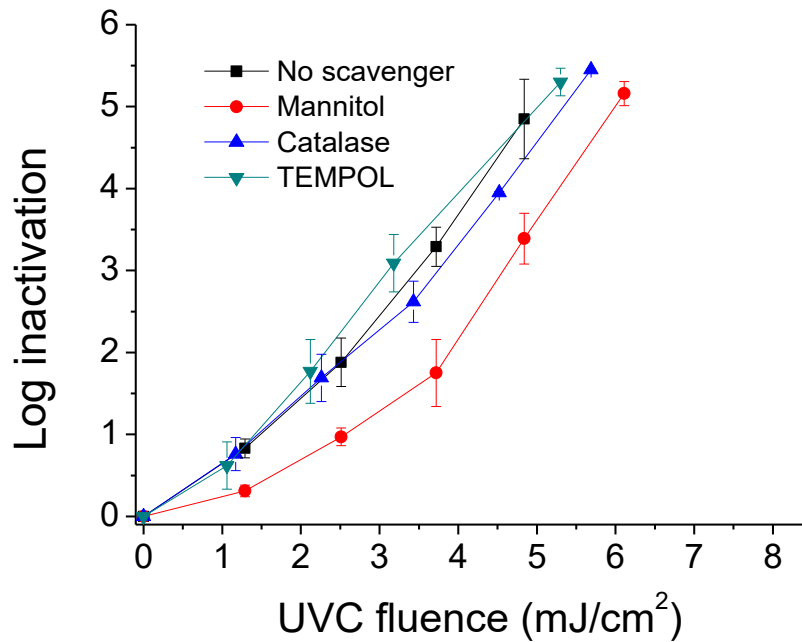


Figure 5.9 *E. coli* inactivation kinetics by 265 nm UVC irradiation after 365 nm UVA pretreatment in the presence of different scavengers. Error bars represent the standard deviation for triplicate runs.

without any scavenger, suggesting that $\bullet\text{O}_2^-$ did not play a role in the process of UVA pretreatment followed by UVC inactivation. The similar result was observed with the addition of catalase (the scavenger of H_2O_2), thus H_2O_2 was not involved in the process either. However, when adding mannitol to remove $\bullet\text{OH}$ in the process, the *E. coli* inactivation kinetics was significantly decreased compared to that without scavenger, which suggested that $\bullet\text{OH}$ played an important role for the improved *E. coli* inactivation by UVC inactivation after UVA pretreatment. Since $\bullet\text{OH}$ was involved only in the process of UVA pretreatment followed by UVC inactivation, but not in solo UVC inactivation, it indicated that $\bullet\text{OH}$ might result from UVA pretreatment.

$\bullet\text{OH}$ radical is highly reactive so that it can nonselectively react and oxidize most organic compounds and inorganic ions with high rate constants usually in the order of $10^6 - 10^9 \text{ M}^{-1} \text{ s}^{-1}$ (Cheng et al., 2016, Dorfman and Adams, 1973, Wang and Xu, 2012). On one hand, it is reasonable to infer that $\bullet\text{OH}$ would react with *E. coli* cells to induce damage on the cells, which would account for the considerable inactivation improvement in the process of UVA pretreatment followed by UVC inactivation. On the other hand, the reaction of highly reactive $\bullet\text{OH}$ and *E. coli* cells is supposed to severely damage the cells and significantly inactivate *E. coli*, as numerous studies on advanced oxidation processes (AOPs) for disinfection suggested (Cho et al., 2004, Chong et al., 2010, Malato et al., 2009). However, although $\bullet\text{OH}$ resulted from UVA pretreatment before UVC irradiation, during 30 minutes 365 nm UVA pretreatment with the UV fluence of 52 J/cm^2 , only 0.2 log inactivation on *E. coli* was achieved, indicating insignificant inactivation by UVA pretreatment. Thus it implies that during UVA pretreatment,

•OH might only damage the cellular functionality to induce nonlethal effect on *E. coli*, but not destruct the cells of *E. coli*. So that after UVA pretreatment, the damaged *E. coli* cells were not significantly inactivated, but became more vulnerable to the following UVC irradiation and also were no longer able to reactivate afterwards. This deduced mechanism is different from the role of •OH generated in AOPs for disinfection. Therefore, further investigation is needed to clarify the mechanism in the process of UVA pretreatment followed by UVC inactivation.

5.3.5 Roles of ROS on *E. coli* reactivation with UVA pretreatment

To explore the mechanism for significant reactivation suppression effect after the process of UVA pretreatment followed by UVC inactivation, it is necessary to examine the roles of ROS on *E. coli* reactivation with UVA pretreatment. Since only •OH, but not H₂O₂ or •O₂⁻, was proved to play a significant role for considerable inactivation improvement of *E. coli* with UVA pretreatment, the role of •OH radical on *E. coli* reactivation with UVA pretreatment was examined using mannitol as scavenger. As shown in Figure 5.10, after 365 nm UVA pretreatment followed by 265 nm UVC inactivation, the presence of mannitol in the system increased the photoreactivation of *E. coli* compare to that without scavenger, suggesting that •OH also played an important role for the reduced *E. coli* reactivation after UVC inactivation with prior UVA pretreatment.

Moreover, in the presence of mannitol, the inactivated *E. coli* was recovered to 20% in the first hour, then leveled off afterwards under the fluorescent lamps visible light. This trend is different from the *E. coli* concentration drop after 2.5 hours photoreactivation without scavenger, suggesting that by removing •OH in the system, *E. coli* was able to retain the photo repair ability, instead of complete loss of photo repair ability so that cannot tolerate the slight UVA in

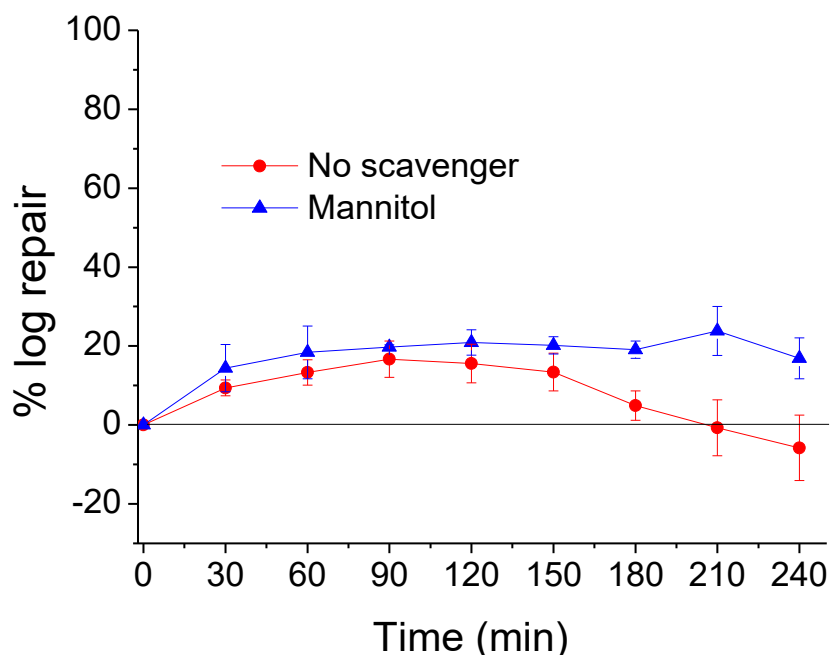


Figure 5.10 *E. coli* photoreactivation after 30 min 365 nm UVA pretreatment followed by 265 nm UVC inactivation for 3.3 log inactivation in the absence and presence of mannitol. Error bars represent the standard deviation for triplicate runs.

the emission of fluorescent lamps visible light after UVA pretreatment. Thus it further indicated that $\bullet\text{OH}$ may result from UVA pretreatment and then damage the cellular functionality to induce nonlethal effect, such as impaired photo repair systems, accounting for the significant reactivation suppression of *E. coli*.

5.3.6 Determination of ROS during UVA pretreatment on *E. coli*

Since $\bullet\text{OH}$ played an important role in the process of UVA pretreatment followed by UVC inactivation of *E. coli* for both considerable inactivation improvement and significant reactivation suppression, it is essential to quantitatively determine the $\bullet\text{OH}$ in order to clarify the mechanism. This process consists of two stages: UVA pretreatment and the following UVC

inactivation. So it is necessary to identify in which stage the $\bullet\text{OH}$ is produced and present before performing the measurement of $\bullet\text{OH}$.

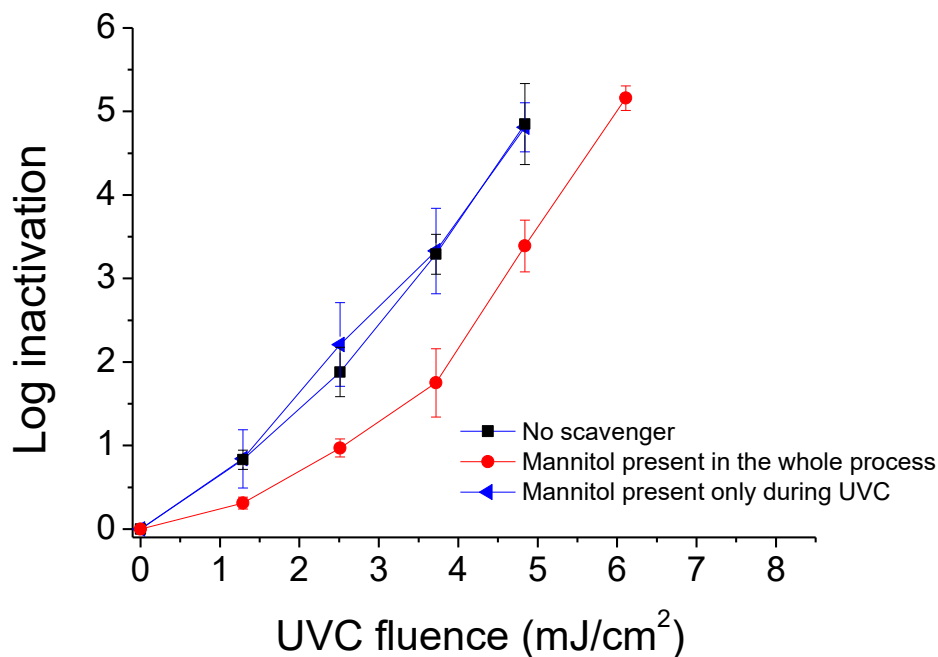


Figure 5.11 *E. coli* inactivation kinetics by 265 nm UVC irradiation after 30 min 365 nm UVA pretreatment in the presence of mannitol during different stages. Error bars represent the standard deviation for triplicate runs.

Mannitol (the scavenger of $\bullet\text{OH}$) was added into the system at different stages in the process of UVA pretreatment followed by UVC inactivation. The results are shown in Figure 5.11. When mannitol was present during the whole process, the *E. coli* inactivation kinetics significantly dropped, indicating the important role of $\bullet\text{OH}$ in the process of UVA pretreatment followed by UVC inactivation. However, when adding mannitol after UVA pretreatment to have it present only during the following UVC inactivation, it did not affect the kinetics of *E. coli* inactivation compared to that without scavenger. This observation suggested that *E. coli* cells were already impacted by $\bullet\text{OH}$ during the UVA pretreatment, so that they were no longer

protected even if removing $\bullet\text{OH}$ during the following UVC irradiation. Thus it demonstrated that $\bullet\text{OH}$ radicals were produced and present only during the UVA pretreatment but not during the following UVC inactivation.

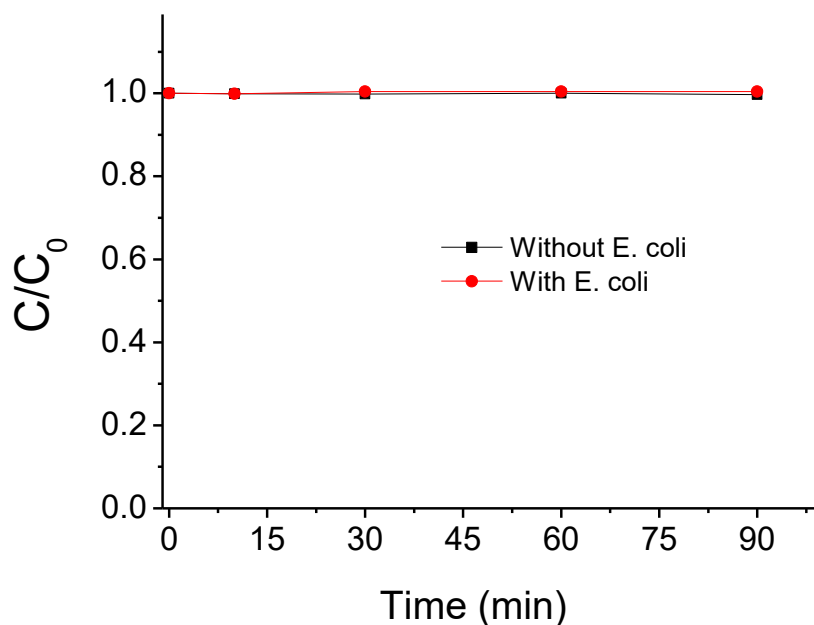


Figure 5.12 Carbamazepine (CBZ) degradation kinetics under 365 nm UVA irradiation in the presence and absence of *E. coli* in water.

Since $\bullet\text{OH}$ radicals were produced during the UVA pretreatment, a probe compound carbamazepine (CBZ) was utilized to indirectly determine the concentration of highly reactive $\bullet\text{OH}$ radicals in water. CBZ was mixed with *E. coli* suspension and then exposed to 365 nm UVA radiation. The degradation of CBZ in water was measured to determine the $\bullet\text{OH}$ concentration. The control experiment was conducted by stirring *E. coli* suspension with CBZ in dark. No change of *E. coli* concentration was observed during the control experiment (Figure B.5 in Appendix B), indicating that CBZ has no harmful effect to *E. coli* cells during the period of those tests with UVA irradiation. CBZ degradation kinetics in water under 365 nm UVA

irradiation is shown in Figure 5.12. No matter if *E. coli* presented in the system or not, no degradation of CBZ was observed, indicating no $\bullet\text{OH}$ radical present in water. On one hand, considering that in this system there are only UVA radiation and *E. coli* cells in water, this observation agrees with the fact that UVA radiation alone is not able to directly generate $\bullet\text{OH}$ radicals in water unless with photocatalysts (e.g. TiO_2) or chemicals (e.g. H_2O_2 , Cl_2) for AOPs (Andreozzi et al., 1999, Kabra et al., 2004, Wang and Xu, 2012). On the other hand, the scavenger experiments have demonstrated $\bullet\text{OH}$ radicals were generated in the system during UVA irradiation. Considering that these scavengers can remove the corresponding ROS both in water and in cells, no detection of $\bullet\text{OH}$ in water indicated that $\bullet\text{OH}$ radicals were produced and present in *E. coli* cells during UVA irradiation.

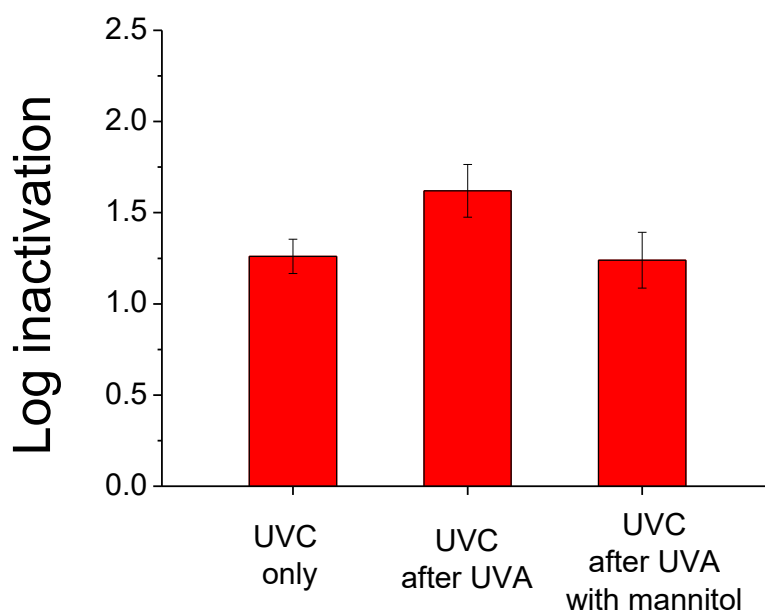


Figure 5.13 *E. coli* inactivation on agar plates by 265 nm UVC irradiation, by 365 nm UVA pretreatment followed by 265 nm UVC irradiation in the absence and presence of mannitol. Error bars represent the standard deviation for triplicate runs.

In the biological systems, $\bullet\text{OH}$ radicals have a very short *in vivo* half-life of 10^{-9} second and high reactivity (Novo and Parola, 2008, Sies, 1993). Thus $\bullet\text{OH}$ radical concentration in cells cannot be directly measured. In order to further verify that $\bullet\text{OH}$ radicals were generated in *E. coli* cells during UVA irradiation, the experiments on surface disinfection in the absence of water were designed and performed. As shown in Figure 5.13, *E. coli* on the surface of agar plate was exposed to 30 seconds 265 nm UVC irradiation and 1.2 log inactivation was observed. When applying 8 minutes 365 nm UVA pretreatment, the same 30 seconds 265 nm UVC irradiation achieved 1.6 log inactivation. This significant improvement of inactivation proved that the process of UVA pretreatment followed by UVC inactivation can also enhance the surface disinfection in addition to water disinfection. However, when mannitol treated *E. coli* cells underwent 8 minutes 365 nm UVA pretreatment, the following 30 seconds 265 nm UVC irradiation only resulted in 1.2 log inactivation, which was decreased to a level equivalent to that without UVA pretreatment. This observation indicated removal of $\bullet\text{OH}$ radicals in *E. coli* cells cancelled out the inactivation improvement by UVA pretreatment. Thus it further demonstrated the role of $\bullet\text{OH}$ in the UVA pretreatment and verified that $\bullet\text{OH}$ radicals were generated in *E. coli* cells but not in water.

Based on these experimental work, it is proved that $\bullet\text{OH}$ radicals, which accounted for the considerable inactivation improvement and significant reactivation suppression in the process of UVA pretreatment followed by UVC inactivation on *E. coli*, were generated in *E. coli* cells during UVA irradiation. Thus it reinforces the deduction for the role of ROS on *E. coli* inactivation and reactivation with UVA pretreatment: $\bullet\text{OH}$ radicals were generated inside *E. coli* cells, so that it only damaged the cellular functionality to induce nonlethal effect, e.g. reacting

with the repair enzymes in cells to impair photo repair systems, instead of destructing the *E. coli* cells from outside by $\bullet\text{OH}$ radicals generated in water in AOPs.

5.3.7 Proposed mechanisms for UVA pretreatment on microorganisms inactivation and reactivation

Based on the investigation of the roles of ROS on *E. coli* inactivation and reactivation and the determination of ROS in the process of UVA pretreatment followed by UVC inactivation, the mechanisms for UVA pretreatment is largely related to the biological processes and ROS in *E. coli* cells other than photochemical reactions during UVA irradiation. Thus the proposal of mechanisms has to be integrated to the context of fundamental biology.

In the biological context, reactive oxygen species (ROS) are formed as natural byproducts during the normal process of cell metabolism, especially in the process of aerobic energy metabolism in aerobic organisms (Novo and Parola, 2008). On one hand, the level of ROS in cells plays an important role in cell signaling for regulation of cellular functions and maintenance of homeostasis (Devasagayam et al., 2004). On the other hand, these ROS are very reactive and can react with cellular components, such as lipids, proteins and DNA, inducing adverse effects on the cells (Halliwell, 1996). Over millions of years' evolution, aerobic organisms have developed strategies and mechanisms at multiple levels to carefully control the generation of ROS and defense the deleterious effects of ROS in cells (Sies, 1993). However, when the cells are exposed to adverse environmental conditions, such as UV, heat or toxic chemicals, the delicately maintained balance of ROS in cells can be disturbed and ROS levels in cells can increase dramatically, resulting in significant oxidative damage to cell components that can impair cellular functions and even lead to cell death, as called oxidative stress (Devasagayam et al., 2004, Lushchak, 2014, Sies, 1986). Among these ROS, $\bullet\text{O}_2^-$ and H_2O_2 can be scavenged by

efficient enzymatic reactions using superoxide dismutase and catalase, respectively, which are contained in most organisms cells as one of defensive mechanisms to oxidative stress (Muller et al., 2007, Reiter et al., 1995). However, $\bullet\text{OH}$ radical cannot be eliminated by an enzymatic reaction. And also, $\bullet\text{OH}$ has a very short half-life of 10^{-9} second and a high reactivity. Thus it does not diffuse from the site of generation and can rapidly react with any surrounding molecules. $\bullet\text{OH}$ radical can damage all types of macromolecules in cells including: carbohydrates (leading to degradation), nucleic acids (leading to DNA damage), lipids (leading to cell membranes damage) and amino acids (leading to proteins denaturation and enzymes inactivation), making it a very dangerous radical to the organisms (Novo and Parola, 2008, Reiter et al., 1995).

Unlike the efficient inactivation by UVC radiation, UVA radiation is poorly absorbed by DNA and thus inefficient in inducing DNA damage for inactivation (Sinha and Hader, 2002). Usually it requires 10^5 times more UV fluence of UVA than UVC radiation to form pyrimidine dimers on DNA for inactivation due to the low absorption of UVA radiation by DNA (Gayan et al., 2014). However, UVA radiation at low UV fluence (compared to the high fluence requirement for inactivation) has been reported to induce sublethal effects on microorganisms especially on *E. coli*, such as growth delay, membrane damage, protein oxidation, decreased energy metabolism, mutation (Bosshard et al., 2010a, Bosshard et al., 2010b, Eisenstark, 1987, Girard et al., 2011, Hoerter et al., 2005, Oppezzo and Pizarro, 2001, Pizarro, 1995, Pizarro and Orce, 1988, Ramabhadran and Jagger, 1976). These sublethal effects are believed to relate to ROS and oxidative stress induced by UVA radiation (Cabiscol et al., 2000, Cadet et al., 2015, Hoerter et al., 2005, Smirnova and Oktyabrsky, 1994, Tyrrell and Keyse, 1990).

As such, by integrating the experimental results in this study with the biology context, the mechanisms for UVA pretreatment on microorganisms inactivation and reactivation can be proposed. For *E. coli* as a representative of bacteria, exposure to UVA radiation with a certain UV fluence can impact its cellular metabolism system, disturb the ROS balance in cells, resulting in significant increase of ROS levels, mostly $\bullet\text{OH}$ radical, to generate oxidative stress. The excess ROS in cells induce oxidative damage to cellular components, such as DNA self-repair enzymes, leading to enzymatic function failure and loss of self-repair ability. Thus *E. coli* becomes more vulnerable to UVC radiation, and is no longer able to reactivate afterwards due to the loss of ability to repair UVC-induce DNA damage. So that considerable inactivation improvement and significant reactivation suppression are achieved by the process of UVA pretreatment followed by UVC inactivation on *E. coli*. As for MS2 as a representative of virus, since it has only RNA inside a protein coat without cellular metabolism system, exposure to UV radiation only induces photochemical reactivations without additional biological effects. Therefore no inactivation improvement is achieved in the process of UVA pretreatment followed by UVC inactivation on MS2.

To the best of the author's knowledge, this is the first study to reveal these effects and mechanisms of UVA pretreatment on microorganisms inactivation and reactivation. Since UVA pretreatment can bring considerable inactivation improvement and significant reactivation suppression on bacteria, this discovery can significantly enhance UV water disinfection and thus may potentially save energy and reduce costs compared to conventional UVC disinfection.

5.3.8 Energy and cost analysis for UVA pretreatment

The process of UVA pretreatment followed by UVC inactivation is demonstrated to be able to significantly improve inactivation and eliminate reactivation of *E. coli* compared to UVC-

only inactivation. For potentially practical application, it is essential to evaluate the energy consumption and the cost of the system. Thus it is necessary to do energy and cost analysis for UVA pretreatment.

UVA pretreatment requires long time UVA irradiation (e.g. 10 ~ 30 minutes 365 nm UVA) for high UVA fluence in order to impact the *E. coli* cells and make them vulnerable to UVC inactivation. The UV fluence for 10 ~ 30 minutes 365 nm UVA exposure is 17 ~ 52 J/cm², which is 3 ~ 4 orders of magnitude higher than the UV fluence for UVC inactivation. This, however, would be balanced by the fact that UVA-LEDs have much higher output power and energy efficiency than UVC-LEDs, and are much more cost efficient. The 365 nm UVA-LED has over 2 orders of magnitude higher output power and energy efficiency compared to 265 nm UVC-LEDs used in this research (Table 5.2). Further, the cost of a 365nm UVA-LEDs is over 2 orders of magnitude lower than a 265 nm UVC-LED in terms of price per watt output in the market (i.e. \$2/W vs. \$1000/W in Table 5.2). Thus the higher energy efficiency and lower cost of UVA-LEDs may have a potential to compensate the higher UV fluence requirement for UVA pretreatment.

Table 5.2 Energy efficiency and cost of UV-LEDs used in this research

UV-LED	Wavelength (nm)	Input Power (W)	Output Power (W)	Energy efficiency	Price per UV-LED	Price per watt output
UVC-LED	265	2.73	0.01	0.3%	\$10	\$1000/W
UVA-LED	365	8.0	2.35	30%	\$5	\$2/W

In order to make to a fair comparison on energy and cost between UVC inactivation with UVA pretreatment and without UVA pretreatment, a given inactivation objective is set for these two processes, e.g. to achieve the same 6 log inactivation of *E. coli*. Based on the inactivation

kinetics (Table 5.1), with 30 minutes 365 nm UVA pretreatment (52 J/cm^2), 6 mJ/cm^2 265nm UVC radiation is able to achieve 6 log inactivation of *E. coli*, while without UVA pretreatment, 7.9 mJ/cm^2 UV fluence is required using 265 nm UVC-LED to achieve the same inactivation level. In addition to achieving the same inactivation of *E. coli*, the process of UVA pretreatment followed by UVC inactivation can also inactivate the repair ability and eliminate reactivation afterwards. For UVC-only inactivation, in order to overcome reactivation potential, extra UV fluence is needed to offset the reactivation. Taking reactivation into consideration, $30 \sim 40 \text{ mJ/cm}^2$ is needed to obtain 6 log inactivation of *E. coli* (Hoyer, 1998, Quek and Hu, 2008, Sommer et al., 2000). Thus it is assumed 30 mJ/cm^2 is required using 265 nm UVC-LEDs to achieve the equivalent inactivation effect as the process of 52 J/cm^2 365 nm UVA-LED pretreatment followed by 6 mJ/cm^2 265nm UVC-LED inactivation. Based on the aforementioned assumptions, the energy consumption can be calculated based on the energy efficiency of these UV-LEDs (Table 5.2). The results are presented in Table 5.3.

With 365 nm UVA-LED pretreatment, the energy consumption of 265 nm UVC-LED inactivation can be significantly decreased from 10 J/cm^2 to 2 J/cm^2 (Table 5.3) due to the effect of UVA pretreatment, which is 0.7 order of magnitude energy saving. However, 30 minutes 365 nm UVA-LED pretreatment consumes 173 J/cm^2 energy, which is higher than the energy saving on UVC-LED inactivation. Thus the total energy consumption is higher than that without UVA pretreatment. If reducing UVA pretreatment to 10 minutes (i.e. 17 J/cm^2 UVA radiation) with slightly increased UVC radiation (6.8 mJ/cm^2), the total energy consumption largely falls off to 59.3 J/cm^2 , but still higher than that without UVA pretreatment (Table 5.3). Thus although the high UVA fluence requirement ($3 \sim 4$ orders of magnitude higher than UVC fluence) can be largely compensated by the high energy efficiency of UVA-LED (2 orders of magnitude higher

Table 5.3 Energy consumption comparisons on 265 nm UVC-LED inactivation with and without 365 nm UVA-LED pretreatment. The third and fourth rows refer to 10 min, 30 min UVA pretreatment, respectively, in which the UV fluence data is derived from Table 5.1 for 6 log inactivation.

	UVA-LED energy consumption	UVC-LED energy consumption	Total energy consumption
265 nm UVC-LED (30 mJ/cm ²) inactivation	–	10 J/cm ²	10 J/cm ²
365 nm UVA-LED (17 J/cm ²) pretreatment followed by 265 nm UVC-LED (6.8 mJ/cm ²) inactivation	57 J/cm ²	2.3 J/cm ²	59.3 J/cm ²
365 nm UVA-LED (52 J/cm ²) pretreatment followed by 265 nm UVC-LED (6 mJ/cm ²) inactivation	173 J/cm ²	2 J/cm ²	175 J/cm ²

than UVC-LEDs), and further offset by 0.7 order of magnitude UVC energy saving due to the effect of UVA pretreatment, the total energy consumption is still 0.5 ~ 1 order of magnitude higher than without UVA pretreatment. Therefore, to take full advantage of UVA pretreatment, the system needs to be well designed by utilizing higher energy efficiency UVA sources and smart reactor designs. In addition, since there is UVA radiation in sunlight reaching on the surface of the earth, the unlimited cost-free sunlight could be a good alternative for UVA pretreatment.

Since UVC-LEDs are much more expensive than UVA-LEDs in terms of price per watt output (Table 5.2), the cost of UV-LEDs should be also taken into consideration for potentially

practical application. To deliver a given amount of UV fluence, it can be done by using more UV-LEDs with a shorter irradiation time for time efficiency, or using less UV-LEDs with a longer exposure time to trade off the cost of UV-LEDs with time. Thus in order to make a fair comparison on the cost of UV-LEDs, a given time, e.g. within 2 minutes, is set to accomplish the different processes of UV inactivation with and without UVA pretreatment in Table 5.3. For 265 nm UVC inactivation, in order to deliver 30 mJ/cm^2 fluence in 2 minutes, 0.25 mW/cm^2 fluence rate is needed for irradiation. Assuming all output from UV-LEDs is delivered to the water, and using the surface area of the water container (64 cm^2), the UV-LEDs with total output power of 16 mW are needed, which cost \$16 based on the UV-LED price per watts output (Table 5.2). Similarly, the cost of UV-LEDs for the process of UVA pretreatment followed by UVC inactivation is calculated and listed in Table 5.4. Note that for the process of UVA pretreatment followed by UVC inactivation, different exposure times are allocated to UVA and UVC irradiation within the total 2 minute time frame. Only the cases for the lowest overall costs of UV-LEDs are listed in Table 5.4.

In some cases with UVA pretreatment, the cost of UVC-LEDs can be cut off (e.g. from \$16 to \$11), however, the total cost of UVC- and UVA-LEDs for the whole process is still higher than that using UVC-LEDs alone (e.g. \$38 vs. \$16) (Table 5.4). It suggests that the lower price of UVA-LEDs compared to expensive UVC-LEDs used in this study does not compensate the cost due to high fluence requirement of UVA pretreatment. Therefore, for practical application, the system needs to be optimized by using cheaper UVA sources, even cost-free sunlight, and customized reactor designs for the high fluence requirement of UVA pretreatment.

Table 5.4 Cost of UV-LEDs for 265 nm UVC inactivation with and without 365 nm UVA pretreatment

	Cost of UVA-LEDs	Cost of UVC-LEDs	Total cost of UV-LEDs
2 minutes 265 nm UVC (30 mJ/cm ²)	—	\$16	\$16
80 s 365 nm UVA (17 J/cm ²) followed by 40 s 265 nm UVC (6.8 mJ/cm ²)	\$27	\$11	\$38
100 s 365 nm UVA (52 J/cm ²) followed by 20 s 265 nm UVC (6 mJ/cm ²)	\$66	\$19	\$85

5.4 Conclusions

In this chapter, a special combination of UV-LEDs with different wavelengths, i.e. UVA pretreatment followed by UVC inactivation, was thoroughly investigated using 365 nm UVA-LED and 265 nm UVC-LED for inactivation and reactivation of different types of microorganisms in water. The new effects and mechanisms of this process were revealed:

- (1) 365 nm UVA pretreatment dramatically improved the *E. coli* inactivation kinetics of 265 nm UVC. This improvement is due to the elimination of shoulder in the kinetics instead of altering the inactivation rate constant. 30 minutes 365 nm UVA pretreatment (52 J/cm²) improved the whole kinetics by 2.2 log inactivation.
- (2) The process of 365 nm UVA pretreatment followed by 265nm UVC inactivation significantly reduced the reactivation of *E. coli*. 30 minutes 365 nm UVA pretreatment

- (52 J/cm²) completely eliminated the reactivation of *E. coli* after 3.3 log inactivation by 265 nm UVC compared to 60 % reactivation without UVA pretreatment.
- (3) The process of 365 nm UVA pretreatment followed by 265nm UVC inactivation has no additional effect on coliphage MS2 with the UVA pretreatment up to 90 min (156 J/cm²).
- (4) Among reactive oxygen species (ROS), •OH radical, but not •O₂⁻ or H₂O₂, played an important role on the effect of UVA pretreatment on *E. coli* for considerable inactivation improvement and significant reactivation suppression. These •OH radicals were produced inside *E. coli* cells, but not in water, during UVA irradiation, instead of UVC irradiation.
- (5) The mechanisms for effects of UVA pretreatment were proposed: UVA irradiation with a certain fluence can impact the metabolism of bacteria, disturb the ROS balance in cells, resulting in increased ROS levels, mainly •OH radical, and oxidative damage to cellular components, such as DNA self-repair enzymes. After enzymes function failure and loss of self-repair ability, bacteria become more vulnerable to UVC inactivation, and are no longer able to reactivate afterwards.
- (6) Energy and cost analysis for UVA pretreatment suggested that the UVA-LED used in this study is not able to make the process economical due to the high fluence requirement for UVA pretreatment. For potentially practical application, it is encouraged to optimize the system by utilizing more energy efficient UVA sources, even unlimited cost-free sunlight, and smart reactor designs tailored for UVA pretreatment.

Chapter 6: Microorganisms inactivation by UV-LEDs pulsed irradiation

6.1 Introduction

In addition to wavelength diversity, another special feature of UV-LEDs is the ability to turn on and off with high frequency due to the nature of semiconductor devices. This feature allows UV-LEDs to easily generate pulsed irradiation which is not viable with UV mercury lamps. Although conventional xenon lamps are capable of emitting pulsed irradiation as well, the pulse pattern is less controllable and the power requirement is much higher compared to that of UV-LEDs. UV-LEDs offer high flexibility for pulse pattern with various frequencies and duty rates, and have low power requirement for operation, which brings broad potential on the application of UV-LEDs pulsed irradiation.

Pulsed irradiation from xenon lamps has been reported to be more effective and efficient for food decontamination and water disinfection compared to continuous UV irradiation from mercury lamps, as reviewed in Chapter 2. Since the newly emerging UV-LEDs are capable of pulsed irradiation with even more options on pulse pattern, it is reasonable to assume that similar enhanced germicidal effect may occur with UV-LEDs pulsed irradiation. On the other hand, the pulsed irradiation produced by xenon lamps is quite different from that of UV-LEDs in terms of emission spectrum, intensity, pulse frequency and duty rate (Song et al., 2016). Therefore, the same effect may not necessarily be observed through UV-LEDs pulsed irradiation and a thorough study is needed to examine the effect of UV-LEDs pulsed irradiation.

In this chapter, a robust comparison of disinfection efficiency between UV-LEDs continuous and pulsed irradiation was conducted to explore the potentially additional effect of pulsed irradiation. The equivalent UV fluence and exposure intensity for continuous and pulsed

irradiation were validated and applied to ensure a fair comparison. Several laboratory water and wastewater samples with different types of microorganisms including *E. coli*, coliphage MS2 and total coliform were examined to cover a range of water quality and microbial species. The effects of pulse patterns such as frequency and duty rate were also examined for UV-LEDs pulsed irradiation. The results were discussed and compared with the studies on conventional xenon lamps pulsed irradiation.

6.2 Experimental design

The 265 nm UV-LED (Table 3.1) was used to perform the tests on continuous and pulsed irradiation. A DC power supply (Aim TTI EX355R) was used to drive the UV-LED at a constant current of 350 mA for both continuous and pulsed irradiation. To generate pulsed irradiation, a fast solid-state relay (SSR, Crydom M-ODC5F) was used to switch the UV-LED on and off instantly. The frequency and duty rate were adjusted by a function generator (GW Instek AFG-2225) and an oscilloscope (GW Instek GDS-1102A-U) was used to measure the waveform of voltage for the UV-LED. The diagram of electronic circuit to generate UV-LED pulsed irradiation and a voltage waveform measured by oscilloscope are illustrated in Figure 6.1. Different levels of frequency (0.1, 1, 10, 100, 1k Hz) and duty rate (10, 25, 50, 75, 90%) were examined for UV-LEDs pulsed irradiation and compared with continuous irradiation. Frequency indicates the number of on-off cycles per second, while duty rate means the percentage of irradiation time in an on-off cycle (Figure 6.1b). In order to conduct a fair comparison of disinfection efficiency between continuous and pulsed irradiation, UV fluence was determined using two types of chemical actinometry, as described in Chapter 3, and then equalized for each irradiation condition by adjusting operation times.

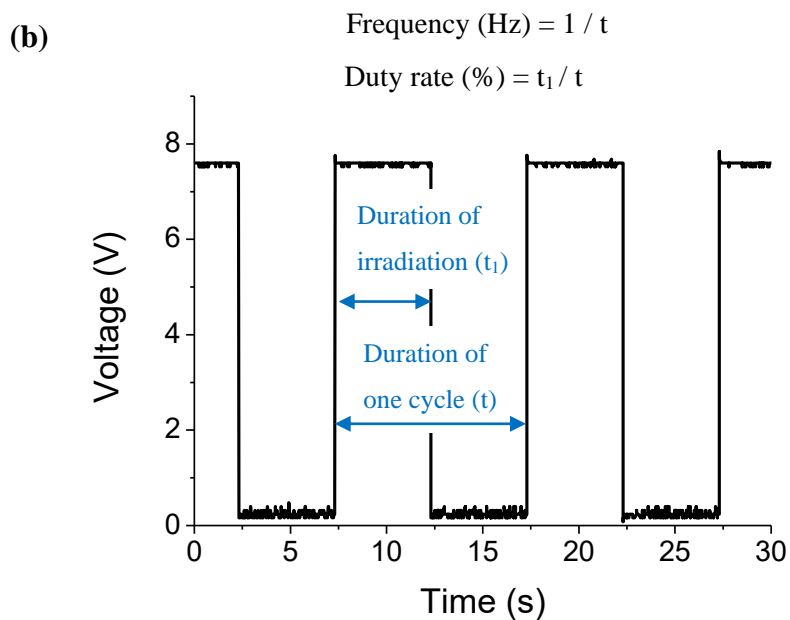
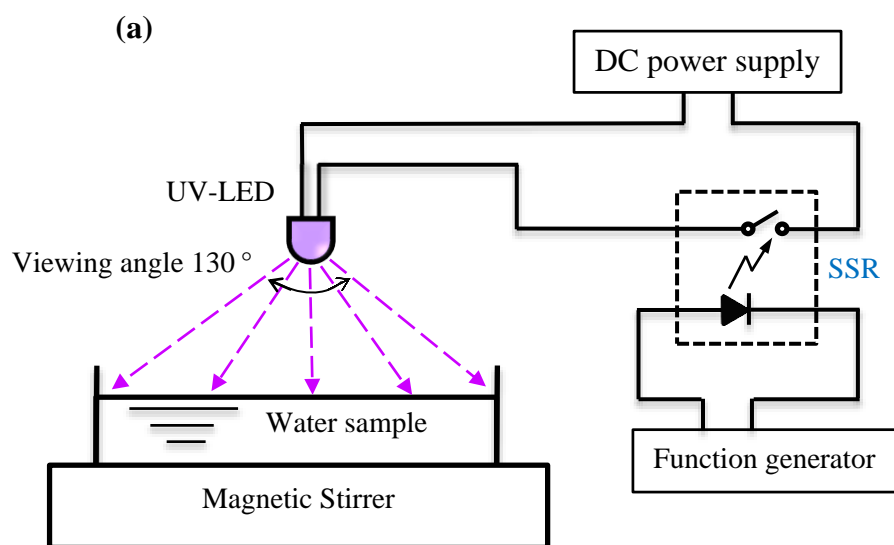


Figure 6.1 Schematic diagram of pulsed UV-LED circuit and experimental apparatus (a); illustration of voltage waveform for pulsed UV-LED irradiation at 0.1 Hz frequency and 50% duty rate (b).

6.3 Results and discussion

6.3.1 Determination of UV fluence for pulsed irradiation

Considering that during the pulse irradiation, the UV-LED is turned on and off repeatedly (Figure 6.1b), the operation time of pulsed irradiation has to be extended in order to achieve equivalent UV fluences as those of continuous irradiation. Based on the definition of duty rate (Figure 6.1b), the operation time of pulsed irradiation can be calculated. For example, pulsed irradiation with 50% duty rate requires theoretically twice longer operation time to emit equivalent UV fluence as that of continuous irradiation. In other words, to match the UV fluence of 40 seconds continuous irradiation, the operation time of pulsed irradiation at 50% duty rate is supposed to be 80 seconds (i.e. calculated operation time). However, the UV fluence results from actinometry did not agree well with this expectation. As shown in Table 6.1, all the pulsed irradiations at 50% duty rate with various frequencies for 80 seconds resulted in higher UV fluence than 40 seconds continuous irradiation by various degrees. Similar inconsistencies were also observed for pulsed irradiation at 10 Hz and various duty rates (Table 6.1). These inconsistencies on UV fluence needed to be addressed and considered before performing proper comparison on disinfection efficiency. Therefore, the voltage waveforms of UV-LED pulsed irradiation with various pulse patterns were examined and monitored by an oscilloscope.

Table 6.1 UV fluence results from iodide-iodate (KI) and ferrioxalate (FeO_x) actinometry for 265 nm UV-LED continuous and pulsed irradiation at various frequencies (Hz) and duty rates (%). Calculated operation time is based on the definition of duty rate (Figure 6.1b), adjusted operation time is based on actual UV fluence measurement in order to ensure the equivalent UV fluence between continuous and pulsed irradiation.

Irradiation mode	UV fluence based on calculated operation time		UV fluence based on adjusted operation time		
	Time (s)	Fluence (KI) (mJ/cm ²)	Time (s)	Fluence (KI) (mJ/cm ²)	Fluence (FeO _x) (mJ/cm ²)
Continuous	40	5.20 (±0.09)	40	5.20 (±0.09)	5.33 (±0.14)
Pulsed 0.1 Hz 50%	80	5.14 (±0.14)	80	5.14 (±0.14)	5.31 (±0.16)
Pulsed 1 Hz 50%	80	5.36 (±0.13)	79	5.25 (±0.16)	5.35 (±0.12)
Pulsed 10 Hz 50%	80	5.68 (±0.17)	73	5.22 (±0.08)	5.23 (±0.18)
Pulsed 100 Hz 50%	80	6.05 (±0.15)	70	5.29 (±0.12)	5.37 (±0.13)
Pulsed 1k Hz 50%	80	5.83 (±0.09)	71	5.19 (±0.10)	5.33 (±0.10)
Pulsed 10 Hz 90%	45	5.36 (±0.15)	43	5.10 (±0.14)	5.30 (±0.17)
Pulsed 10 Hz 75%	53	5.45 (±0.17)	50	5.09 (±0.13)	5.26 (±0.16)
Pulsed 10 Hz 25%	160	5.88 (±0.14)	139	5.12 (±0.10)	5.23 (±0.13)
Pulsed 10 Hz 10%	400	6.27 (±0.18)	333	5.22 (±0.19)	5.35 (±0.14)

As shown in Figure 6.2, the voltage waveforms of UV-LED when emitting pulsed irradiation are not perfect squares, although the function generator is set to output square waveforms. Instead, there is a slight peak at the beginning of each square waveform. This imperfection of voltage waveforms for pulsed UV-LED is probably due to the imperfection of UV-LED and DC power supply when operated in a fast-switch circuit. The measured waveforms

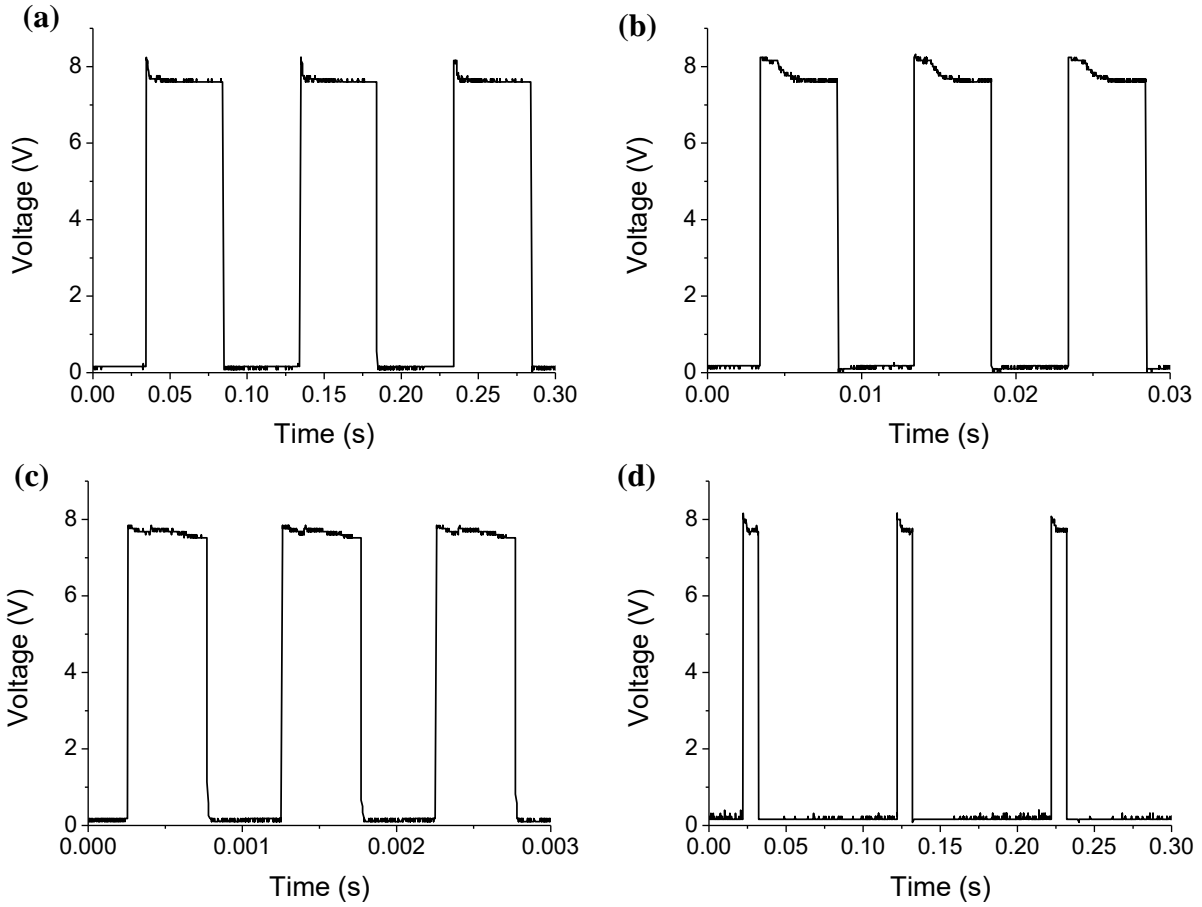


Figure 6.2 Measured waveforms of UV-LED pulsed irradiation at 50% duty rate with 10 Hz (a), 100 Hz (b) and 1k Hz (c), as well as at 10% duty rate with 10 Hz (d)

revealed the imperfection of the waveform under practical operating conditions, which could explain the inconsistency of UV fluence results based on calculated operation time for pulsed irradiation. The tiny peak at the beginning of each pulse contributed slightly stronger UV radiation intensity during that very short period, and the accumulation of these peaks resulted in a higher UV fluence for pulsed irradiation with calculated operation time. The measured voltage waveforms well explained and confirmed the UV fluence results from actinometry. Therefore, the operation time of UV-LED pulsed irradiation has to be adjusted, instead of using calculated

operation time, in order to deliver equivalent UV fluence between continuous and pulsed irradiation. Thus two different types of actinometry were used to double check the UV fluence of pulsed irradiation with adjusted operation time (Table 6.1) for equivalent UV fluence and accurate comparison of disinfection efficiency between continuous and pulsed irradiation. Moreover, the measured waveform from the oscilloscope also confirmed that the voltage of UV-LED during exposure period in pulsed irradiation (Figure 6.2) is equivalent to that of continuous irradiation (Figure B.6 in Appendix B), indicating that the current and intensity are also in an equivalent level when comparing the disinfection efficiency of UV-LED continuous and pulsed irradiation.

Once the equivalent UV fluence was confirmed for 265 nm UV-LED continuous and pulsed irradiation with various pulse patterns, the disinfection efficiency was compared for the inactivation of pure *E. coli* and MS2 in lab buffered water, as well as total coliform and *E. coli* in wastewater.

6.3.2 UV-LEDs pulsed irradiation on *E. coli* inactivation

With the equivalent UV fluence, the inactivation of *E. coli* showed comparable results under various frequencies and duty rates (Figure 6.3). The statistical analysis using two-tailed paired t-test showed no significant difference in the log inactivation between the continuous and pulsed irradiation with various frequencies of 0.1 Hz ($p=0.19$), 1 Hz ($p=0.06$), 10 Hz ($p=0.08$), 100 Hz ($p=0.07$), 1k Hz ($p=0.62$). As for the effect of duty rate, the inactivation results of only 90% and 75% duty rates were significantly different ($p=0.001$, 0.007 , respectively); however, instead of enhanced germicidal effect reported by few other studies (Li et al., 2010, Tran et al., 2014, Wengraitis et al., 2013), pulsed irradiation at 90% and 75% duty rate resulted in slightly lower inactivation compared to continuous irradiation at equivalent UV fluence. The results

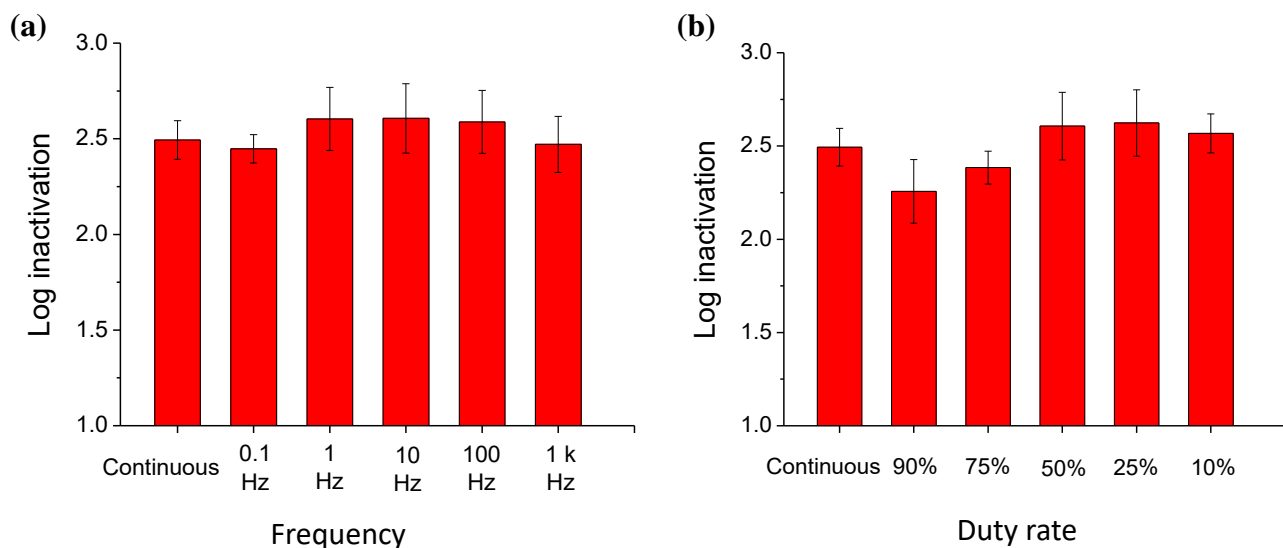


Figure 6.3 *E. coli* inactivation by 265 nm UV-LED continuous and pulsed irradiation with various pulse patterns at equivalent UV dose 4.9 mJ/cm²: (a) various frequencies at 50% duty rate; (b) various duty rates at 10 Hz frequency. Error bars represent the standard deviation for triplicate runs.

showed that 265 nm UV-LED continuous and pulsed irradiation induced comparable *E. coli* inactivation at various frequencies and duty rates, with the exception of 90% and 75% duty rate. As such, no significant enhanced germicidal effect on *E. coli* was observed for pulsed irradiation compared to continuous irradiation at equivalent UV fluence.

6.3.3 UV-LEDs pulsed irradiation on coliform inactivation in wastewater

Total coliform and *E. coli* in real wastewater were also used to examine the disinfection efficiency of UV-LEDs pulsed irradiation and effects of different pulse patterns at equivalent UV fluence. The results revealed comparable inactivation for both total coliform and *E. coli* under pulsed irradiation with various frequencies and duty rates (Figure 6.4). The statistical analysis showed no significant difference in terms of log inactivation between continuous and pulsed irradiation with each pulse pattern. The results on wastewater are fairly consistent with that of *E.*

coli in lab prepared water, both indicating comparable germicidal effect from 265 nm UV-LED pulsed irradiation over continuous irradiation at equivalent UV fluence.

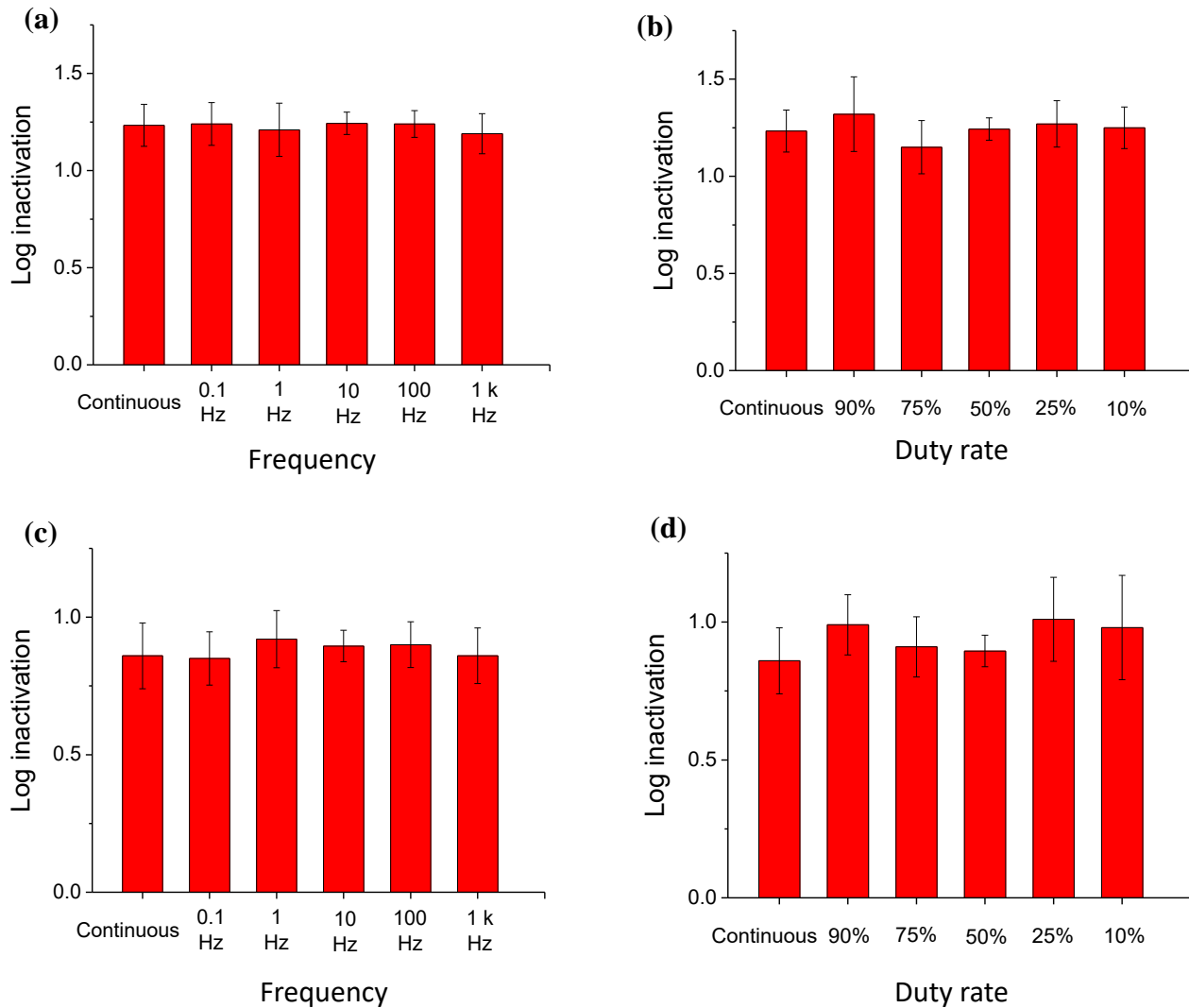


Figure 6.4 265 nm UV-LED continuous and pulsed irradiation with various pulse patterns at equivalent UV fluence 2.7 mJ/cm² on inactivation of total coliform (a, b) and *E. coli* (c, d) in wastewater. Error bars represent the standard deviation for triplicate runs.

These results are different from the two earlier studies that reported 3.8 times and 2.5 times greater germicidal efficiency by pulsed irradiation by 272 nm and 365 nm UV-LEDs, respectively, compared to those by continuous irradiation for *E. coli* inactivation (Li et al., 2010,

Wengraitis et al., 2013). Their observation seemed surprisingly impressive given the initially low output power UV-LEDs (a few milliwatts for UVC-LED and a few watts for UVA-LED), when compared to the powerful xenon lamps pulsed irradiation (6 MW per pulse) which showed to be only 2.4 times more effective than mercury lamps continuous irradiation (15 W) for *E. coli* inactivation (Bohrerova et al., 2008). The disagreement between our results and the ones reporting higher germicidal efficiency for pulsed UV-LEDs may be linked to: UV fluence determination method and disinfection medium. Firstly, the method for UV fluence determination may play a significant role on inconsistent results between this study and the two earlier studies. Li et al. (2010) measured the intensity of continuous and pulsed UV-LED irradiation and used calculated operation time for pulsed irradiation, e.g. the operation time for 50% duty rate pulse was twice as long as that of continuous irradiation, to estimate the same total fluence for all irradiation mode. Wengraitis et al. (2013), on the other hand, used radiometer for pulsed irradiation measurement but applied different UV fluence in pulse mode for examining disinfection efficiency and then divided the log inactivation by UV fluence for UV sensitivity comparison in terms of log inactivation per mJ/cm^2 .

In this study, two different types of chemical actinometry method were used to determine the exact UV fluence for continuous and pulsed irradiation. This was then used to adjust the operation time to ensure the equivalent UV fluence for different irradiation modes. As discussed earlier, due to the imperfection of pulse waveforms, UV-LED pulsed irradiation with theoretically calculated operation time may not guarantee the equivalent UV fluence. In fact, all of the pulsed modes using calculated operation time resulted in higher UV fluence than that of continuous irradiation which served as a baseline for disinfection efficiency comparison (Table 6.1). As a result, using theoretically calculated operation time for pulsed irradiation without

additional validation (such as chemical actinometry) may lead to an unfair comparison with continuous irradiation due to unequal UV fluence, thereby causing the discrepancy among previous studies (without UV fluence validation by actinometry) and this study. Secondly, the two initial studies applied UV-LEDs pulsed irradiation to *E. coli* biofilm on culture plates while in this study *E. coli* was suspended in water. The difference in disinfection medium may affect the inactivation results since it is reported that microorganisms cultivated on the surface may be less resistant to UV irradiation than those in liquid (Mamane-Gravetz et al., 2005).

6.3.4 UV-LEDs pulsed irradiation on MS2 inactivation

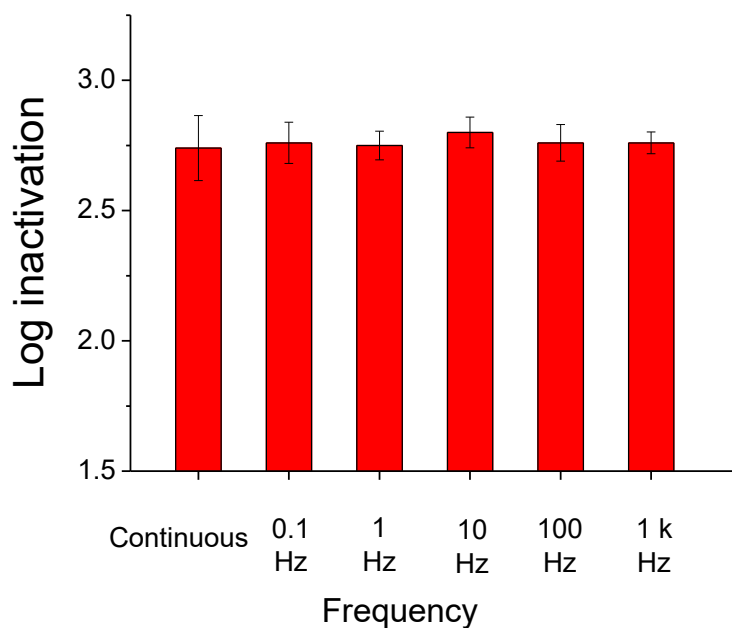


Figure 6.5 MS2 inactivation by 265 nm UV-LED continuous and pulsed irradiation with various frequencies at 50% duty rate with equivalent UV fluence 40 mJ/cm². Error bars represent the standard deviation for triplicate runs.

MS2 as a typical bacteriophage is commonly used to represent viruses for disinfection study. Thus, it was investigated in this study for the effect of UV-LED pulsed irradiation. As shown in Figure 6.5, 265 nm UV-LED pulsed irradiation with various frequencies achieved

almost identical MS2 inactivation and no significant difference was observed on log inactivation between pulsed and continuous irradiation at equivalent UV fluence. Once again, this observation agrees well with that of total coliform and *E. coli* in this study, suggesting comparable germicidal effect from 265 nm UV-LED pulsed and continuous irradiation at equivalent UV fluence.

To the best of the authors' knowledge, this is the first study using UV-LEDs to compare disinfection efficiency of continuous and pulsed irradiation on a virus. Hence, the only related research for comparison with our results would be those using conventional xenon lamps pulsed irradiation, which will be discussed later. On the other hand, MS2 is widely used as a model microorganism for the assessment of Reduction Equivalent Fluence (REF) for validation of UV reactors in North America (Mamane-Gravetz et al., 2005), i.e., the log inactivation of MS2 is used to validate the UV fluence of a reactor based on the known MS2 fluence-response kinetics. Our results of total coliform and *E. coli* reveal that the inactivation by UV-LEDs only depends on UV fluence regardless of continuous or pulsed irradiation. It is known that MS2 is more resistant to UV irradiation compared to *E. coli*. Thus, it is reasonable to assume that MS2 inactivation by UV-LEDs is also UV fluence-dependent no matter continuous or pulsed irradiation. Therefore, the identical MS2 inactivation (Figure 6.5) could be used to indicate that the UV fluence applied in each irradiation mode was equivalent, and to demonstrate that our method using chemical actinometry for UV fluence determination of UV-LED pulsed irradiation was valid.

6.3.5 Other features of UV-LEDs pulsed irradiation

Since during pulse irradiation, the UV-LED is turned on and off repeatedly, this may bring potentially more features of UV-LED pulsed irradiation compared to continuous irradiation.

Based on the adjusted operation time of pulsed irradiation for equivalent UV fluence with continuous irradiation (Table 6.1), the total UV-LED ‘on’ time during ‘on-off’ cycles in pulsed irradiation was compared with that of continuous irradiation and listed in Table 6.2.

Table 6.2 Comparisons of total UV-LED ‘on’ time between continuous and pulsed irradiation. Operation time for equivalent UV fluence is from Table 6.1. Total UV-LED ‘on’ time during ‘on-off’ cycles is based on the definition of duty rate in Figure 6.1(b).

Irradiation mode	Operation time (s) for equivalent UV fluence	Total UV-LED ‘on’ time (s) during ‘on-off’ cycles	UV-LED ‘on’ time saving (or input power saving)
Continuous	40	40	—
Pulsed 0.1 Hz 50%	80	40	0%
Pulsed 1 Hz 50%	79	39.5	1%
Pulsed 10 Hz 50%	73	36.5	9%
Pulsed 100 Hz 50%	70	35	13%
Pulsed 1k Hz 50%	71	35.5	11%
Pulsed 10 Hz 90%	43	38.7	3%
Pulsed 10 Hz 75%	50	37.5	6%
Pulsed 10 Hz 25%	139	34.8	13%
Pulsed 10 Hz 10%	333	33.3	17%

As shown in Table 6.2, to deliver the equivalent UV fluence, the total UV-LED ‘on’ times in pulsed irradiation modes are all less than that of continuous irradiation in varied degrees. For example, it took 70 seconds pulsed irradiation at 100 Hz frequency with 50% duty rate to deliver the equivalent UV fluence as 40 seconds continuous irradiation. However, the total UV-LED ‘on’ time during ‘on-off’ cycles in this pulse pattern was only 35 seconds (i.e. $70 \times 50\% = 35$),

which is 13% less than 40 seconds continuous mode. Similarly, pulsed irradiation at 10 Hz frequency with 10% duty rate can save 17% total UV-LED ‘on’ time (Table 6.2). Since the life span of UV-LED counts its total time being turned on, the UV-LED ‘on’ time saving indicates life span extension by up to 17% by operating UV-LED in pulsed irradiation compared to continuous irradiation, which could be a useful feature for certain applications. Moreover, the UV-LED only consumes input power during the period being turned on, so that the input power and energy consumption can be also saved by up to 17% when operating UV-LED in pulsed irradiation, thus potentially promoting low cost UV-LED applications without compromising inactivation effectiveness.

The temperature of UV-LED during operation is another important consideration for UV-LED application as it can significantly affect UV-LED’s performance and may cause the UV-LED overheating or even burning out if lack of proper thermal management (Kheyrandish et al., 2017). When performing the UV inactivation tests in this study, a heat sink was used to dissipate the heat generation during UV-LED operation (Figure 3.1). So that the temperature of UV-LED was well maintained below 25 °C during operation. However, the size of the heat sink is much larger than that of the UV-LED itself, which may impact the compactness of the UV-LED devices in practical application. In the absence of heat sink, the temperature of UV-LED during operation was measured and monitored (Figure 6.6). When running the UV-LED in continuous irradiation, its temperature quickly increased to 50 °C within 15 seconds, which reached the maximum operating temperature of this UV-LED and may cause burning out if proceeding. However, operation in pulsed irradiation at 50% duty rate with various frequencies reduced temperature rise to reach 45 °C after running for 25 seconds (Figure 6.6a). The trends on temperature change of the UV-LED in pulsed irradiation at 50% duty rate are all similar for

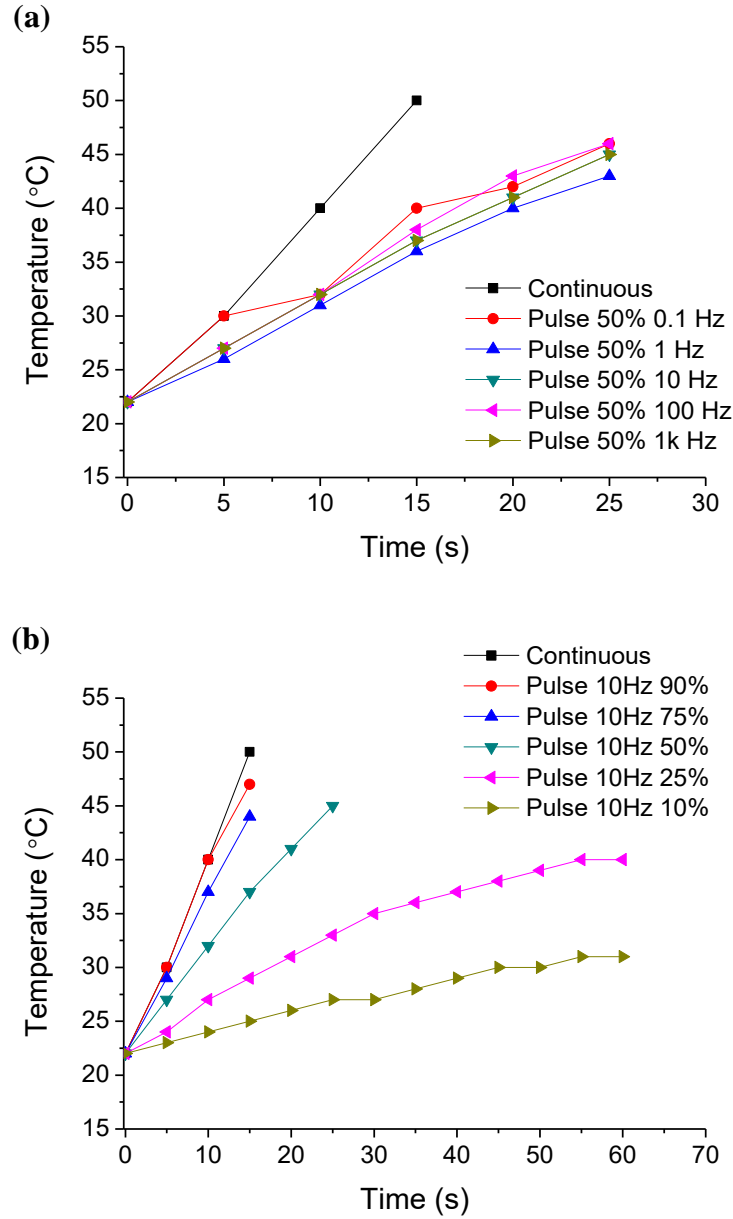


Figure 6.6 Temperature of UV-LED when operating in continuous and pulsed mode with various pulse patterns in the absence of heat sink: (a) various frequencies at 50% duty rate; (b) various duty rates at 10 Hz frequency.

various frequencies from 0.1 Hz to 1k Hz, indicating that frequency has little impact on the temperature control of UV-LED in pulsed irradiation. On the other hand, operating UV-LED in pulsed irradiation at 10 Hz frequency with various duty rates significantly decreased the

temperature climbing (Figure 6.6b). With lower duty rates, the UV-LED temperature rises were slower and reached lower temperature in the long time run. For pulsed irradiation at 10% duty rate, the temperature of UV-LED leveled off at 30 °C after running for 1 minute while it reached and stayed 40 °C for 25% duty rate. Therefore, operating UV-LED in pulsed irradiation provides the potential to eliminate the heat sink for more compact UV-LED devices and reactors while maintaining the comparable radiation intensity and inactivation effects.

In summary, although operating UV-LED in pulsed irradiation takes longer operation time than in continuous mode, it is in exchange for life span extension, energy consumption saving and better thermal management, which could be an option for certain applications that cost being higher priority of consideration than operation time such as remote small communities with scarce resources and limited water demand.

6.3.6 Discussion

The concept of pulsed UV irradiation originated from xenon lamps pulsed irradiation studies that reported enhanced germicidal effect by applying xenon lamps pulsed irradiation on various microorganisms for food decontamination and water disinfection (Bohrerova et al., 2008, Elmnasser et al., 2007, Gomez-Lopez et al., 2007). In this study, this concept was applied by using UV-LEDs in order to explore the potential of this important feature of UV-LEDs for a more effective inactivation of model bacteria and viruses. It was observed comparable disinfection efficiency by UV-LED pulsed and continuous irradiation, instead of enhanced germicidal effect, on the typical bacteria (total coliform, *E. coli*) and virus (coliphage MS2) inactivation. This is in agreement with a recent study of Gillespie et al. (2017), in which 405 nm LEDs pulsed exposure showed similar performance on bacterium *Staphylococcus aureus* inactivation when compared with the continuous exposure. The results might be largely

attributed to the substantial differences on pulse patterns between UV-LEDs pulsed irradiation and xenon lamps pulsed irradiation in terms of emission spectrum, intensity, pulse frequency and duty rate. The emission wavelengths from xenon lamps range from 100 nm to 1100 nm, including UV radiation, visible light and infrared with the output power of each pulse up to 35 MW. Each pulse has a duration of nanoseconds to milliseconds and typically 1 to 20 pulses are emitted in one second (Oms-Oliu et al., 2010). On the other hand, UV-LEDs emit nearly monochromatic radiation at a selectable wavelength with the output power of up to dozens milliwatts for UVC-LED or several watts for UVA-LEDs (Note that UV-LEDs are still at the early development stages and have relatively low output). The pattern of UV-LEDs pulsed irradiation is fully adjustable in terms for frequency and duty rate with a wide range. Since pulse patterns play an important role for enhanced germicidal effect by xenon lamps pulsed irradiation (Elmnasser et al., 2007), it is necessary to distinguish and identify which patterns result in the enhanced germicidal effect by xenon lamps pulsed irradiation in order to interpret the observation on UV-LEDs pulsed irradiation and explore its potential.

Many studies have compared disinfection efficiency between xenon lamps pulsed irradiation and mercury lamps continuous irradiation and proposed the possible mechanisms to interpret enhanced germicidal effects from xenon lamps pulsed irradiation. Literally, pulsation was regarded as the factor accounting for xenon lamps' enhanced disinfection. However, three major differences are integrated together in xenon lamps pulsed irradiation when comparing with mercury lamps continuous irradiation: very broad spectrum, much higher intensity, and pulsed radiation emission, which cannot be isolated to differentiate and identify the exact role of pulsation. For UV-LEDs irradiation in this study, the wavelength, UV fluence, and intensity during exposure period were all kept the same for the pulsed and continuous irradiation.

Therefore, such experiments provided a unique opportunity to distinguish the effect of pulsed wave on microorganisms inactivation. The results in this study reveal that applying the same amount of UV irradiation with the same UV wavelength and intensity in the repeated pulse is not able to induce additional inactivation effect compared to applying UV irradiation continuously. This information not only encourages a better understanding of pulsed UV irradiation inactivation of microorganisms, but also has important implications on the application of UV-LEDs for disinfection.

Previous studies borrowed the inactivation mechanisms from xenon lamps pulsed irradiation to promote UV-LEDs pulsed irradiation inactivation, suggesting that UV-LEDs pulsed irradiation may also induce additional cellular damage by repeated pulse disturbance of UV irradiation (Li et al., 2010, Tran et al., 2014, Wengraitis et al., 2013). However, such interpretation of UV-LEDs pulsed irradiation may not be appropriate due to the substantial differences of the pulse patterns between UV-LEDs and xenon lamps as discussed above. UV radiation not only induces photochemical reactions on cellular components, but also may impact biological processes in the cells (Harm, 1980). Thus, the repeated pulse from UV irradiation may induce stress and turbulence on the biological processes in the cells and may potentially impact the activity of the cells in addition to photochemical reactions with DNA or RNA. However, considering the significantly low output power of the current UV-LEDs compared to that of xenon lamps, the mild stress and turbulence on the cells from UV-LEDs pulsed irradiation is probably not sufficient to induce additional lethal effects such as photophysical and photothermal damage to the cells. Therefore, no additional inactivation is observed in both this study and a recent study of Gillespie et al. (2017) when applying UV-LEDs pulsed irradiation to either bacteria or virus.

Since applying UV irradiation in the repeated pulse is not able to induce additional lethal effects compared to applying the same UV irradiation continuously, the reported enhanced germicidal effect from xenon lamps pulsed irradiation might be largely attributed to extremely high intensity. The peak power of xenon lamps pulsed irradiation is typically in megawatt (MW) range and can be up to 35 MW (Oms-Oliu et al., 2010), which is around 9 orders of magnitude higher than that of current UVC-LEDs (i.e. MW vs. mW). Firstly, at very high UV intensity, multiphoton absorption by one molecule may happen due to very high photon flows, which breaks down the Second Law of Photochemistry under the normal conditions with regular UV lamps (Bolton and Cotton, 2008). Secondly, it is reported that applying the same UV fluence with higher order of magnitude intensity can achieve higher inactivation than that with lower order of magnitude intensity (Sommer et al., 1998). Thirdly, such a strong power delivered in a very short time (nanoseconds to milliseconds for each pulse) is probably capable to not only result in severe impact on the cells of microorganisms, but also cause local overheating of the cells due to the huge amount of energy, which were observed microscopically by some studies on xenon lamps and proposed to be photophysical and photothermal effects, respectively (Elmnasser et al., 2007, Krishnamurthy et al., 2010, Wekhof et al., 2001). Therefore, the enhanced germicidal effect was extensively observed by xenon lamps pulsed irradiation in previous studies but not by UV-LEDs pulsed irradiation in this study.

The understanding of xenon lamps and UV-LEDs pulsed irradiation on microorganisms inactivation has important implications on the application of UV-LEDs for disinfection. Since high intensity of UV irradiation probably plays a significant role to enhance the inactivation efficiency while repeated pulse does not, it would be ideal to apply high intensity UV irradiation continuously to maximize the inactivation efficiency and to reduce the required operation time

than applying pulsed irradiation. However, the continuous irradiation in high intensity may not be always practical due to the significant heat generation for high output power UV sources such as xenon lamps. Operating the high output power UV sources in pulsation allows a better thermal management due to a short pulse duration and a cooling period between each pulse while maximizing the intensity during the pulse (Krishnamurthy et al., 2004). Thus, this concept could encourage the manufacturing and application of high output power UV-LEDs. The newly emerging UV-LED is still in its infancy and currently the wall plug efficiency of UV-LEDs is relatively low at less than 10% (Harris et al., 2013). As a result, majority of the input power is converted into heat during UV-LEDs operation. Moreover, the tiny area of the diodes (typically several mm²) makes it difficult to efficiently dissipate the generated heat, which brings issues on overheating of UV-LEDs and limits the development and application of high output power UV-LEDs. The findings in this study suggest that pulsed irradiation could be a promising way to apply high output power UV-LEDs. When operating in pulsed irradiation, the heat is only generated during the short pulse and there is a cooling period between each pulse, thus temperature of the diodes could be maintained below the critical damage threshold to protect the UV-LEDs and extend the lifetime. Moreover, the high intensity during the short pulse has a potential to enhance the inactivation, provided that the output power of UV-LEDs is continuously improved and the intensity reaches a certain threshold, likely to a level comparable to that of xenon lamps pulsed irradiation. Therefore, the development and application of high output UV-LEDs in pulsed irradiation is encouraged to capitalize on this important feature of UV-LEDs.

6.4 Conclusions

In this chapter, UV-LEDs continuous and pulsed irradiation were compared for the inactivation of pure *E. coli* and MS2 in buffered lab water as well as wild *E. coli* and total coliform in wastewater. Through these comparisons, the role of pulsed irradiation on microorganisms inactivation was distinguished. And also, more features of UV-LED pulsed irradiation were revealed:

- (1) The comparisons of UV-LED continuous and pulsed irradiation were based on the equivalent UV fluence which was validated by two different types of chemical actinometry. The operation time of pulsed irradiation has to be adjusted to match the equivalent UV fluence with continuous irradiation instead of using theoretically calculated operation time.
- (2) Comparable inactivation was observed by 265 nm UV-LED continuous and pulsed irradiation with various frequencies (0.1, 1, 10, 100, 1k Hz) and duty rates (10, 25, 50, 75, 90%) for both typical bacteria (coliform, *E. coli*) and virus (MS2) in buffered lab water and wastewater under equivalent UV fluence.
- (3) Operating UV-LED in pulsed irradiation takes longer operation time than in continuous mode, but it is in exchange for life span extension, energy consumption saving and better thermal management.
- (4) At current UV-LEDs outputs the continuous and pulsed irradiation can be used to obtain similar inactivation but pulsed irradiation can help better thermal management for high output UV-LEDs.

Chapter 7: Conclusions and recommendations

7.1 Overall conclusions

This research explored the potential for the application of the emerging UV-LEDs for water disinfection with the focus on two special features of UV-LEDs: multiple wavelengths and pulsed irradiation. The impacts of UV-LEDs multiple wavelengths and pulsed irradiation on microorganisms inactivation were investigated thoroughly by applying various wavelengths combinations and pulse patterns on different types of microorganisms. Based on the studies performed in this research, following conclusions were derived:

(1) UV-LEDs multiple wavelengths:

Unlike the fixed spectrum of polychromatic radiation from medium pressure mercury lamps, the effects of UV-LEDs multiple wavelengths depend on the wavelength combinations among UVA (315 – 400 nm), UVB (280 – 315 nm) and UVC (200 – 280 nm) and the manner to apply different wavelengths, as well as the different types of microorganisms:

- Combinations of UVC and UVB radiation simultaneously or sequentially on bacteria or viruses always achieve additive effect on inactivation without additional effect due to the same type of DNA damage induced by UVC/UVB and the related photochemical reactions following the Second Law of Photochemistry.
- Combining UVA with UVC or UVB simultaneously or applying UVA after UVC/UVB reduce the overall disinfection efficacy on bacterium *E. coli* due to the DNA repair in bacteria cells and the photoreactivation effect of UVA radiation. On the other hand, such

combinations have only additive effect on phage MS2 inactivation due to the absence of biological processes such as photoreactivation in viruses.

- Applying UVA before UVC with a certain UVA fluence as pretreatment can dramatically improve UVC inactivation kinetics and significantly reduce reactivation afterwards on bacterium *E. coli*, but not on virus MS2. 365 nm UVA pretreatment with UV fluence of 52 J/cm² can improve the whole 265 nm UVC inactivation kinetics of *E. coli* by 2.2 log, and completely eliminate the reactivation of bacterium *E. coli* compared to 60% reactivation after UVC-only inactivation.

(2) UV-LEDs pulsed irradiation:

Unlike enhanced germicidal effect from xenon lamps pulsed irradiation compared to mercury lamps continuous irradiation, no additional effect was achieved by UV-LEDs pulsed irradiation compared to UV-LEDs continuous irradiation.

- Comparable inactivation was observed by 265 nm UV-LED continuous and pulsed irradiation with various frequencies (0.1, 1, 10, 100, 1k Hz) and duty rates (10, 25, 50, 75, 90%) for both typical bacteria (coliform, *E. coli*) and virus (MS2) in buffered lab water and wastewater under equivalent UV fluence.
- Applying the same amount of UV radiation with the same UV wavelength and intensity in the repeated pulse always achieves comparable inactivation effect as applying the same UV radiation continuously.
- At current UV-LEDs outputs the continuous and pulsed irradiation can be used to obtain similar inactivation but pulsed irradiation can help towards better thermal management for high output UV-LEDs.

(3) The mechanism for additional effects from UV-LEDs multiple wavelengths:

The effects of UVA pretreatment on inactivation of bacterium *E. coli* were firstly revealed in this research for considerable inactivation improvement and significant reactivation suppression. The mechanisms were investigated and proposed through detailed experimental work:

- Reactive oxygen species (ROS), mainly $\bullet\text{OH}$, but not $\bullet\text{O}_2^-$ or H_2O_2 , played an important role on the effect of UVA pretreatment on *E. coli* for considerable inactivation improvement and significant reactivation suppression. These $\bullet\text{OH}$ were produced inside the *E. coli* cells, but not in water, during UVA irradiation, instead of UVC irradiation.
- During UVA pretreatment, $\bullet\text{OH}$ generated in *E. coli* cells only damage the cellular functionality to induce nonlethal effect on *E. coli*, such as impairing self-repair systems, instead of inflicting damage to the *E. coli* cell structure from outside by $\bullet\text{OH}$ generated in water in advanced oxidation processes (AOPs).
- The mechanisms for the effects of UVA pretreatment were proposed: UVA irradiation with a certain fluence can impact the metabolism of bacteria, disturb the ROS balance in cells, resulting in increased ROS levels, mainly $\bullet\text{OH}$, and oxidative damage to cellular components, such as DNA self-repair enzymes. After enzymes function failure and loss of self-repair ability, bacteria become more vulnerable to UVC inactivation, and are no longer able to reactivate afterwards.

7.2 Contributions and significance of this research

This research was an initiative to explore the potential to capitalize on the two important features of emerging UV-LEDs, multiple wavelengths and pulsed irradiation, for water

disinfection. The outcome of this research not only can serve as a starting point to develop effective and efficient systems for practical application of UV-LEDs, but also contribute to the fundamental knowledge on the effects of UV radiation on bacterial cells:

First, utilizing the wavelength diversity of UV-LEDs, this research revealed the effects of UV wavelength combinations among UVA, UVB and UVC on microorganisms inactivation, which are not available among previous studies on polychromatic radiation from medium pressure mercury lamps due to the fix spectrum. Thus, it allows understanding of the biological effects of UV radiation with different wavelength combinations.

Second, the effects and mechanisms of UVA pretreatment on microorganisms inactivation were revealed in this research, especially on bacterium *E. coli* for considerable inactivation improvement and significant reactivation suppression. This finding expands the existing knowledge on biological effects of UVA radiation. As summarized in Table 7.1, the effect of UVA radiation on bacterium *E. coli* inactivation depends on the UV fluence and the manner in which UVA is applied. This research not only reinforces the previous understanding on UVA effect on the inactivation of microorganisms, but also extends it with a newly discovered biological effect of UVA radiation.

Third, utilizing the special feature of UV-LEDs on pulsed irradiation, the role of pulsed irradiation on microorganisms inactivation was distinguished and identified through detailed and well-controlled comparisons between UV-LEDs continuous and pulsed irradiation, which is not viable with xenon lamps pulsed irradiation. The findings on UV-LEDs pulsed irradiation not only clarify the effect of pulsation on UV disinfection, but also promote a better understanding on xenon lamps pulsed irradiation inactivation.

Table 7.1 Summary of effects and mechanisms of applying UVA 365 nm on bacterium *E. coli* inactivation in different manners with different ranges of UV fluence.

Manner to apply UVA	UVA fluence	Effect	Mechanism	Note
Apply UVA after UVC	0 ~ 10 J/cm ²	Reactivation	Photo repair of UV-damaged DNA by photo-activated repair enzymes	Based on this study and previous studies
Apply UVA before UVC	10 ~ 100 J/cm ²	Improve inactivation and reduce reactivation	UVA impacts cells metabolism, disturbs ROS balance in cells, resulting increased ROS levels in cells and oxidative damage to DNA repair enzymes, leading to loss of self-repair ability and vulnerability to UV inactivation	Revealed in this study
Apply UVA only	> 100 J/cm ²	Inactivation	DNA damage due to photochemical reactions	Based on fundamental UV disinfection

The contributions through this research are of considerable significance for both engineering application in practice and future research in academia:

The findings in the research can serve as a starting point to develop effective and efficient systems for practical application of UV-LEDs. Based on the findings in this research, some considerations should be taken into account for UV-LEDs reactor designs:

- 1) When combining UVC- and UVB-LEDs in a disinfection reactor, the inactivation effect of each wavelength can be simply added up for overall inactivation effect.
- 2) It is not recommended to combine UVA-LEDs with UVC-/UVB-LEDs simultaneously or apply UVA-LEDs after UVC-/UVB-LEDs, because the photoreactivation effect of UVA may reduce the overall inactivation effect.
- 3) For the reactor designs on UVA pretreatment prior to UVC/UVB inactivation, in order to take full advantage of UVA pretreatment, the systems should be carefully optimized by taking energy consumption and cost of UVA sources into consideration.
- 4) To utilize high output UV-LEDs, operation in pulsed irradiation can be an alternative for better thermal management, although it may take longer operation time.

The unique characteristics of UV-LEDs compared to traditional UV mercury lamps, such as compactness, portability, robustness, wavelength diversity, and pulsed irradiation, provide flexible and diverse options to novel reactor designs. These information regarding the effects of UV-LEDs multiple wavelengths and pulsed irradiation derived from this research is of immense importance to take full advantage of the features of UV-LEDs for practical application.

The discovery of effects and mechanisms of UVA pretreatment on microorganisms inactivation opens the door for new biological effects of UVA radiation. Based on the proposed mechanisms in this research, $\bullet\text{OH}$ generated in *E. coli* cells accounts for the effects of UVA pretreatment through oxidative damage to DNA repair enzymes for nonlethal effect. On the other hand, $\bullet\text{OH}$ is highly reactive and can indiscriminately react with any surrounding molecules to

induce damage in cells. Thus, once excess $\bullet\text{OH}$ is generated in cells under UVA irradiation, they most likely damage other cellular components as well for more biological effects to be discovered. Since UVA pretreatment can achieve nonlethal effect on *E. coli* cells to affect the cellular functionality without killing them, there is a potential on utilizing UVA radiation to purposely alter the cells functionality without killing the cells. This potential could bring impact on the field of microbiology and medicine, and hence catalyze new applications of UVA radiation to more fields.

7.3 Recommendations for future work

This research is an exploratory study aiming to thoroughly investigate the potential on capitalizing the two important features of UV-LEDs. Considering the wide range in UV wavelength (200 ~ 400 nm) and a large variety of microorganisms, it is infeasible to cover all the UV wavelengths and all types of microorganisms in one study. Instead, this study selected some representative UV wavelengths in different UV ranges and the typical microorganisms of different types. Although the findings can be reasonably applied to a larger range of UV wavelengths and microorganisms that are not limited to the specific wavelengths and microorganisms in this research, it is highly recommended to test more wavelengths, e.g. UVA-LEDs with longer wavelengths that have higher output power with lower price, and more microorganisms, especially UV-resistant microorganisms such as bacterial spores, viruses, protozoa, to more confidently extend the findings in this research to a wider range of UV wavelengths and a larger variety of microorganisms. Similar as action spectrum (i.e. relative response versus wavelength) of UVC inactivation, the effect of UVA pretreatment may also have action spectrum with a potential peak UVA wavelength for most efficient pretreatment. Thus it is highly encouraged to examine more UVA wavelengths and establish action spectrum of UVA

pretreatment, which is of great importance for further understanding and application of UVA pretreatment.

Moreover, the effects and mechanisms of UVA pretreatment on microorganisms inactivation were firstly revealed in this study and there is little related information in literature, thus further investigation is needed for a thorough understanding on the effects and mechanisms of UVA pretreatment. The observations in this research suggested that the effects of UVA pretreatment on *E. coli* inactivation and reactivation are UV fluence-dependent with a threshold to take effect, thus it would be of great interest to investigate the quantitative relationships among UVA fluence, the damage on DNA repair systems, and the extent on inactivation improvement and reactivation suppression. Once determined, these quantitative relationships could also promote a better understanding on the related mechanisms.

Furthermore, since the proposed mechanisms of UVA pretreatment largely involve the biological processes such as metabolism and reactive oxygen species (ROS) in cells, it is encouraged to further investigate UVA pretreatment mechanisms from the view of molecular microbiology. Due to the complexity of physiological processes that occur in microorganisms, it is necessary to utilize advanced techniques to detect the cellular components such as DNA, proteins, enzymes in cells in order to further interpret the mechanisms of UVA pretreatment in the molecular level.

Last but not least, research on UV-LEDs reactor and system designs is highly encouraged for practical application of UV-LEDs. The massive special features of UV-LEDs not only make them a promising alternative to conventional UV sources such as mercury lamps, but also could open the door to new applications of UV-LEDs. Thus it is highly recommended to take full

advantage of the special features of UV-LEDs for creative reactor designs and novel applications.

Bibliography

- Allied Analytics LLP, 2014. Global UV Disinfection Equipment Market - Size, Share, Global Trends, Company Profiles, Analysis, Segmentation and Forecast, 2013 - 2020. Research and Markets. <http://www.researchandmarkets.com/reports/3066124/> (Retrieved on Jan.18, 2018).
- Adams, M.H., 1959. Bacteriophages. Interscience Publishers, New York.
- Andreozzi, R., Caprio, V., Insola, A. and Marotta, R., 1999. Advanced oxidation processes (AOP) for water purification and recovery. *Catalysis Today*. 53(1), 51-59.
- Aoyagi, Y., Takeuchi, M., Yoshida, K., Kurouchi, M., Yasui, N., Kamiko, N., Araki, T. and Nanishi, Y., 2011. Inactivation of Bacterial Viruses in Water Using Deep Ultraviolet Semiconductor Light-Emitting Diode. *Journal of Environmental Engineering-Asce*. 137(12), 1215-1218.
- APHA, AWWA and WEF, 2012. Standard methods for the examination of water and wastewater, 22nd edition: 9221C, 9223B. American Public Health Association (APHA): Washington, DC, USA.
- Aravind, L., Walker, D.R. and Koonin, E.V., 1999. Conserved domains in DNA repair proteins and evolution of repair systems. *Nucleic Acids Research*. 27(5), 1223-1242.
- Autin, O., Romelot, C., Rust, L., Hart, J., Jarvis, P., MacAdam, J., Parsons, S.A. and Jefferson, B., 2013. Evaluation of a UV-light emitting diodes unit for the removal of micropollutants in water for low energy advanced oxidation processes. *Chemosphere*. 92(6), 745-751.
- Beck, S.E., Rodriguez, R.A., Linden, K.G., Hargy, T.M., Larason, T.C. and Wright, H.B., 2014. Wavelength Dependent UV Inactivation and DNA Damage of Adenovirus as Measured by

- Cell Culture Infectivity and Long Range Quantitative PCR. *Environmental Science & Technology*. 48(1), 591-598.
- Beck, S.E., Ryu, H., Boczek, L.A., Cashdollar, J.L., Jeanis, K.M., Rosenblum, J.S., Lawal, O.R. and Linden, K.G., 2017. Evaluating UV-C LED disinfection performance and investigating potential dual-wavelength synergy. *Water Research*. 109, 207-216.
- Beck, S.E., Wright, H.B., Hargy, T.M., Larason, T.C. and Linden, K.G., 2015. Action spectra for validation of pathogen disinfection in medium-pressure ultraviolet (UV) systems. *Water Research*. 70, 27-37.
- Bohrerova, Z. and Linden, K.G., 2007. Standardizing photoreactivation: Comparison of DNA photorepair rate in *Escherichia coli* using four different fluorescent lamps. *Water Research*. 41(12), 2832-2838.
- Bohrerova, Z., Shemer, H., Lantis, R., Impellitteri, C.A. and Linden, K.G., 2008. Comparative disinfection efficiency of pulsed and continuous-wave UV irradiation technologies. *Water Research*. 42(12), 2975-2982.
- Bolton, J.R. and Cotton, C.A., 2008. *The Ultraviolet Disinfection Handbook*. American Water Works Association, Denver.
- Bolton, J.R. and Linden, K.G., 2003. Standardization of methods for fluence (UV dose) determination in bench-scale UV experiments. *Journal of Environmental Engineering-Asce*. 129(3), 209-215.
- Bolton, J.R., Stefan, M.I., Shaw, P.S. and Lykke, K.R., 2011. Determination of the quantum yields of the potassium ferrioxalate and potassium iodide-iodate actinometers and a method for the calibration of radiometer detectors. *Journal of Photochemistry and Photobiology a-Chemistry*. 222(1), 166-169.

- Bosshard, F., Bucheli, M., Meur, Y. and Egli, T., 2010a. The respiratory chain is the cell's Achilles' heel during UVA inactivation in *Escherichia coli*. *Microbiology-Sgm.* 156, 2006-2015.
- Bosshard, F., Riedel, K., Schneider, T., Geiser, C., Bucheli, M. and Egli, T., 2010b. Protein oxidation and aggregation in UVA-irradiated *Escherichia coli* cells as signs of accelerated cellular senescence. *Environmental Microbiology.* 12(11), 2931-2945.
- Bowker, C., Sain, A., Shatalov, M. and Ducoste, J., 2011. Microbial UV fluence-response assessment using a novel UV-LED collimated beam system. *Water Research.* 45(5), 2011-2019.
- Brownell, S.A., Chakrabarti, A.R., Kaser, F.M., Connelly, L.G., Peletz, R.L., Reygadas, F., Lang, M.J., Kammen, D.M. and Nelson, K.L., 2008. Assessment of a low-cost, point-of-use, ultraviolet water disinfection technology. *Journal of Water and Health.* 6(1), 53-65.
- Cabiscol, E., Tamarit, J. and Ros, J., 2000. Oxidative stress in bacteria and protein damage by reactive oxygen species. *International Microbiology.* 3, 3-8.
- Cadet, J., Douki, T. and Ravanat, J.L., 2015. Oxidatively Generated Damage to Cellular DNA by UVB and UVA Radiation. *Photochemistry and Photobiology.* 91(1), 140-155.
- Chatterley, C. and Linden, K., 2010. Demonstration and evaluation of germicidal UV-LEDs for point-of-use water disinfection. *Journal of Water and Health.* 8(3), 479-486.
- Chen, R.Z., Craik, S.A. and Bolton, J.R., 2009. Comparison of the action spectra and relative DNA absorbance spectra of microorganisms: Information important for the determination of germicidal fluence (UV dose) in an ultraviolet disinfection of water. *Water Research.* 43(20), 5087-5096.

- Chen, Y.M., Lu, A.H., Li, Y., Zhang, L.S., Yip, H.Y., Zhao, H.J., An, T.C. and Wong, P.K., 2011. Naturally Occurring Sphalerite As a Novel Cost-Effective Photocatalyst for Bacterial Disinfection under Visible Light. *Environmental Science & Technology*. 45(13), 5689-5695.
- Cheng, M., Zeng, G.M., Huang, D.L., Lai, C., Xu, P., Zhang, C. and Liu, Y., 2016. Hydroxyl radicals based advanced oxidation processes (AOPs) for remediation of soils contaminated with organic compounds: A review. *Chemical Engineering Journal*. 284, 582-598.
- Chevremont, A.C., Boudenne, J.L., Coulomb, B. and Farnet, A.M., 2013a. Fate of carbamazepine and anthracene in soils watered with UV-LED treated wastewaters. *Water Research*. 47(17), 6574-6584.
- Chevremont, A.C., Boudenne, J.L., Coulomb, B. and Farnet, A.M., 2013b. Impact of watering with UV-LED-treated wastewater on microbial and physico-chemical parameters of soil. *Water Research*. 47(6), 1971-1982.
- Chevremont, A.C., Farnet, A.M., Coulomb, B. and Boudenne, J.L., 2012a. Effect of coupled UV-A and UV-C LEDs on both microbiological and chemical pollution of urban wastewaters. *Science of the Total Environment*. 426, 304-310.
- Chevremont, A.C., Farnet, A.M., Sergent, M., Coulomb, B. and Boudenne, J.L., 2012b. Multivariate optimization of fecal bioindicator inactivation by coupling UV-A and UV-C LEDs. *Desalination*. 285, 219-225.
- Cho, M., Chung, H., Choi, W. and Yoon, J., 2004. Linear correlation between inactivation of E-coli and OH radical concentration in TiO₂ photocatalytic disinfection. *Water Research*. 38(4), 1069-1077.

- Chong, M.N., Jin, B., Chow, C.W.K. and Saint, C., 2010. Recent developments in photocatalytic water treatment technology: A review. *Water Research*. 44(10), 2997-3027.
- Close, J., Ip, J. and Lam, K.H., 2006. Water recycling with PV-powered UV-LED disinfection. *Renewable Energy*. 31(11), 1657-1664.
- Cortat, B., Garcia, C.C.M., Quinet, A., Schuch, A.P., de Lima-Bessa, K.M. and Menck, C.F.M., 2013. The relative roles of DNA damage induced by UVA irradiation in human cells. *Photochemical & Photobiological Sciences*. 12(8), 1483-1495.
- Devasagayam, T., Tilak, J., Boloor, K., Sane, K.S., Ghaskadbi, S.S. and Lele, R., 2004. Free radicals and antioxidants in human health: current status and future prospects. *Journal of Association of Physicians of India (JAPI)*. 52(10), 794-804.
- DiRuggiero, J. and Robb, F.T., 2004. Early Evolution of DNA Repair Mechanisms. In: *The Genetic Code and the Origin of Life*. Springer, Boston, MA.
- Dorfman, L.M. and Adams, G.E., 1973. Reactivity of the hydroxyl radical in aqueous solutions. *National Standard Reference Data System*.
- Eisenstark, A., 1987. Mutagenic and lethal effects of near-ultraviolet radiation (290-400 nm) on bacteria and phage. *Environmental and Molecular Mutagenesis*. 10(3), 317-337.
- Elmnasser, N., Guillou, S., Leroi, F., Orange, N., Bakhrouf, A. and Federighi, M., 2007. Pulsed-light system as a novel food decontamination technology: a review. *Canadian Journal of Microbiology*. 53(7), 813-821.
- Fine, F. and Gervais, P., 2004. Efficiency of pulsed UV light for microbial decontamination of food powders. *Journal of Food Protection*. 67(4), 787-792.
- Fridovich, S.E. and Porter, N.A., 1981. Oxidation of arachidonic-acid in micelles by superoxide and hydrogen-peroxide. *Journal of Biological Chemistry*. 256(1), 260-265.

- Gates, F.L., 1930. A Study of the bactericidal action of Ultra Violet Light. *The Journal of general physiology*. 14(1), 31-42.
- Gayán, E., Condon, S. and Alvarez, I., 2014. Biological Aspects in Food Preservation by Ultraviolet Light: a Review. *Food and Bioprocess Technology*. 7(1), 1-20.
- Gillespie, J.B., Maclean, M., Given, M.J., Wilson, M.P., Judd, M.D., Timoshkin, I.V. and MacGregor, S.J., 2017. Efficacy of Pulsed 405-nm Light-Emitting Diodes for Antimicrobial Photodynamic Inactivation: Effects of Intensity, Frequency, and Duty Cycle. *Photomedicine and Laser Surgery*. 35(3), 150-156.
- Girard, P.M., Francesconi, S., Pozzebon, M., Graindorge, D., Rochette, P., Drouin, R. and Sage, E., 2011. UVA-induced damage to DNA and proteins: direct versus indirect photochemical processes. *Journal of Physics: Conference Series*. 261.
- Goldstein, S. and Czapski, G., 1984. Mannitol as an OH• scavenger in aqueous solutions and in biological systems. *International Journal of Radiation Biology*. 46(6), 725-729.
- Goldstein, S. and Rabani, J., 2008. The ferrioxalate and iodide-iodate actinometers in the UV region. *Journal of Photochemistry and Photobiology a-Chemistry*. 193(1), 50-55.
- Gomez-Lopez, V.M., Ragaert, P., Debevere, J. and Devlieghere, F., 2007. Pulsed light for food decontamination: a review. *Trends in Food Science & Technology*. 18(9), 464-473.
- Halliwell, B., 1996. Antioxidants in human health and disease. *Annual Review of Nutrition*. 16, 33-50.
- Hamamoto, A., Mori, M., Takahashi, A., Nakano, M., Wakikawa, N., Akutagawa, M., Ikehara, T., Nakaya, Y. and Kinouchi, Y., 2007. New water disinfection system using UVA light-emitting diodes. *Journal of Applied Microbiology*. 103(6), 2291-2298.

- Harm, W., 1980. Biological Effects of Ultraviolet Radiation. Cambridge University Press, New York. 127-130.
- Harris, G.D., Adams, V.D., Sorensen, D.L. and Curtis, M.S., 1987. Ultraviolet inactivation of selected bacteria and viruses with photoreactivation of the bacteria. *Water Research*. 21(6), 687-692.
- Harris, T.R., Pagan, J. and Batoni, P., 2013. Optical and Fluidic Co-Design of a UV-LED Water Disinfection Chamber. *ECS Transactions*. 45(17), 11-18.
- Hatami, H., 2013. Importance of water and water-borne diseases: On the occasion of the world water day (March 22, 2013). *International journal of preventive medicine*. 4(3), 243.
- He, Y.Y. and Hader, D.P., 2002. Involvement of reactive oxygen species in the UV-B damage to the cyanobacterium *Anabaena* sp. *Journal of Photochemistry and Photobiology B-Biology*. 66(1), 73-80.
- Hijnen, W.A.M., Beerendonk, E.F. and Medema, G.J., 2006. Inactivation credit of UV radiation for viruses, bacteria and protozoan (oo)cysts in water: A review. *Water Research*. 40(1), 3-22.
- Hoerter, J.D., Arnold, A.A., Kuczynska, D.A., Shibuya, A., Ward, C.S., Sauer, M.G., Gizachew, A., Hotchkiss, T.M., Fleming, T.J. and Johnson, S., 2005. Effects of sublethal UVA irradiation on activity levels of oxidative defense enzymes and protein oxidation in *Escherichia coli*. *Journal of Photochemistry and Photobiology B-Biology*. 81(3), 171-180.
- Hoyer, O., 1998. Testing performance and monitoring of UV systems for drinking water disinfection. *Water Supply*. 16(1-2), 424-429.

- Hwang, K.S., Jeon, Y.S., Choi, T.I. and Hwangbo, S., 2013. Combination of Light Emitting Diode at 375 nm and Photo-reactive TiO₂ Layer Prepared by Electrostatic Spraying for Sterilization. *Journal of Electrical Engineering & Technology*. 8(5), 1169-1174.
- Ibrahim, M.A.S., MacAdam, J., Autin, O. and Jefferson, B., 2014. Evaluating the impact of LED bulb development on the economic viability of ultraviolet technology for disinfection. *Environmental Technology*. 35(4), 400-406.
- IUVA, 2015. Proposed Testing Protocol for Measurement of UV-C LED Lamp Output. *IUVA NEWS*. 17(2), 7.
- Jagger, J., 1967. Introduction to research in ultraviolet photobiology. Prentice-Hall, Inc., New Jersey.
- Jo, W.K. and Tayade, R.J., 2014. New Generation Energy-Efficient Light Source for Photocatalysis: LEDs for Environmental Applications. *Industrial & Engineering Chemistry Research*. 53(6), 2073–2084.
- Kabra, K., Chaudhary, R. and Sawhney, R.L., 2004. Treatment of hazardous organic and inorganic compounds through aqueous-phase photocatalysis: A review. *Industrial & Engineering Chemistry Research*. 43(24), 7683-7696.
- Kalisvaart, B.F., 2004. Re-use of wastewater: preventing the recovery of pathogens by using medium-pressure UV lamp technology. *Water Science and Technology*. 50(6), 337-344.
- Keener, L. and Krishnamurthy, K., 2014. Shedding Light on Food Safety: Applications of Pulsed Light Processing. *Food Safety Magazine*. <http://www.foodsafetymagazine.com/magazine-archive1/junejuly-2014/shedding-light-on-food-safety-applications-of-pulsed-light-processing/> (Retrieved on Jan.18, 2018).

- Khan, M.A., Shatalov, M., Maruska, H.P., Wang, H.M. and Kuokstis, E., 2005. III-nitride UV devices. *Japanese Journal of Applied Physics*. 44(10), 7191-7206.
- Kheyrandish, A., Mohseni, M. and Taghipour, F., 2017. Development of a method for the characterization and operation of UV-LED for water treatment. *Water Research*. 122, 570-579.
- Krishnamurthy, K., Demirci, A. and Irudayaraj, J., 2004. Inactivation of *Staphylococcus aureus* by pulsed UV-light sterilization. *Journal of Food Protection*. 67(5), 1027-1030.
- Krishnamurthy, K., Demirci, A. and Irudayaraj, J.M., 2007. Inactivation of *staphylococcus aureus* in milk using flow-through pulsed UV-Light treatment system. *Journal of Food Science*. 72(7), M233-M239.
- Krishnamurthy, K., Tewari, J.C., Irudayaraj, J. and Demirci, A., 2010. Microscopic and Spectroscopic Evaluation of Inactivation of *Staphylococcus aureus* by Pulsed UV Light and Infrared Heating. *Food and Bioprocess Technology*. 3(1), 93-104.
- Kuhn, H.J., Braslavsky, S.E. and Schmidt, R., 2004. Chemical actinometry. *Pure and Applied Chemistry*. 76(12), 2105-2146.
- Kuo, J., Chen, C.L. and Nellor, M., 2003. Standardized collimated beam testing protocol for water/wastewater ultraviolet disinfection. *Journal of Environmental Engineering-Asce*. 129(8), 774-779.
- Lejeune, D., Hasanuzzaman, M., Pitcock, A., Francis, J. and Sehgal, I., 2006. The superoxide scavenger TEMPOL induces urokinase receptor (uPAR) expression in human prostate cancer cells. *Molecular Cancer*. 5.

- Li, G.-Q., Wang, W.-L., Huo, Z.-Y., Lu, Y. and Hu, H.-Y., 2017. Comparison of UV-LED and low pressure UV for water disinfection: Photoreactivation and dark repair of *Escherichia coli*. *Water Research*. 126, 134-143.
- Li, J., Hirota, K., Yumoto, H., Matsuo, T., Miyake, Y. and Ichikawa, T., 2010. Enhanced germicidal effects of pulsed UV-LED irradiation on biofilms. *Journal of Applied Microbiology*. 109(6), 2183-2190.
- Liang, J.L., Deng, J., Li, M. and Tong, M.P., 2016. Bactericidal activity and mechanism of AgI/AgBr/BiOBr_{0.75}I_{0.25} under visible light irradiation. *Colloids and Surfaces B-Biointerfaces*. 138, 102-109.
- Linden, K.G., Shin, G. and Sobsey, M.D., 2001. Comparative effectiveness of UV wavelengths for the inactivation of *Cryptosporidium parvum* oocysts in water. *Water Science and Technology*. 43(12), 171-174.
- Lushchak, V.I., 2014. Free radicals, reactive oxygen species, oxidative stress and its classification. *Chemico-Biological Interactions*. 224, 164-175.
- Malato, S., Fernandez-Ibanez, P., Maldonado, M.I., Blanco, J. and Gernjak, W., 2009. Decontamination and disinfection of water by solar photocatalysis: Recent overview and trends. *Catalysis Today*. 147(1), 1-59.
- Mamane-Gravetz, H., Linden, K.G., Cabaj, A. and Sommer, R., 2005. Spectral sensitivity of *Bacillus subtilis* spores and MS2 Coliphage for validation testing of ultraviolet reactors for water disinfection. *Environmental Science & Technology*. 39(20), 7845-7852.
- Marugan, J., van Grieken, R., Pablos, C. and Sordo, C., 2010. Analogies and differences between photocatalytic oxidation of chemicals and photocatalytic inactivation of microorganisms. *Water Research*. 44(3), 789-796.

- Mori, M., Hamamoto, A., Takahashi, A., Nakano, M., Wakikawa, N., Tachibana, S., Ikehara, T., Nakaya, Y., Akutagawa, M. and Kinouchi, Y., 2007. Development of a new water sterilization device with a 365 nm UV-LED. *Medical & Biological Engineering & Computing*. 45(12), 1237-1241.
- Morton, R. and Haynes, R., 1969. Changes in the ultraviolet sensitivity of *Escherichia coli* during growth in batch cultures. *Journal of bacteriology*. 97(3), 1379-1385.
- Muller, F.L., Lustgarten, M.S., Jang, Y., Richardson, A. and Van Remmen, H., 2007. Trends in oxidative aging theories. *Free Radical Biology and Medicine*. 43(4), 477-503.
- Muller, J., 2011. Seeing the light: the benefits of UV water treatment. *Water Online*. <http://www.wateronline.com/doc/seeing-the-light-the-benefits-of-uv-0001> (Retrieved on Jan.18, 2018).
- Muramoto, Y., Kimura, M. and Nouda, S., 2014. Development and future of ultraviolet light-emitting diodes: UV-LED will replace the UV lamp. *Semiconductor Science and Technology*. 29(8).
- Nair, A.J., 2010. *Comprehensive Biotechnology XI*. Firewall Media. .
- Nakahashi, M., Mawatari, K., Hirata, A., Maetani, M., Shimohata, T., Uebanso, T., Hamada, Y., Akutagawa, M., Kinouchi, Y. and Takahashi, A., 2014. Simultaneous Irradiation with Different Wavelengths of Ultraviolet Light has Synergistic Bactericidal Effect on *Vibrio parahaemolyticus*. *Photochemistry and Photobiology*. 90(6), 1397-1403.
- Novo, E. and Parola, M., 2008. Redox mechanisms in hepatic chronic wound healing and fibrogenesis. *Fibrogenesis & tissue repair*. 1(1), 5.
- Oguma, K., Katayama, H., Mitani, H., Morita, S., Hirata, T. and Ohgaki, S., 2001. Determination of pyrimidine dimers in *Escherichia coli* and *Cryptosporidium parvum* during UV light

- inactivation, photoreactivation, and dark repair. *Applied and Environmental Microbiology*. 67(10), 4630-4637.
- Oguma, K., Katayama, H. and Ohgaki, S., 2002. Photoreactivation of *Escherichia coli* after low- or medium-pressure UV disinfection determined by an endonuclease sensitive site assay. *Applied and Environmental Microbiology*. 68(12), 6029-6035.
- Oguma, K., Kita, R., Sakai, H., Murakami, M. and Takizawa, S., 2013. Application of UV light emitting diodes to batch and flow-through water disinfection systems. *Desalination*. 328, 24-30.
- Oguma, K., Rattanakul, S. and Bolton, J.R., 2016. Application of UV Light-Emitting Diodes to Adenovirus in Water. *Journal of Environmental Engineering*. 142(3).
- Oms-Oliu, G., Martin-Belloso, O. and Soliva-Fortuny, R., 2010. Pulsed Light Treatments for Food Preservation. A Review. *Food and Bioprocess Technology*. 3(1), 13-23.
- Oppezzo, O.J. and Pizarro, R.A., 2001. Sublethal effects of ultraviolet A radiation on *Enterobacter cloacae*. *Journal of Photochemistry and Photobiology B-Biology*. 62(3), 158-165.
- Pablos, C., Marugan, J., van Grieken, R. and Serrano, E., 2013. Emerging micropollutant oxidation during disinfection processes using UV-C, UV-C/H₂O₂, UV-A/TiO₂ and UV-A/TiO₂/H₂O₂. *Water Research*. 47(3), 1237-1245.
- Payne, G. and Sancar, A., 1990. Absolute action spectrum of E-FADH₂ and E-FADH₂-MTHF forms of *Escherichia coli* DNA photolyase. *Biochemistry*. 29(33), 7715-7727.
- Pizarro, R.A., 1995. UV-A oxidative damage modified by environmental conditions in *Escherichia coli*. *International Journal of Radiation Biology*. 68(3), 293-299.

- Pizarro, R.A. and Orce, L.V., 1988. Membrane damage and recovery associated with growth delay induced by near-UV radiation in *Escherichia coli* K-12. *Photochemistry and Photobiology*. 47(3), 391-397.
- Quek, P.H. and Hu, J.Y., 2008. Indicators for photoreactivation and dark repair studies following ultraviolet disinfection. *Journal of Industrial Microbiology & Biotechnology*. 35(6), 533-541.
- Rahn, R.O., Bolton, J. and Stefan, M.I., 2006. The iodide/iodate actinometer in UV disinfection: Determination of the fluence rate distribution in UV reactors. *Photochemistry and Photobiology*. 82(2), 611-615.
- Rahn, R.O., Stefan, M.I., Bolton, J.R., Goren, E., Shaw, P.S. and Lykke, K.R., 2003. Quantum yield of the iodide-iodate chemical actinometer: Dependence on wavelength and concentration. *Photochemistry and Photobiology*. 78(2), 146-152.
- Ramabhadran, T.V. and Jagger, J., 1976. Mechanism of growth delay induced in *Escherichia coli* by near ultraviolet radiation. *Proceedings of the National Academy of Sciences of the United States of America*. 73(1), 59-63.
- Reiter, R.J., Melchiorri, D., Sewerynek, E., Poeggeler, B., Barlowwalden, L., Chuang, J.I., Ortiz, G.G. and Acunacastroviejo, D., 1995. A review of the evidence supporting melatonin's role as an antioxidant. *Journal of Pineal Research*. 18(1), 1-11.
- Rincon, A.G. and Pulgarin, C., 2004. Bactericidal action of illuminated TiO₂ on pure *Escherichia coli* and natural bacterial consortia: post-irradiation events in the dark and assessment of the effective disinfection time. *Applied Catalysis B-Environmental*. 49(2), 99-112.

- Rincon, A.G. and Pulgarin, C., 2007. Absence of E-coli regrowth after Fe^{3+} and TiO_2 solar photoassisted disinfection of water in CPC solar photoreactor. *Catalysis Today*. 124(3-4), 204-214.
- Ronto, G., Gaspar, S. and Berces, A., 1992. Phage T7 in biological UV dose measurement. *Journal of Photochemistry and Photobiology B: Biology*. 12(3), 285-294.
- Ruh, J., Vogel, F., Schmidt, E., Werner, M., Klar, E., Secchi, A., Gebhard, M.M., Glaser, F. and Herfarth, C., 2000. Effects of hydrogen peroxide scavenger Catalase on villous microcirculation in the rat small intestine in a model of inflammatory bowel disease. *Microvascular Research*. 59(3), 329-337.
- Rybicki, E., 1990. The classification of organisms at the edge of life or problems with virus systematics. *South African Journal of Science*. 86(4), 182-186.
- Sancar, A., 2003. Structure and function of DNA photolyase and cryptochrome blue-light photoreceptors. *Chemical Reviews*. 103(6), 2203-2237.
- Sanz, E.N., Davila, I.S., Balao, J.A.A. and Alonso, J.M.Q., 2007. Modelling of reactivation after UV disinfection: Effect of UV-C dose on subsequent photoreactivation and dark repair. *Water Research*. 41(14), 3141-3151.
- Shang, C., Cheung, L.M., Ho, C.M. and Zeng, M.Z., 2009. Repression of photoreactivation and dark repair of coliform bacteria by TiO_2 -modified UV-C disinfection. *Applied Catalysis B-Environmental*. 89(3-4), 536-542.
- Shen, B., Jensen, R.G. and Bohnert, H.J., 1997. Mannitol protects against oxidation by hydroxyl radicals. *Plant Physiology*. 115(2), 527-532.
- Sies, H., 1986. Biochemistry of oxidative stress. *Angewandte Chemie-International Edition in English*. 25(12), 1058-1071.

- Sies, H., 1993. Strategies of antioxidant defense. *European Journal of Biochemistry*. 215(2), 213-219.
- Sinha, R.P. and Hader, D.P., 2002. UV-induced DNA damage and repair: a review. *Photochemical & Photobiological Sciences*. 1(4), 225-236.
- Smirnova, G.V. and Oktyabrsky, O.N., 1994. Near-ultraviolet radiation and hydrogen peroxide modulate intracellular levels of potassium and thiols in *Escherichia coli*. *Current Microbiology*. 28(2), 77-79.
- Sommer, R., Haider, T., Cabaj, A., Pribil, W. and Lhotsky, M., 1998. Time dose reciprocity in UV disinfection of water. *Water Science and Technology*. 38(12), 145-150.
- Sommer, R., Lhotsky, M., Haider, T. and Cabaj, A., 2000. UV inactivation, liquid-holding recovery, and photoreactivation of *Escherichia coli* O157 and other pathogenic *Escherichia coli* strains in water. *Journal of Food Protection*. 63(8), 1015-1020.
- Song, K., Mohseni, M. and Taghipour, F., 2016. Application of ultraviolet light-emitting diodes (UV-LEDs) for water disinfection: A review. *Water Research*. 94, 341–349.
- Taniyasu, Y. and Kasu, M., 2010. Improved Emission Efficiency of 210-nm Deep-ultraviolet Aluminum Nitride Light-emitting Diode. *NTT Technical Review*. 8(8), 1-5.
- Taniyasu, Y., Kasu, M. and Makimoto, T., 2006a. An aluminium nitride light-emitting diode with a wavelength of 210 nanometres. *Nature*. 441(7091), 325-328.
- Taniyasu, Y., Kasu, M. and Makimoto, T., 2006b. Aluminum Nitride Deep-ultraviolet Light-emitting Diodes. *NTT Technical Review*. 4(12), 54-58.
- Thamilselvan, S., Byer, K.J., Hackett, R.L. and Khan, S.R., 2000. Free radical scavengers, catalase and superoxide dismutase provide protection from oxalate-associated injury to LLC-PK1 and MDCK cells. *Journal of Urology*. 164(1), 224-+.

- Thiagarajan, V., Byrdin, M., Eker, A.P.M., Muller, P. and Brettel, K., 2011. Kinetics of cyclobutane thymine dimer splitting by DNA photolyase directly monitored in the UV. *Proceedings of the National Academy of Sciences of the United States of America*. 108(23), 9402-9407.
- Tran, T., Racz, L., Grimaila, M.R., Miller, M. and Harper, W.F., 2014. Comparison of continuous versus pulsed ultraviolet light emitting diode use for the inactivation of *Bacillus globigii* spores. *Water Science and Technology*. 70(9), 1473-1480.
- Tyrrell, R.M. and Keyse, S.M., 1990. New trends in photobiology - the interaction of UVA radiation with cultured-cells. *Journal of Photochemistry and Photobiology B-Biology*. 4(4), 349-361.
- USEPA, 1999. Wastewater Technology Fact Sheet Ultraviolet Disinfection. Washington DC, Office of Water, EPA 832-F-99-064.
- USEPA, 2006. Ultraviolet disinfection guidance manual for the final long term 2 enhanced surface water treatment rule. Washington DC, Office of Water, EPA 815-R-06-007.
- Vilhunen, S., Sarkka, H. and Sillanpaa, M., 2009. Ultraviolet light-emitting diodes in water disinfection. *Environmental Science and Pollution Research*. 16(4), 439-442.
- Vogna, D., Marotta, R., Andreozzi, R., Napolitano, A. and d'Ischia, M., 2004. Kinetic and chemical assessment of the UV/H₂O₂ treatment of antiepileptic drug carbamazepine. *Chemosphere*. 54(4), 497-505.
- Wang, J.L. and Xu, L.J., 2012. Advanced Oxidation Processes for Wastewater Treatment: Formation of Hydroxyl Radical and Application. *Critical Reviews in Environmental Science and Technology*. 42(3), 251-325.

- Wekhof, A., Trompeter, F.-J. and Franken, O., 2001. Pulsed UV disintegration (PUVD): a new sterilisation mechanism for packaging and broad medical-hospital applications. Proceedings of the First International Conference on Ultraviolet Technologies, Washington, DC, USA, 14–16 June 2001. pp. 1–15.
- Wengraitis, S., McCubbin, P., Wade, M.M., Biggs, T.D., Hall, S., Williams, L.I. and Zulich, A.W., 2013. Pulsed UV-C Disinfection of *Escherichia coli* With Light-Emitting Diodes, Emitted at Various Repetition Rates and Duty Cycles. *Photochemistry and Photobiology*. 89(1), 127-131.
- WHO, 2014. Progress on Drinking Water and Sanitation. http://apps.who.int/iris/bitstream/10665/112727/1/9789241507240_eng.pdf (Retrieved on Jan.18, 2018).
- Wikipedia, Light-emitting diode. https://en.wikipedia.org/wiki/Light-emitting_diode (Retrieved on Jan.18, 2018).
- Wikipedia, p–n junction. https://en.wikipedia.org/wiki/P%E2%80%93n_junction (Retrieved on Jan.18, 2018).
- Wikipedia, Virus. <https://en.wikipedia.org/wiki/Virus> (Retrieved on Jan.18, 2018).
- Wilcox, C.S. and Pearlman, A., 2008. Chemistry and Antihypertensive Effects of Tempol and Other Nitroxides. *Pharmacological Reviews*. 60(4), 418-469.
- Wurtele, M.A., Kolbe, T., Lipsz, M., Kulberg, A., Weyers, M., Kneissl, M. and Jekel, M., 2011. Application of GaN-based ultraviolet-C light emitting diodes - UV LEDs - for water disinfection. *Water Research*. 45(3), 1481-1489.
- Xiong, P. and Hu, J.Y., 2013. Inactivation/reactivation of antibiotic-resistant bacteria by a novel UVA/LED/TiO₂ system. *Water Research*. 47(13), 4547-4555.

- Yamada, J., Yoshimura, S., Yamakawa, H., Sawada, M., Nakagawa, M., Hara, S., Kaku, Y., Iwama, T., Naganawa, T., Banno, Y., Nakashima, S. and Sakai, N., 2003. Cell permeable ROS scavengers, Tiron and Tempol, rescue PC12 cell death caused by pyrogallol or hypoxia/reoxygenation. *Neuroscience Research*. 45(1), 1-8.
- Zimmer-Thomas, J.L., Slawson, R.M. and Huck, P.M., 2007. A comparison of DNA repair and survival of *Escherichia coli* O157 : H7 following exposure to both low- and medium-pressure UV irradiation. *Journal of Water and Health*. 5(3), 407-415.
- Zimmer, J.L. and Slawson, R.M., 2002. Potential repair of *Escherichia coli* DNA following exposure to UV radiation from both medium- and low-pressure UV sources used in drinking water treatment. *Applied and Environmental Microbiology*. 68(7), 3293-3299.

Appendices

Appendix A Microorganisms cultivation and enumeration for UV disinfection

A.1 *E. coli* stock preparation

- (1) Prepare materials:

E. coli ATCC 11229: from American Type Culture Collection (ATCC)

LB broth (agar), phosphate buffered saline (PBS): from Sigma-Aldrich

Glycerol solution: Mix deionized (DI) water with 63 g glycerol to a total volume of 100 mL, then autoclave at 121 °C for 20 min.

- (2) Dissolve *E. coli* freeze-dried power (ATCC) with 1 mL LB broth, then mix with 9 mL broth.
- (3) Cultivate *E. coli* with LB broth in a shaker-incubator at 37 °C and 200 rpm for 24 h.
- (4) Mix 10 mL cultivated *E. coli* solution with 10 mL prepared glycerol solution using vortex, then split by 2 mL in 10 sterile tubes. Store them in deep freezer (-30 °C) as *E. coli* stock and use within six months.

A.2 *E. coli* sample preparation and enumeration

- (1) Take *E. coli* stock from deep freezer and allow it thaw in room temperature for 10 minutes.
- (2) Mix 0.5 mL *E. coli* stock with 9.5 mL LB broth, then cultivate in a shaker-incubator at 37 °C and 200 rpm.
- (3) Measure absorbance at 600 nm (i.e. OD600) for growing *E. coli* solution every 30 min to construct the growth curve as shown in Figure A.1.

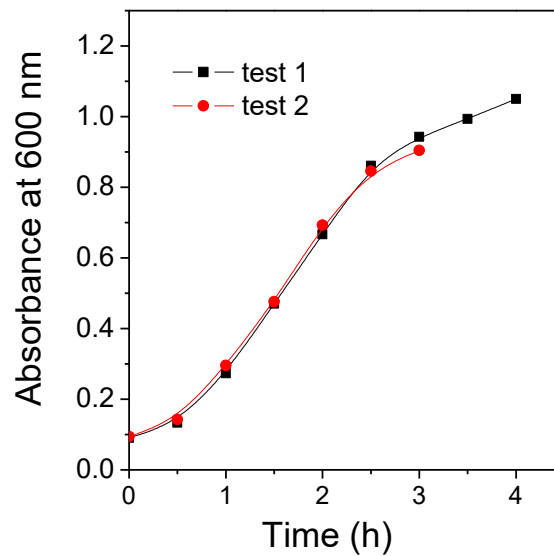


Figure A.1 Growth curve of *E. coli* solution

- (4) Based on the growth curve, exponential phase is determined between 1.5 to 3 h. Therefore, fresh *E. coli* solution of 3 h growth (exponential phase) is used to prepare the water sample for UV disinfection experiment.
- (5) Fresh *E. coli* solution of 3 h growth is centrifuged at 3300 rpm for 5 min, then supernatant is discarded. The settled *E. coli* cells on the bottom are re-suspended in PBS. Repeat the centrifuge and PBS washing for 3 times. Then concentrated *E. coli* solution in PBS is obtained.
- (6) Dilute the concentrated *E. coli* solution with PBS to a concentration around $10^6 \sim 10^7$ CFU/mL as the initial solution for UV disinfection.
- (7) Collect *E. coli* samples before and after UV exposure, then do serial dilution using PBS for each sample.
- (8) Spread 20 μ L each dilution of *E. coli* samples in prepared LB agar plate for triplicates. Then turn over and cultivate these agar plates in an incubator at 37 °C for 16 h.
- (9) Count the colonies on the agar plates, the agar plates with 20~200 colonies are used to calculate the *E. coli* concentration and log inactivation. The agar plates with *E. coli*

colonies are illustrated as Figure A.2:

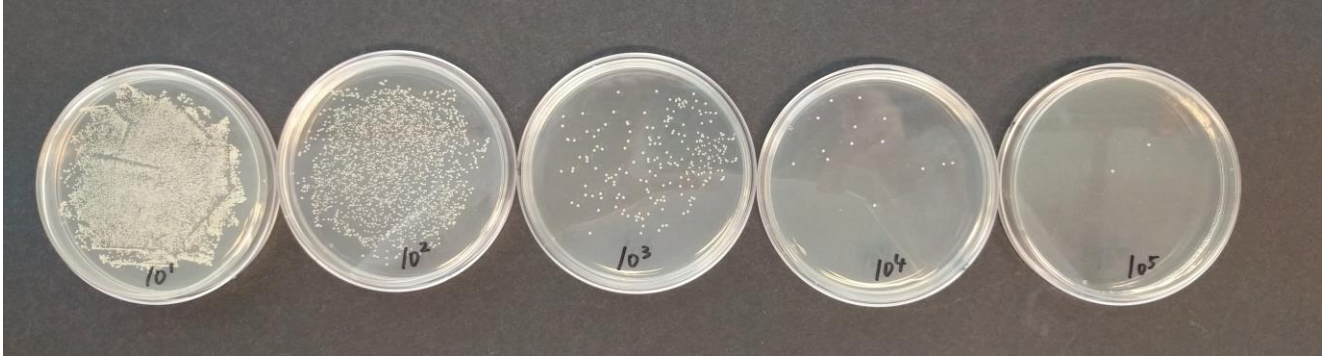


Figure A.2 *E. coli* colonies on agar plates

A.3 MS2 phage stock preparation

(1) Prepare materials:

E. coli ATCC 15597: from American Type Culture Collection (ATCC)

MS2 ATCC 15597-B1: from American Type Culture Collection (ATCC)

LB broth (agar), phosphate buffered saline (PBS), CaCl_2 : from Sigma-Aldrich

CaCl_2 solution: dissolve 3 mg $\text{CaCl}_2 \cdot 2\text{H}_2\text{O}$ into 10 mL DI water, then autoclave at 121 °C for 20 min.

(2) Prepare *E. coli* ATCC 15597 stock using the same procedure as Appendix A.1.

(3) Prepare fresh *E. coli* ATCC 15597 solution in exponential phase by following the step (1) ~ (4) in Appendix A.2.

(4) Dissolve MS2 freeze-dried powder (ATCC) with 1 mL LB broth, then mix with 9 mL fresh *E. coli* ATCC 15597 solution in exponential phase and 200 μL prepared CaCl_2 solution. Cultivate the mixture in a shaker-incubator at 37 °C and 200 rpm for 24 h.

(5) Centrifuge cultivated MS2 and *E. coli* mixture at 3300 rpm for 5 min. Then filter the supernatant by using 0.45 μm filter. Collect filtrate as MS2 stock. Store it in refrigerator at 4 °C, and use within one month.

A.4 MS2 phage sample preparation and enumeration

(1) Prepare materials:

Bottom agar plates: Mix 8 g LB broth power, 4.8 g agar power with 400 mL DI water, autoclave at 121 °C for 20 min, then make agar plates.

Upper agar: Mix 8 g LB broth power, 4 g agar power and 0.32 g $\text{CaCl}_2 \cdot 2\text{H}_2\text{O}$ with 400 mL DI water, autoclave at 121 °C for 20 min, then slightly cool down and keep it warm at around 45~50 °C.

Fresh *E. coli* ATCC 15597 solution: Follow the step (1) ~ (4) in Appendix A.2 to prepare fresh *E. coli* ATCC 15597 solution in exponential phase

(2) Dilute MS2 stock solution with PBS to a concentration around $10^6 \sim 10^7$ PFU/mL as the initial solution for UV disinfection.

(3) Collect MS2 samples before and after UV exposure, then do serial dilution using PBS for each sample.

(4) Transfer 1 mL each dilution of MS2 samples in prepared bottom agar plate for triplicates.

(5) Mix fresh *E. coli* ATCC 15597 solution and warm upper agar, then pour into bottom agar plate, slightly shake to mix, allow to cool down and harden.

(6) Turn over and cultivate these agar plates in an incubator at 37 °C for 16 h.

(7) Count the plaques on the agar plates: the clear circular zones in the dark yellow lawn of host *E. coli* are identified as MS2 plaques. The agar plates with 20~200 plaques are used to calculate the MS2 concentration and log inactivation. The agar plates with MS2 plaques are illustrated as Figure A.3:

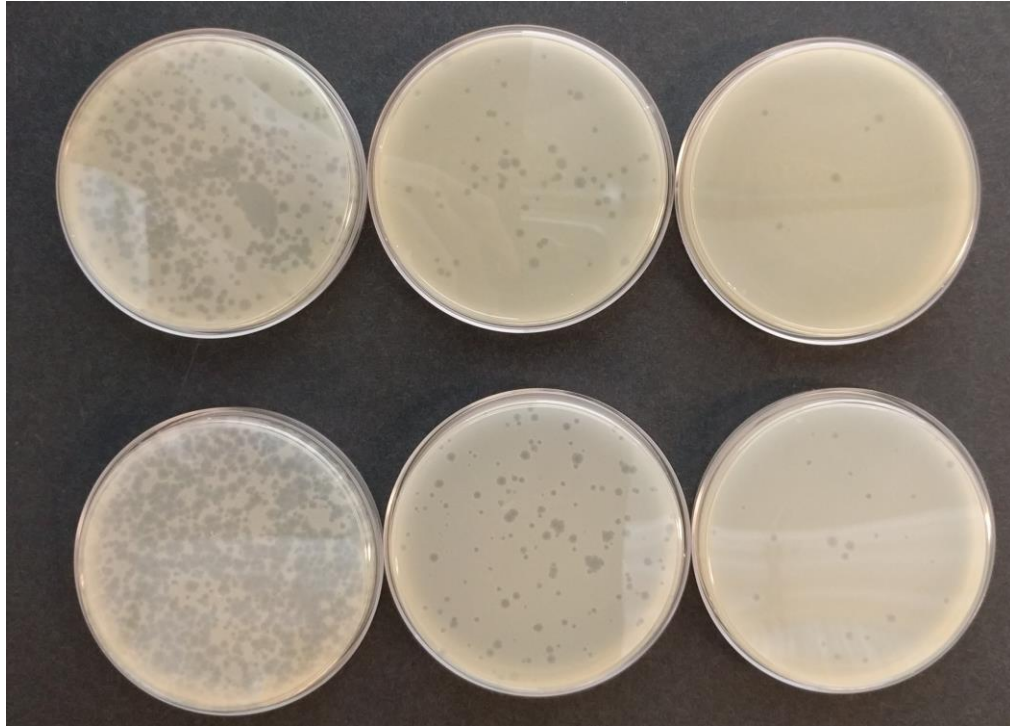


Figure A.3 MS2 plaques on *E. coli* agar plates

Appendix B Supplementary data

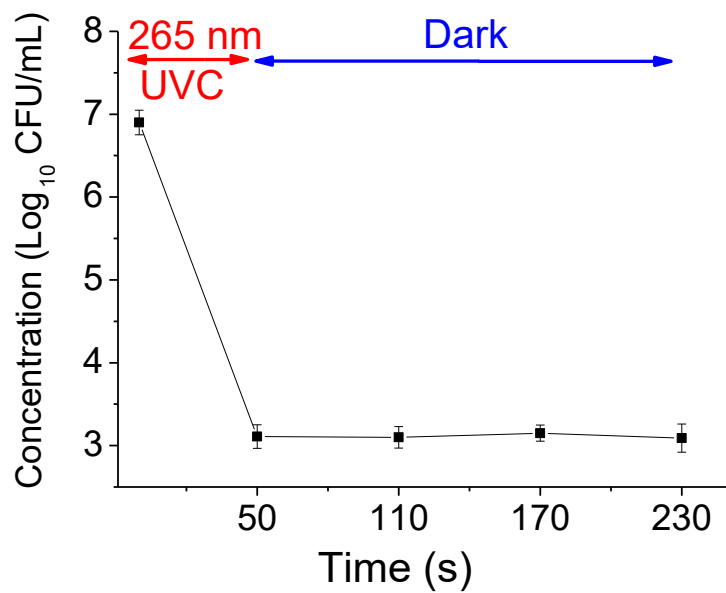


Figure B.1 Dark control for *E. coli* concentration change after 50 s 265 nm UVC-LED exposure.

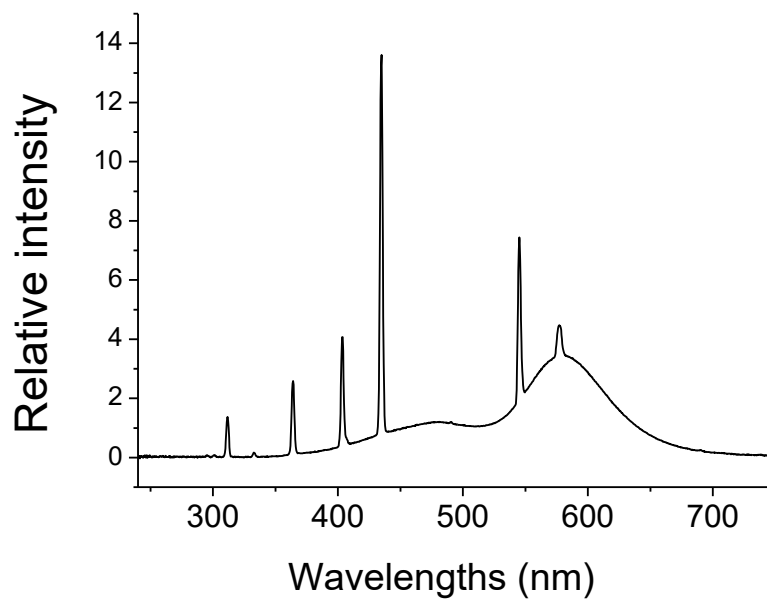


Figure B.2 The emission spectrum from fluorescent lamps for photoreactivation experiments

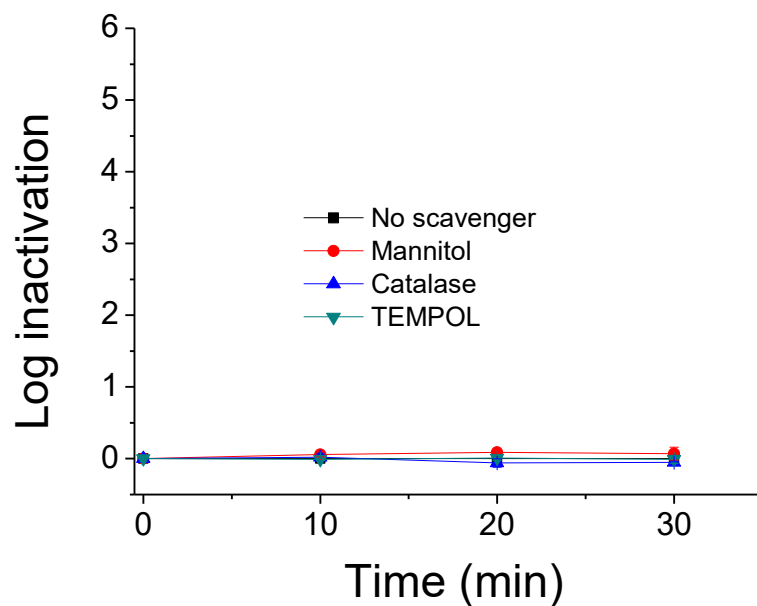


Figure B.3 Effect of different scavengers (0.5 mol/L mannitol, 1 mg/mL catalase, 1 mmol/L TEMPOL) on the viability of *E. coli* cells as control. Error bars represent the standard deviation for triplicate runs.

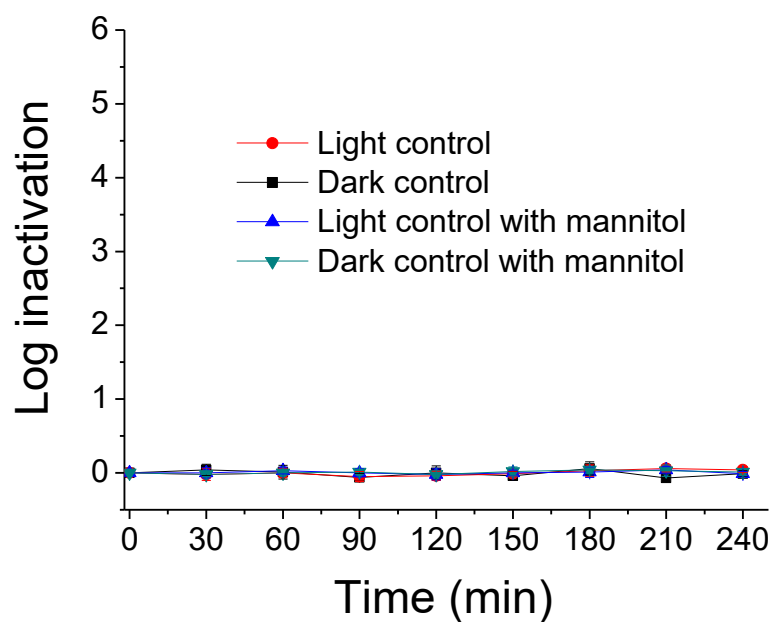


Figure B.4 The viability of *E. coli* cells under fluorescent lamps visible light and in dark as light and dark control for reactivation experiment. Error bars represent the standard deviation for triplicate runs.

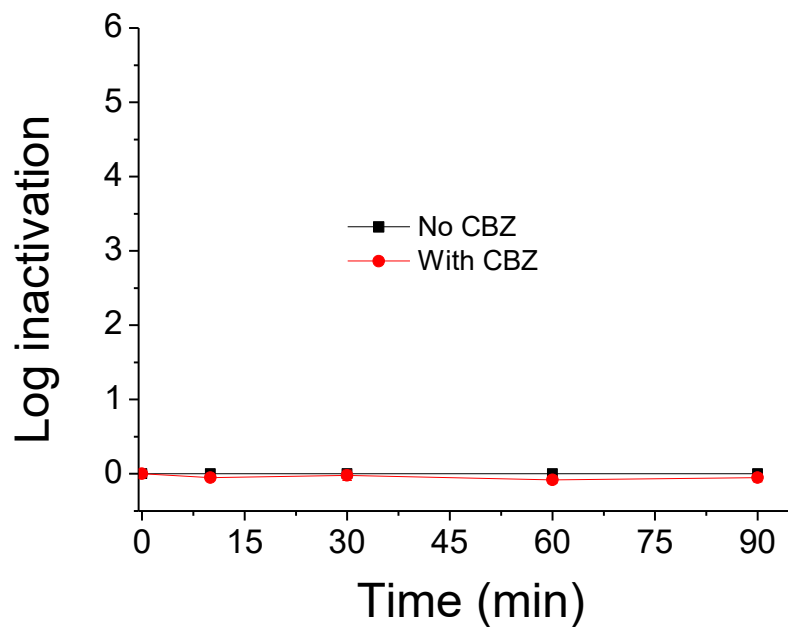


Figure B.5 Effect of carbamazepine (CBZ, 400 ppb) on the viability of *E. coli* cells as control. Error bars represent the standard deviation for triplicate runs.

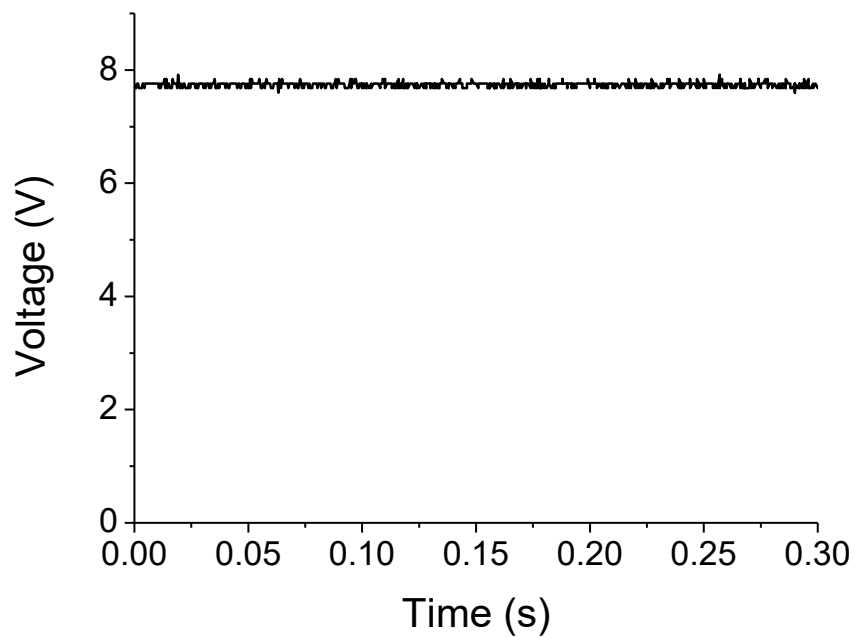


Figure B.6 Measured voltage waveform for UV-LED continuous irradiation